In presenting the dissertation as a partial fulfillment of the requirements for an advanced degree from the Georgia Institute of Technology, I agree that the Library of the Institution shall make it available for inspection and circulation in accordance with its regulations governing materials of this type. I agree that permission to copy from, or to publish from, this dissertation may be granted by the professor under whose direction it was written, or, in his absence, by the dean of the Graduate Division when such copying or publication is solely for scholarly purposes and does not involve potential financial gain. It is understood that any copying from, or publication of, this dissertation which involves potential financial gain will not be allowed without written permission.

_____

THE ROLE OF A PERMEABLE BED IN INCIPIENT SEDIMENT MOTION

A THESIS

Presented to

The Faculty of the Graduate Division

by

Charles Samuel Martin

In Partial Fulfillment

of the Requirements for the Degree

Doctor of Philosophy

in the School of Civil Engineering

Georgia Institute of Technology

May, 1964

THE ROLE OF A PERMEABLE BED IN

INCIPIENT SEDIMENT MOTION

Approved:

Date approved by Chairman: May 28, 1964

ACKNOWLEDGMENTS

The writer would like to express his sincere appreciation to all who had a part in making this thesis possible. Special thanks are due Dr. M. R. Carstens, thesis advisor and chairman of the thesis reading committee, who initially suggested the problem and offered excellent guidance throughout the duration of the study. The other members of the reading committee were Dr. A. B. Vesic and Dr. P. G. Mayer. The aid given by Dr. Vesic on the soil mechanics phase of the study and in translating a foreign technical paper is greatly appreciated. The translation of another foreign paper by Dr. Mayer is likewise appreciated. The help given by Mr. Homer Bates, laboratory technician, in carrying out the experimental program was invaluable. The personnel at the Rich Electronic Computer Center were more than helpful in aiding the writer in composing computer programs.

While conducting the study, the writer was given partial, and sometimes complete, financial support by the United States Mine Defense Laboratory, Panama City, Florida, through Contract Nobs-84237, Bureau of Ships, Department of the Navy. The writer is grateful to the Navy Department, especially the Mine Defense Laboratory, for the financial support.

TABLE OF CONTENTS

TABLE OF CONTENTS (Continued)

TABLE OF CONTENTS (Continued)

LIST OF TABLES

LIST OF TABLES (Continued)

LIST OF ILLUSTRATIONS

Figure — Page

TEXT

LIST OF ILLUSTRATIONS (Continued)

APPENDIX

NOMENCLATURE

Symbol	Quantity	Dimensions (F,L,T)
	TEXT	
a	amplitude of displacement of simple-harmonic oscillation; amplitude of oscillating plate	L
a_1, a_2, a_3, a_4	arbitrary constants	$L^{1/2}$
A	projected area of bed particle	L^2
A_s	surface area of bed particle	L^2
A_o, A_n	Euler coefficients of Fourier cosine series	L
B	free-surface width of trapezoidal canal	L
c	celerity of simple-harmonic water wave	LT^{-1}
C_f	local skin friction coefficient	none
C	flow coefficient for permeable bed	none
$C_\perp$	flow coefficient for flow perpendicular to the bed	none
$C_{\parallel}$	flow coefficient for flow parallel with the bed	none
C_D	drag coefficient	none
C_L	lift coefficient	none
d	mean diameter of bed particle	L
D	diameter of cylindrical tube; depth of water in sea and in canal	L
$e = \Delta\forall_v / \Delta\forall_s$	voids ratio	none
E	complete elliptic integral of the second kind	none

NOMENCLATURE (Continued)

Symbol	Quantity	Dimensions (F,L,T)
f	Darcy-Weisbach resistance coefficient	none
$f(\ ), f'(\ ), f''(\ )$	functional expressions	none
$f_1(\ ),\ f_2(\ )$	functional expressions	none
F	total fluid-resistance force on bed particle	F
F_D	component of fluid-resistance force parallel to bed	F
F_L	component of fluid-resistance force normal to bed	F
F_{AM}	added-mass force on bed particle	F
F_p	pressure force on bed particle resulting from fluid acceleration	F
F_s	seepage force on bed particle resulting from seepage flow through bed	F
$F_{\parallel}$	force on bed particle parallel to bed	F
$F_{\perp}$	force on bed particle perpendicular to bed	F
g	acceleration due to gravity	LT^{-2}
$h = p/\gamma + y$	piezometric head in permeable bed	L
$h_o(x)$	piezometric-head variation on sea bed	L
H	total wave amplitude from trough to crest	L
k	modulus of Jacobian elliptic functions	none
k'	complementary modulus of Jacobian elliptic functions	none
$K(k) = K$	complete elliptic integral of the first kind	none

NOMENCLATURE (Continued)

Symbol	Quantity	Dimensions (F,L,T)
$K(k')=K'(k)=K'$	associated complete elliptic integral of the first kind	none
K_{AM}	added-mass coefficient	none
L	length of water wave	L
m	integer	none
m	linear momentum of bed particle	FT
M	mass of fluid displaced by bed particle	FT^2L^{-1}
M_s	mass of bed particle	FT^2L^{-1}
n	integer	none
p	fluid pressure at a point	FL^{-2}
$q(k) = q$	Jacobi's nome	none
R	average bearing force between bed particles	F
R_1, R_2	particle-to-particle reaction forces on bed particles	F
$R^* = u^* d/\nu$	Reynolds number based on diameter of bed particle and shear velocity	none
$s = \gamma_s/\gamma$	ratio of specific weight of bed material to specific weight of fluid; specific gravity when bed material is submerged in liquid	none
S	bottom slope of an open channel	none
t	time	T
T	wave period and period of simple-harmonic oscillation	T
u	fluid velocity parallel to bed	LT^{-1}
$u_d = [u]_{y=0.35d}$	fluid velocity 0.35d from theoretical bed	LT^{-1}

NOMENCLATURE (Continued)

Symbol	Quantity	Dimensions (F,L,T)
$u^* = \sqrt{\tau/\rho}$	shear velocity	LT^{-1}
U_m	maximum velocity of oscillating plate and maximum fluid velocity outside boundary layer for simple-harmonic and cnoidal waves	LT^{-1}
v_s	seepage velocity normal to bed or porous wall	LT^{-1}
V	velocity outside boundary layer	LT^{-1}
$\overline{V}$	mean velocity in channel and pipe	LT^{-1}
$\overline{V}_o$	mean velocity at entrance to cylindrical pipe having porous walls	LT^{-1}
V_t	terminal velocity of bed particle	LT^{-1}
$\Delta\forall$	incremental volume of mass of fluid and bed material	L^3
$\Delta\forall_s$	incremental volume of solids (bed material) in mass of fluid and bed material	L^3
$\Delta\forall_v$	incremental volume of voids (fluid) in mass of fluid and bed material	L^3
W	effective weight force of bed particle in fluid	F
x	horizontal coordinate	L
x'	coordinate parallel to bed	L
$X(x)$	functional expression	$L^{1/2}$
y	vertical coordinate	L
y_o	depth of liquid in open channel	L
y_t	wave trough for cnoidal wave	L
y'	coordinate normal to bed	L

NOMENCLATURE (Continued)

Symbol	Quantity	Dimensions
$Y(y)$	functional expression	$L^{1/2}$
α	angle bed makes with horizontal	none
β	angle seepage force makes with bed	none
γ	specific weight of fluid	FL^{-3}
γ_s	specific weight of solids (bed material)	FL^{-3}
δ'	thickness of laminar sublayer	L
η	vertical coordinate describing cnoidal wave shape	L
θ	phase angle	none
κ	coefficient of permeability	LT^{-1}
λ_n	eigenvalue	L^{-1}
μ	dynamic viscosity of fluid	FTL^{-2}
ν	kinematic viscosity of fluid	L^2T^{-1}
ρ	mass density of fluid	FT^2L^{-4}
σ_g	geometric standard deviation of bed particle diameter	none
τ	boundary shear stress	FL^{-2}
Φ	angle of repose	none
$\chi(\ )$	function expression	none
ψ	stream function	L
ω	frequency of simple-harmonic oscillation	T^{-1}

Subscripts Not Defined Above

c	refers to the critical state of incipient motion
s	refers to seepage

NOMENCLATURE (Continued)

Symbol	Quantity	Dimensions
	APPENDIX	
a	amplitude of displacement of water in test section of U-tube	L
A	cross-sectional area of the vertical legs of the U-tube	L^2
A_a, A_c	cross-sectional areas of streamtube	L^2
A_o, A_n	Euler coefficients of Fourier cosine series	L
B_n	Euler coefficients of Fourier sine series	L
c	damping coefficient for U-tube	FTL^{-1}
C_1, C_2	arbitrary constants	L
k	equivalent spring constant	FL^{-1}
ℓ	length of contracted area of streamtube	L
M	effective mass of water in U-tube	FT^2L^{-1}
n	integer	none
p	air pressure on free surface in U-tube	FL^{-2}
p_o	maximum air pressure on free surface in U-tube	FL^{-2}
r_o	radius of lower cylindrical insert in U-tube	L
s	displacement of water in test section of U-tube prior to separation	L
t	time	T
t_s	time elapsed until initiation of separation	T
T	period of oscillation in U-tube	T
u	velocity of water in test section of U-tube	LT^{-1}

NOMENCLATURE (Continued)

Symbol	Quantity	Dimensions
V	velocity of fluid in streamtube	LT^{-1}
x	horizontal coordinate	L
z	displacement of free surface in U-tube	L
$\dot{z}$	velocity of free surface in U-tube	LT^{-1}
$\ddot{z}$	acceleration of free surface in U-tube	LT^{-2}
γ	specific weight of water	FL^{-3}
δ	logarithmic decrement for damping in U-tube	none

SUMMARY

The effect of a permeable bed on incipient sediment motion is investigated by considering the pertinent forces acting on bed particles. A general incipient-motion criterion is formulated in terms of forces

$$\tan \Phi = \frac{\sum F_{\parallel}}{\sum F_{\perp}}$$

in which Φ is the angle of repose of the bed material, $\sum F_{\parallel}$ is the sum of the forces acting parallel to the bed, and $\sum F_{\perp}$ is the sum of the forces acting perpendicular to the bed. The forces finally considered in the analysis are the fluid-resistance force, F, which has components of drag and lift, the seepage force, F_s, which is caused by flow through the bed, and the effective weight force, W, of the bed particles. The magnitudes of the fluid-resistance force and the seepage force are determined from analyses of results of experiments for which only one of these two forces is present.

The magnitude of the fluid-resistance force is determined by analyzing results of the writer and others for the case for which the seepage force is absent. For bed particles immersed in a laminar boundary layer incipient motion is found to occur if

$$\frac{\tau_c}{(\gamma_s - \gamma)\, d \tan \Phi} \gtrsim 0.19$$

in which τ_c is the critical boundary shear stress (viscous shear), γ_s

is the specific weight of the bed material, γ is the specific weight of the fluid, and d is the mean diameter of the bed particle. For bed particles immersed in a turbulent boundary layer, the incipient-motion criteria developed are believed to depend measurably on the intensity of the turbulent fluctuations in the vicinity of the bed. An incipient-motion criterion in terms of a velocity in the vicinity of the bed is developed. The bed velocity is defined as

$$u_d = [u]_{y=0.35d}$$

in which u_d is the fluid velocity outside the laminar sublayer. The theoretical wall ($y = 0$) is found to be located essentially 0.2 d below the plane tangent to the top of the uppermost bed particles. For values of the shear-velocity Reynolds number, $R_c^* \tilde{>} 18$, the incipient-motion parameter

$$\frac{u_{dc}}{\sqrt{(\gamma_s/\gamma - 1)\, gd \tan \Phi}}$$

in which u_{dc} is the critical bed velocity, and g is the acceleration of gravity, is shown to be essentially a constant, which depends upon the level of turbulence intensity. This parameter has the value 1.1 for flows having high turbulence intensities and 1.9 for flows having low turbulence intensities. For oscillatory flow incipient motion occurs if

$$\frac{U_{mc}}{\sqrt{(\gamma_s/\gamma - 1)\, gd \tan \Phi}} \tilde{>} 3.2$$

in which U_{mc} is the critical maximum fluid velocity outside the boundary

layer. Shields' parameter, $\tau_c/(\gamma_s-\gamma)d$, is shown to vary widely for turbulent boundary layers.

The magnitude of the seepage force, F_s, is determined from tests for which the fluid-resistance force is absent. In order to ascertain the magnitude of F_s at the bed experiments were conducted for the effect of seepage on the stability of slopes. For the writer's tests, the seepage velocity was perpendicular and directed either out of or into the bed. The seepage force was determined by analyzing the experimental results in light of the above general incipient-motion criterion. The seepage force, F_s, on the uppermost layer of bed particles is found to be a constant times the seepage force on the bed particles several layers beneath the top layer. This constant is called a flow coefficient, C, and is thought to depend only on the shape and packing of the bed particles. For flow perpendicular to the bed the flow coefficient is independent of the direction of the seepage flow provided that Darcy's Law is satisfied. The value of C is 0.7 for uniform, nearly spherical, glass beads and between 0.9 and 0.95 for uniform, well-rounded, sand. The experimental results come from tests of others as well as the writer. For seepage flow parallel with the bed, $C = 0.97$. In determining the seepage force at the bed for any given seepage flow perpendicular to or parallel with the bed the piezometric-head variation within the bed is required.

An experiment was conducted for which both the fluid-resistance force, F, and the seepage force, F_s, were present. Water was pumped up through a bed (glass beads) over which water was made to oscillate simple harmonically. It was found that the seepage force caused by the

flow out of the bed did not aid incipient motion. The bed particles were observed only to rock back and forth. It is concluded that once a bed particle rocks out of its recess it momentarily loses its seepage force and hence incipient motion is not enhanced.

A survey of the literature on boundary-layer control shows that seepage out of or into a bed can have a considerable effect on the flow characteristics above the bed. Seepage out of a bed may enhance boundary-layer transition whereas seepage into a bed may delay transition. Except for the cases for which transition is enhanced or delayed, seepage causes the boundary shear stress to decrease for flow out of a bed and to increase for flow into the bed. Except for the case for which boundary-layer transition is enhanced, seepage flow out of a bed can only hinder incipient motion inasmuch as the boundary shear stress is reduced and, as concluded above, the seepage force can not aid incipient motion for flow out of a bed. Seepage flow into a bed can either hinder or aid incipient motion, depending upon the relative magnitude of the seepage force and the fluid-resistance force (boundary shear). In considering the effect of seepage on incipient motion the altering of the flow characteristics above the bed by seepage most certainly has to be considered.

The results obtained from the analyses of the magnitude of the fluid-resistance force and the magnitude of the seepage force and from the literature survey concerning the altering of the flow characteristics by seepage, are all considered in an approximate analysis in order to obtain order-of-magnitude effects of seepage on incipient motion. Two practical cases for which the fluid-resistance force and the seepage force are present are then investigated to show what effect seepage has

on incipient motion.

The first physical situation considered is that of seepage in and out of an ocean bed under water waves. The piezometric-head variation within the bed is determined analytically for simple-harmonic and cnoidal waves by solving Laplace's equation for laminar flow through porous media. Some calculations are made to determine order-of-magnitude effects of seepage on incipient motion. For small bed particles, the effect of seepage on incipient motion is essentially negligible. For fairly large bed particles the seepage flow out of the bed under a wave trough can reduce the boundary shear stress more than 20 per cent. This reduction delays incipient motion. For large bed particles under the wave crest the seepage flow into the bed may or may not hinder incipient motion. The overall effect of seepage on incipient motion of bed particles under water waves is probably minor as both the motivating force (boundary shear) and the resisting force (seepage force) depend on the same parameter, the wave amplitude, H.

The second physical case considered is that of seepage into a canal bed. The piezometric-head gradient at the bed is given for a trapezoidal and for an infinitely wide canal. For the condition for which the ground-water table is significantly below the free surface in a canal the seepage force plays a predominant role in inhibiting incipient motion for small bed particles ($d \tilde{<} 0.2$ mm). For bed particles larger than 0.2 mm the effect of seepage on incipient motion becomes less and less. For very large bed particles the seepage flow into the canal bed may even aid incipient motion inasmuch as the boundary shear stress is increased considerably.

CHAPTER I

INTRODUCTION

Description of the Problem

The seepage of water through soil is a problem frequently encountered by engineers. In many such problems it is necessary to investigate the interaction and behavior of the water and soil wherever the water enters or leaves the soil bed. For example, soils engineers might be concerned with the problem of soil rupture due to water flowing out of the bed on the downstream side of a sheet piling. Soils engineers might also be faced with the problem of the effect of seepage on the stability of banks. Oceanographers may desire to know the contribution to water wave damping by seepage of water in and out of a sandy sea bed. In all seepage problems the seepage flow through the porous medium creates hydrodynamic forces on the particulate matter comprising the medium. The central topic of this study is the seepage force acting on the bed particles comprising the uppermost layer of the bed. The uppermost bed particles experience an upward seepage force wherever the fluid flows out of the bed and, conversely, a downward seepage force wherever the fluid flows into the bed. The effect of the seepage force on the initial motion of the uppermost bed particles is considered in this study. The problem to be studied, then, is the role of a permeable bed in incipient motion of bed particles. The instability of the bed as a mass is not considered in this study.

Review of the Literature

The role of the seepage force in promoting or hindering sediment movement has been mentioned by some researchers, but to the writer's knowledge neither analytical nor experimental studies have been performed in which the seepage force was considered as one of the forces influencing incipient motion. Eagleson and Dean (1) comment that a permeable bed may influence incipient motion of bed particles under water waves. Water flows out of the bed under a wave trough and into the bed under a wave crest. Simons (2) observed that extensive erosion occurred in an otherwise stable irrigation canal during a wind storm which generated waves up to two feet in height. He believed that the stability of the canal might have been destroyed by wave-induced flow out of the bed. Posey (3) states that upward flow in the porous bed downstream from a bridge pier enhances sediment movement. Lane (4) mentions that, for seepage flow out of a canal bed containing a wide range of grain sizes, the fine material is transported into the spaces between the larger material and deposited there, forming a more resistant bed because of a concreting action.

Purpose and Scope of the Investigation

The objective of this investigation is to determine quantitatively the effect a permeable bed has on incipient sediment motion. This objective is attained by analyzing the seepage force as well as the other forces which act on bed particles. Criteria for incipient motion are formulated from experimental results. These criteria are applied to two practical cases for which a permeable bed exists; namely (1) incipient motion of bed particles under water waves, and (2) incipient motion of bed particles in an unlined canal.

CHAPTER II

FORCES ON BED PARTICLES

Incipient motion of bed particles is obviously the consequence of forces acting upon the particles. The hydrodynamic forces acting upon a single particle on the bed at a given instant are dependent upon the fluid motion in the vicinity of the particle. The complexity of formulating a meaningful force analysis is apparent when one considers that a particle on the bed may be submerged in either a laminar or turbulent boundary layer and that bed particles are neither uniform in size nor shape. Nevertheless, force analyses which are perforce simplified are invaluable in devising organized experimental programs.

The forces which may act on any single stationary particle on the bed are shown in Figure 1, in which α is the angle that the bed makes with the horizontal. These forces are constituted as follows:

(a) Effective weight force, W, is the weight of the particle minus the buoyant force

$$W = g(M_s - M) \tag{1}$$

in which g is the acceleration of gravity, M_s is the mass of the bed particle and M is the mass of the displaced fluid.

(b) Particle-to-particle reaction forces, R_1 and R_2, are the forces of adjacent bed particles on the particle in question. These forces constitute the normal and tangential forces at points of contact of adjacent bed particles.

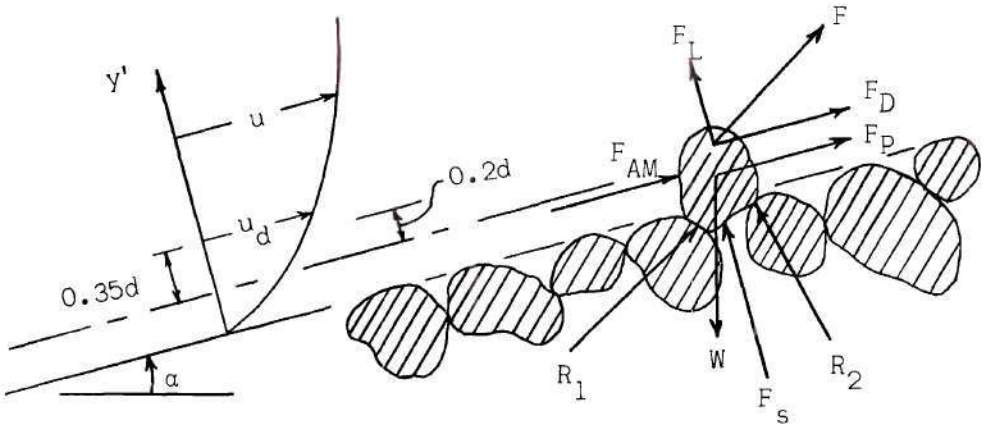

Figure 1. Sketch of Forces Acting upon a Bed Particle.

(c) Pressure force, F_P, is the pressure force on the particle resulting from the pressure gradient in an accelerating fluid

$$F_P = M\, du/dt \qquad (2)$$

in which u is the fluid velocity above the bed.

(d) The added-mass pressure force, F_{AM}, is the pressure force on the particle resulting from the additional fluid acceleration required to move the fluid past the particle

$$F_{AM} = K_{AM}\, M\, du/dt \qquad (3)$$

in which K_{AM} is the added-mass coefficient. The value of K_{AM} varies with the flow pattern around the particle, being one-half for irrotational flow past a spherical particle in a fluid of infinite expanse.

(e) The fluid-resistance force, F, due solely to the velocity, u, parallel to the bed, is usually resolved into a lift force, F_L,

normal to the bed and a drag force, F_D, parallel to the bed

$$F_L = C_L A \rho \frac{u|u|}{2} \tag{4}$$

and

$$F_D = C_D A \rho \frac{u|u|}{2} \tag{5}$$

in which C_L is the coefficient of lift, C_D is the coefficient of drag, A is the projected area of the particle in a plane normal to the direction of the flow, and ρ is the mass density of the fluid.

(e) The seepage force, F_s, is caused by flow out of or into the bed. It is associated with the pressure gradient across a bed particle. The magnitude of the seepage force will be investigated in Chapter IV.

The seepage force is the main topic of this study. In the following, a general criterion for incipient motion will be formulated.

Incipient-Motion Criterion

The stability of a mass of bed particles submerged in a quiescent fluid is used as the basis for the criterion for incipient motion. The resistance of bed particles to motion can be readily determined by observation of the angle the bed makes with the horizontal at the threshold of instability. This angle is usually called the angle of repose, Φ, and can be measured several ways; for example, either by pouring a pile of bed material and measuring the final slope or by tilting a plane bed until failure occurs and measuring the angle of the bed at failure. It is well known that the angle of repose is not a physical constant of the

bed material; it depends upon the density of packing within the bed, the stress level within the bed, geometrical conditions and the method of formation of a slope. Nevertheless, for a given bed at the threshold of instability the force of gravity down the face of the bed is just counterbalanced by the resisting particle-to-particle reactions of adjacent particles. By definition the angle of repose

$$\tan \Phi = \frac{g(M_s - M) \sin \Phi}{g(M_s - M) \cos \Phi}$$

in which $g(M_s - M) \sin \Phi$ is the component of the gravity force parallel to the bed and $g(M_s - M) \cos \Phi$ is the component of the gravity force perpendicular to the bed. For incipient motion for which the fluid is in motion, causing other forces to exist, the angle of repose may be expressed

$$\tan \Phi = \frac{\sum F_{\parallel}}{\sum F_{\perp}}$$

in which $\sum F_{\parallel}$ is the summation of all the external forces (excluding reaction forces) acting parallel to the bed and $\sum F_{\perp}$ is the summation of all the external forces acting perpendicular to the bed. At incipient motion the angle Φ is the angle between the plane normal to the bed and the plane describing the line of action of the reaction force, R_2 (Figure 1). The other reaction force depicted in Figure 1, R_1, approaches zero by virtue of the definition of incipient motion.

If the magnitude and direction of the various forces which act on bed particles are known, incipient motion can be easily predicted. Unfortunately the magnitude and direction of fluid-induced forces are quite

difficult to determine. In Chapter III the fluid-resistance force, F, will be considered; in Chapter IV the seepage force, F_s, will be considered. The forces resulting from unsteady nature of flows, namely F_{AM} and F_p, are not considered to be significant in this study.

CHAPTER III

INCIPIENT MOTION WITHOUT A PERMEABLE BED EFFECT

The magnitude of the fluid-resistance force, F, will now be investigated by analyzing incipient-motion results for which the seepage force, F_s, is absent. The two main forces which are present in this analysis are the effective weight force, W, and the fluid-resistance force, F. For the results to be analyzed here, the boundary layer in which the bed particles are immersed is either laminar or turbulent. Both unidirectional and oscillatory flows are considered. An incipient-motion criterion based on a critical bottom velocity is introduced as well as Shields' incipient-motion criterion based on a critical tractive force. All analyses are conducted for test results for which cohesionless, uniform sand grains (or artificial beads) comprise a homogeneous bed.

Incipient-Motion Criteria

For flow up a plane bed which is lying at an angle α with the horizontal the incipient-motion criterion, Equation (6) can be expressed

$$\tan \Phi = \frac{F_D - W \sin \alpha}{W \cos \alpha - F_L} \tag{7}$$

Inasmuch as the bed particles are immersed in a nonuniform flow field and the flow may be either laminar or turbulent the magnitudes of the two components, F_D and F_L, of the total resistance force are not easily ascertained. The fluid-resistance force on any bed particle is comprised

of both viscous resistance and form resistance. The former is caused by fluid deformation and the latter is caused by a pressure variation over the surface of the particles. For bed particles immersed in a laminar boundary layer or laminar sublayer the viscous resistance force predominates. For bed particles projecting through the laminar sublayer the force due to form resistance predominates.

Laminar Boundary Layer

For a laminar boundary layer the lift force, F_L, which depends on the pressure variation over the surface of the bed particle, can be expected to be negligible. The drag force, F_D, depends mainly on the boundary shear force. With the lift force being neglected Equation (6) becomes

$$\tan \Phi = \frac{\tau_c A - g(M_s - M) \sin \alpha}{g(M_s - M) \cos \alpha}$$

in which τ_c is the critical boundary shear stress and A is the projected area of the particle in a plane parallel to the direction of flow. Since the projected area A is proportional to the diameter, d, of the bed particles squared and M and M_s are proportional to the diameter of the particles cubed

$$\tau_c \propto (\gamma_s - \gamma)(\tan \Phi \cos \alpha + \sin \alpha)$$

in which γ_s is the specific weight of the bed material and γ is the specific weight of the fluid. The above relationship may be expressed

$$\frac{\tau_c}{(\gamma_s - \gamma)\, d(\tan \Phi \cos \alpha + \sin \alpha)} = \text{constant} \qquad (8)$$

The magnitude of the constant has to be determined experimentally.

Turbulent Boundary Layer

For bed particles immersed in a turbulent boundary layer the fluid-resistance force is due mainly to the pressure variation over the surface of the bed particles. The lift force can no longer be considered negligible. The condition for incipient motion, Equation (7),is, upon using Equations (1), (4), and (5)

$$\tan \Phi = \frac{C_D A \frac{\rho u^2}{2} - g(M_s - M) \sin \alpha}{g(M_s - M) \cos \alpha - C_L A \frac{\rho u^2}{2}}$$

in which u in this case is a velocity in the vicinity of the bed, and A is the projected area of the bed particle in a plane normal to the direction of the flow. Since A is proportional to d^2 and M_s and M are proportional to ρd^3 the above expression can be reduced to

$$(C_D + C_L \tan \Phi) \frac{\rho u^2}{2} \propto (\gamma_s - \gamma) d(\tan \Phi \cos \alpha + \sin \alpha)$$

The fluid-resistance coefficients, C_D and C_L, depend upon the flow pattern around the particle and upon a Reynolds number. The combination of these two are fairly well represented by a function depending on R^*, the shear velocity Reynolds number

$$R^* = \frac{\rho u^* d}{\mu} = \frac{u^* d}{\nu}$$

in which the shear velocity $u^* = \sqrt{\tau/\rho}$, in which τ is the boundary shear stress. The above proportionality can be approximated by

$$\frac{u_{dc}}{\sqrt{(s-1)\, gd\, [\tan \Phi \cos \alpha + \sin \alpha]}} = f(R_c^*) \qquad (9)$$

in which u_{dc} is the velocity above the top layer of bed particles, $s = \gamma_s/\gamma$, and R_c^* is based on the critical boundary shear stress, τ_c. Inasmuch as the velocity in the vicinity of the particles is related to the shear velocity, u^*, the above relationships can also be expressed as

$$\frac{\tau_c}{(\gamma_s - \gamma)d\, [\tan \Phi \cos \alpha + \sin \alpha]} = f'(R_c^*) \qquad (10)$$

If the bed is horizontal ($\alpha = 0$) and if $\tan \Phi$ is disregarded, Equation (10) is recognized as the parameter introduced by Shields (5). Shields' parameter is

$$\frac{\tau_c}{(\gamma_s - \gamma)d} = f''(R_c^*) \qquad (11)$$

in which τ_c is the critical tractive force per unit area on the bed. The critical tractive force is transmitted to the individual bed particles by means of pressure variation and viscous shear variation over the surface of the particles. For a turbulent boundary layer the pressure variation constitutes most of the tractive force.

The two criteria for incipient motion, Equations (9) and (10), should be of equal suitability in predicting conditions for initial motion. Only in application (design of a stable bed) would one criterion be preferred to the other. For example in the design of a stable canal bed in uniform flow Equation (10) would be preferred since the tractive force on the bed can be determined from mechanics; whereas, for the design against

localized scour, which usually occurs in a nonuniform flow zone, Equation (9) would be preferred.

In the following, incipient-motion results obtained by various investigators are analyzed for laminar and for turbulent boundary layers. The analyses are performed such that the LHS of Equations (8), (9), (10), and (11) can be evaluated.

Incipient-Motion Results for a Laminar Boundary Layer

For fluid motion in a known laminar boundary layer the boundary shear stress can be determined from

$$\tau = \mu \left[\frac{\partial u}{\partial y'} \right]_{y'=0} \tag{12}$$

in which u is the fluid velocity at a distance y' from the boundary. Experimental results for incipient motion are available for three different laminar flows for which the velocity distribution, u, is known from solutions to the Navier-Stokes equations.

Laminar Flow in an Open Channel

White (6) investigated incipient motion of sand grains immersed in laminar flow in an open channel. The channel had a slope of 1 in 28. For such a mild slope only a slight error is introduced by assuming $\alpha = 0$. The velocity distribution in terms of y, the vertical coordinate, is

$$u = 3\bar{V} \left[\frac{y}{y_o} - \frac{1}{2} \left(\frac{y}{y_o} \right)^2 \right]$$

in which $\bar{V}$ is the average velocity in the channel and y_o is the depth of the liquid in the channel. The LHS of Equation (8) becomes

$3\mu\bar{V}/(\gamma_s - \gamma)dy_o \tan \Phi$. Because of the difficulty in measuring the small depth of flow, y_o, White found τ_c by measuring the flow rate and using $\tau = \gamma y_o S$, in which S is the slope of the free surface. White's results are tabulated below. The angle of repose for the Aylesford sand appears to be abnormally large.

Material	d(mm)	Angle of Repose (Φ)	Value of LHS of Equation (8)	R_c^*
Aylesford Sand	0.21	54°	0.194	0.04
Leighton Buzzard Sand	0.90	46°	0.162	0.30

Laminar Boundary Layer in a Converging Flow

White also conducted incipient-motion tests for a converging laminar boundary layer by designing a constant-drag nozzle. The design of the nozzle cross section was based on the laminar boundary-layer equations. By measuring the pressure variation on the boundary of the nozzle he was able to solve for the boundary shear stress. White's results are

Material	d(mm)	Angle of Repose (Φ)	Value of LHS of Equation (8)	R_c^*
Sand	0.122	45°	0.204	2.1

White's results for bed particles completely immersed in a laminar boundary layer do not substantiate Shields'[1] proposition that the critical boundary shear varies inversely with the shear velocity Reynolds number. The LHS of Equation (8) appears to be a constant for $R_c^* < 2.1$.

---

[1]Shields (5) concluded that, for $R_c^* \gtrsim 1.8$, $\tau_c/(\gamma_s - \gamma)d = 0.1/R_c^*$. He did not confirm this conclusion by experiment.

Laminar Boundary Layer in Oscillatory Flow

Incipient-motion results for bed particles in a laminar boundary layer which is undergoing simple-harmonic motion have been collected by Manohar (7) and by the writer. Manohar obtained incipient-motion results for sand and artificial materials by oscillating a bed under an otherwise quiescent tank of water. The writer investigated incipient motion of sand and of artificial material which rested in the test section of a large U-tube. The velocity distributions relative to the bed for the two cases of simple-harmonic motion are identical and hence the boundary shear stresses will be equal. In the case of the U-tube the velocity distribution for fluid oscillating simple harmonically above a plane boundary can be resolved from a solution presented by Schlichting (8)

$$u = a\omega \left[\sin \omega t - \exp\left(-\sqrt{\omega/2\nu}\, y\right) \sin\left(\omega t - \sqrt{\omega/2\nu}\, y\right)\right] \quad (13)$$

in which a is the amplitude of oscillation, and ω is the angular velocity of oscillation. Upon using Equation (12) the maximum value of the LHS of Equation (8) becomes $a\sqrt{\mu}\,\sqrt{\rho}\,\omega^{3/2}/(\gamma_s - \gamma)d \tan \Phi$. From experimental data corresponding to the condition of incipient motion the LHS of Equation (8) can be evaluated. The forces due to the unsteady nature of the flow, F_{AM} and F_P, are neglected.

The U-tube described in the Appendix was the facility used by the writer to study incipient motion. The flow within the test section of the U-tube is simple harmonic. The velocity within the test section, outside the boundary layer, is

$$u = \frac{2a\pi}{T} \sin\left[\frac{2\pi t}{T}\right]$$

in which 2a is the total amplitude of displacement of the water, and T is the resonant period of oscillation of the U-tube. The total amplitude, 2a, can be varied from 0 to 40 in, whereas T varies from 3.59 to 3.73 sec. For laminar flow the velocity distribution within the boundary layer is given by Equation (13). The test section is 1 ft (vertical) by 4 ft (horizontal) in cross section and 10 ft long. The central portion of the test-section floor is depressed in order to form a container for the sediment. The depressed area for the sediment is 6 ft long by 4 ft wide by 4 in deep. Artificial glass beads and natural Ottawa sand were used as the bed materials. The glass beads are quite uniform in size and nearly spherical in shape. The Ottawa sand is also uniform in size but well-rounded in shape. From sieve analysis the mean diameter as well as the standard deviation from the mean of the materials was obtained. The natural angle of repose of the materials under water was determined by pouring a pile and then measuring its final slope. These physical characteristics, as well as the specific gravity, of the bed materials are tabulated below.

Physical Characteristics of Bed Materials

Material	d(mm)	Geometric Standard Deviation (σ_g)	Specific Gravity (s)	Angle of Repose (Φ)
Glass Beads	0.297	1.06	2.47	24°
Ottawa Sand	0.585	1.16	2.62	32.5°

The bed was screeded with a 2- by 2-in board in order to render it plane. The total amplitude of oscillation, 2a, was increased in steps until sediment particles began to oscillate. Whenever a large number of particles oscillated as much as a distance of several grain diameters, incipient motion was said to exist. The amplitude and period of oscillation as well

as the water temperature were then recorded. For incipient motion:

Material	2a (in)	T (sec)	Temperature (°F)
Glass Beads	11.0	3.56	54
Ottawa Sand	13.1	3.58	68

Dye was injected into the boundary layer by means of a tube and hypodermic needle which projected through the floor of the test section and into the sand. The tip of the needle was only several grain diameters below the top of the sand bed. The breakdown of the dye in the boundary layer was observed as the amplitude of oscillation was increased. Incipient motion for the glass beads occurred just prior to transition of the boundary layer whereas for the sand it occurred for a turbulent boundary layer. The value of

$$\frac{\tau_c}{(\gamma_s-\gamma)\ d\ \tan\Phi} = \frac{a\sqrt{\mu}\sqrt{\rho}\ \ \omega^{3/2}}{(\gamma_s-\gamma)\ d\ \tan\Phi}$$

at incipient motion of the glass beads is 0.191. The value of $\tau_c/(\gamma_s-\gamma)d \tan\Phi$ could not be determined for the sand inasmuch as no theoretical equation corresponding to Equation (13) exists for oscillating flow with a turbulent boundary layer. The writer was able to run only two incipient-motion tests for the two bed materials available since the frequency of oscillation of the U-tube is essentially constant. Manohar, however, was able to run many incipient-motion tests as he could vary both amplitude, a, and frequency, ω, of oscillation.

The results of Manohar's incipient-motion tests are listed in Table 1. The values of the parameter $\tau_c/(\gamma_s-\gamma)d$ rather than the LHS of Equation (8) are listed inasmuch as Manohar did not experimentally determine

Table 1. Incipient-Motion Results for an Oscillatory Laminar Boundary Layer (Manohar's Data)

a (in)	ω(rad/sec)	$\tau_c/(\gamma_s-\gamma)d$
Glass Beads: d = 0.235 mm, Specific gravity = 2.49, Temperature = 70° F		
24.0	0.433	0.0501
23.0	0.511	0.0615
22.0	0.556	0.0670
21.0	0.546	0.0622
20.0	0.556	0.0607
19.0	0.583	0.0620
18.0	0.641	0.0677
17.0	0.698	0.0728
16.0	0.690	0.0673
15.0	0.740	0.0700
14.0	0.739	0.0651
13.0	0.785	0.0664
12.0	0.821	0.0654
11.0	0.923	0.0652
10.0	0.996	0.0729
9.0	1.020	0.0680
8.0	1.200	0.0772
7.0	1.255	0.0722
6.0	1.415	0.0740
5.0	1.543	0.0703
4.0	1.714	0.0658
	Average =	0.0680
Sand: d = 0.280 mm, Specific gravity = 2.65, Temperature = 74° F		
24.0	0.571	0.0560
23.0	0.588	0.0561
22.0	0.610	0.0566
21.0	0.655	0.0602
20.0	0.667	0.0589
19.0	0.678	0.0573
18.0	0.721	0.0596
17.0	0.757	0.0605
16.0	0.743	0.0555
15.0	0.825	0.0606

(Continued)

Table 1. Incipient-Motion Results for an Oscillatory Laminar Boundary Layer (Manohar's Data) (Continued)

a (in)	ω(rad/sec)	$\tau_c/(\gamma_s-\gamma)d$
14.0	0.860	0.0603
13.0	0.905	0.0606
12.0	0.926	0.0578
11.0	1.042	0.0630
10.0	1.105	0.0628
9.0	1.270	0.0695
8.0	1.330	0.0666
7.0	1.420	0.0641
		Average = 0.0603

the angle of repose, Φ. It is apparent that $\tau_c/(\gamma_s-\gamma)d$ is essentially constant for each bed material. There is only a minor variation of this parameter with the frequency of oscillation, indicating that the inertia forces due to the unsteady nature of the flow are not significant. Manohar assumed that the angle of repose for both his 0.235 mm glass beads and 0.280 mm sand was 45° in water. The writer feels that 45° is too high for the angle of repose of small, uniform grains. The writer has measured the angle of repose of 0.220 mm and 0.297 mm glass beads to be 22° and 24°, respectively. An approximation for Φ for Manohar's glass beads would be an interpolation between the results of the writer, from which $\Phi = 22.4°$. For $\Phi = 22.4°$ the LHS of Equation (8) is 0.165 for Manohar's glass beads. The value of Φ for Manohar's sand would likely be greater due to more angularity. Based on information available to the writer, Manohar's sand most likely varies between 25° and 30°. If $\Phi = 25°$, the LHS of Equation (8) is 0.130.

Summary

Incipient-motion results for three entirely different laminar

boundary layers have been analyzed. The results are summarized below.

Type of Laminar Flow	Investigator	d(mm)	Φ	$\frac{\tau_c}{(\gamma_s-\gamma)d \tan \Phi}$
Open channel	White	0.21	54°	0.194
Open channel	White	0.90	46°	0.162
Converging nozzle	White	0.122	45°	0.204
Oscillatory (U-tube)	Martin	0.297	24°	0.191
Oscillatory (Oscillating plate)	Manohar	0.235	22.4° (Assumed)	0.165
Oscillatory (Oscillating plate)	Manohar	0.280	25° (Assumed)	0.130

Except for Manohar's 0.280 mm sand the parameter $\tau_c/(\gamma_s-\gamma)d \tan \Phi$ appears to have a constant value in the neighborhood of 0.16 to 0.20. The reason for the large discrepancy between the value of the parameter for Manohar's sand and the other values is not apparent. As shown in Table 1 the parameter $\tau_c/(\gamma_s-\gamma)d$ for Manohar's sand is essentially constant over a wide range of frequencies, precluding the possibility of any large experimental error. The assumed angle of repose may be in error but, in the writer's opinion, only on the low side.

In any event it is concluded that for a laminar boundary layer the LHS of Equation (8) is a constant. If an average value is taken of all the above results except Manohar's, Equation (8) may be expressed

$$\frac{\tau_c}{(\gamma_s-\gamma)\, d\, [\tan \Phi \cos + \sin \alpha]} = 0.19$$

or

$$\frac{\mu \left[\frac{\partial u}{\partial y'} \right]_{y'=0}}{(\gamma_s - \gamma)\, d \left[\tan \Phi \cos \alpha + \sin \alpha \right]} = 0.19 \qquad (14)$$

For any given velocity distribution in laminar flow the conditions for incipient motion for a given bed can be predicted by Equation (14) as long as cohesive forces between grains are absent.

Incipient-Motion Results for a Turbulent Boundary Layer

For bed particles immersed in a turbulent boundary layer the viscous force becomes insignificant and the pressure force becomes dominant. For hydraulically smooth boundaries for which there is a small degree of turbulence and a laminar sublayer exists, Equation (14) is applicable. According to Schlichting (9) a boundary consisting of uniform sand grains is considered smooth if $R^* \lesssim 5$, transitional if $5 \lesssim R^* \lesssim 70$, and rough if $R^* \gtrsim 70$. For sand grains comprising a transitional boundary the predominant force may be composed of viscous shear stresses for R^* near 5 and normal stresses (pressure) for R^* near 70. For a rough boundary the dominant force is pressure. The parameters $f(R_c^*)$ and $f'(R_c^*)$ will be delineated from experimental results on both transitional and rough boundaries.

In evaluating the relationship $f(R_c^*)$ the question arises as to the appropriate velocity u_d to be used in the analysis. Einstein and El-Samni (10) determined a lift coefficient for particles immersed in a hydraulically rough boundary-layer flow in terms of a difference in pressure between the top of the particles and the space between the particles

$$\Delta p = C_L \frac{\rho u^2}{2}$$

Their experiments were conducted by using 69 mm diameter hemispheres placed in a hexagonal pattern on the bottom of a flume and by also using 61 mm mean diameter gravel placed 6-8 inches thick on a flume. The hemispheres were uniform in size but the gravel had a considerable spread in size. They found that, for the hemispheres, the lift coefficient had a constant value of 0.178 if the velocity u was measured 0.35 d from the theoretical wall which was determined to be 0.20 d below a plane tangent to the top of the spheres. The theoretical wall was determined as being the origin of the logarithmic velocity distribution. Other origins failed to produce a logarithmic profile in the vicinity of the wall. For the gravel the same value of the lift coefficient and the same reference plane for the velocity u were found provided the sieve size used was the grain size of which 35 percent of the mixture by weight was smaller. Iwagaki and Tsuchiya (11) measured the velocity profile above stream beds comprised of sand grains having mean diameters of 0.223 mm and 1.435 mm. For each boundary a logarithmic velocity profile was obtained outside the laminar sublayer if the theoretical wall was located 0.25 d below the plane tangent to the top layer of particles. The two flow rates used were at incipient motion of the sand grains. The value of R_c^* was 2.4 and 35 for the 0.223 mm and 1.435 mm diameter particles, respectively. The smaller grain size material produced a hydraulically smooth boundary whereas the larger grain size produced a boundary which was in the transitional zone, $5 < R^* < 70$. But in both cases the theoretical wall for the logarithmic velocity profiles coincided. For turbulent oscillatory flow over a bed Kalkanis (12) found the theoretical wall to be 0.2d below the plane tangent to the top of the bed. He found this to be true for nearly uniform particles having

sizes of 1.68 mm, 2.18 mm, and 2.82 mm.

The theoretical wall for turbulent velocity profiles appears to be approximately 0.2d below the top of beds comprised of uniform grains. If Einstein's and El-Samni's findings for a constant C_L are utilized the velocity u_d to be used in incipient motion calculations should be

$$u_d = [u]_{y = 0.35d} \tag{15}$$

with the origin for y being 0.2d below the plane tangent to the top layer of particles, as shown in Figure 1.

The accepted equations for velocity distributions for turbulent flow will be used to evaluate u_d from incipient-motion results. The generalized velocity distribution for turbulent flow is, from Nikuradse (13)

$$\frac{u}{u^*} - 5.75 \log_{10} \frac{y}{d} = \chi(R^*) \tag{16}$$

in which χ is a parameter which depends on the ratio of the thickness of the laminar sublayer to the diameter of the sand grains. For a hydraulically smooth boundary, for which $R^* \lesssim 5$

$$\chi(R^*) = 5.5 + 5.75 \log_{10} R^*$$

and

$$\frac{u}{u^*} = 5.5 + 5.75 \log_{10} \frac{u^* y}{\nu} \tag{17}$$

For a transitional boundary, for which $5 \lesssim R^* \lesssim 70$, $\chi(R^*)$ has not been expressed mathematically, to the writer's knowledge; but Nikuradse has

delineated $X(R^*)$ graphically from experimental results. For a hydraulically rough boundary, for which $R^* \gtrsim 70$, $X(R^*) = 8.5$ and

$$\frac{u}{u^*} = 8.5 + 5.75 \log_{10} \frac{y}{d} \qquad (18)$$

For smooth boundaries and for some transitional boundaries the velocity at $y = 0.35\ d$ occurs within the laminar sublayer. Inasmuch as $f(R_c^*)$ is sought for turbulent flows u_d will be computed only for those flows for which the laminar sublayer thickness $\delta' < 0.35d$. The thickness of the laminar sublayer for smooth boundaries is given by Rouse (14) to be

$$\delta' = \frac{11.6\nu}{u^*}$$

For transitional and rough boundaries, however, the actual laminar sublayer decreases as the roughness and R^* increase. The variation of $u^*\delta'/\nu$ with R^* has been determined by Rotta (15). Using Rotta's results the actual laminar sublayer thickness at $R^* = 18$ is 0.35d. For $R^* \lesssim 18$ the velocity u_d, as defined, will be within the laminar sublayer provided the theoretical wall is the same for both the laminar and turbulent velocity profiles. The characteristic velocity for smooth and transitional boundaries which provides meaningful results on fluid-resistance may not be at $y = 0.35d$. Inasmuch as neither the theoretical wall describing the velocity distribution within the laminar sublayer nor the appropriate characteristic velocity is known the parameter $f(R_c^*)$ will be delineated only for $R_c^* > 18$.

For $18 < R_c^* < 70$

$$\frac{u_{dc}}{u_c^*} = -2.6 + X(R_c^*) \tag{19}$$

and for $R_c^* > 70$

$$\frac{u_{dc}}{u_c^*} = 5.9 \tag{20}$$

Using these relationships incipient-motion data from several investigators are analyzed.

Unidirectional Converging Flow

White (6) also determined the conditions for incipient motion of bed particles placed in converging flow of both air and water. For these low viscosity fluids and a converging flow the boundary layer is quite thin. He measured both the critical velocity outside the boundary layer and the critical tractive force for incipient motion. From White's measured values of $f'(R_c^*)$ the values of $f(R_c^*)$ can be computed from Equations (9), (19), and (20). For $18 < R_c^* < 70$

$$f(R_c^*) = [X(R_c^*) - 2.6] \sqrt{f'(R_c^*)} \tag{21}$$

and, for $R_c^* > 70$

$$f(R_c^*) = 5.9 \sqrt{f'(R_c^*)} \tag{22}$$

The results of this analysis and White's experimental results are given in Table 2, in which V is the velocity outside the boundary layer. The incipient-motion parameter, $f(R_c^*)$, based on the bed velocity will be taken to be a constant 1.95 for $33 \lesssim R_c^* \lesssim 1280$. Also the parameter

$f'(R_c^*)$ based on the critical tractive force is essentially a constant, having a value of 0.11. Both of these incipient-motion parameters should remain constant for values of $R_c^* > 1280$ provided there is no radical change in the wake between grains and the turbulence intensity remains essentially the same.

Table 2. Incipient-Motion Results for Unidirectional Flow (White's Data)

Bed Material	d(mm)	Fluid	γ_s/γ	α	Φ	V (ft/sec)	R_c^*	$f'(R_c^*)$	$f(R_c^*)$
Sand	0.90	Water	2.6	0°	45°	1.25	33	0.119	2.1
Steel Shot	0.71	Water	7.9	0°	34.4°	2.03	35	0.094	1.9
Sand	0.90	Air	2100	0°	45°	37.5	80	0.098	1.9
Sand	5.6	Water	2.6	-24.2°	45°	1.84	360	0.114	2.0
Sand	5.6	Water	2.6	0°	45°	2.46	480	0.101	1.9
Sand	5.6	Water	2.6	26.2°	45°	2.98	590	0.113	2.0
Sand	5.6	Air	2100	0°	45°	88.4	1280	0.102	1.9

Open-Channel Flow

There are data available for turbulent boundary layers which are developed, or partially developed, in contrast with White's study for thin, undeveloped boundary layers. As reported by Mavis, Ho, and Tu (16), Ho and Tu conducted incipient-motion tests in a flume, using water as the fluid and sixteen different sizes of bed material. Ho conducted the first series of tests and, subsequently, Tu repeated Ho's tests. They measured the velocity profile above the bed at the condition of incipient motion.

Upon using their measured values of the fluid velocity at 0.025 ft and at 0.05 ft above the top of the bed, and assuming that the kinematic viscosity of the water was $(10^{-5})ft^2/sec$, the velocities u_c^* and u_{dc} were computed by the writer from Equations (15) and (16). Inasmuch as the angles of repose of the bed material are not reported the LHS of Equation (9) can not be determined. However if the angle of repose is disregarded, and since the bed in their experiments was horizontal, the LHS of Equation (9) reduces to $u_{dc} / \sqrt{(s-1)\ gd}$.

The LHS of Equation (10) reduces to Shields' parameter, Equation (11). The results for both parameters are tabulated in Table 3. The velocity results reported by Mavis et al. are the arithmetic mean of eight to ten observations on the sand and crushed stone and four observations on the Haydite. The values of u_{dc} listed in Table 3 are the average of those computed from measure velocities at 0.025 ft and 0.050 ft from the bed. Upon comparing the results of Mavis et al. with the results of White for $33 < R_c^* < 360$ a wide discrepancy is apparent. White's results for the incipient-motion criterion based on velocity are such that the parameter $u_{dc} / \sqrt{(s-1)\ gd}$ is twice that for the results of Mavis et al. In order to have equal values of the parameter $f(R_c^*)$ for the two series of tests the angle of repose for the bed materials of Mavis et al. would have to be 14°. This computed value is evidently entirely too small for bed material greater than 1.0 mm in size. If the angle of repose for their bed materials for which incipient motion occurred in the range of $32 < R_c^* < 320$ were assumed to be 35°, a suitable value, the value of $f(R_c^*)$ is approximately 1.1. The corresponding

Table 3. Incipient-Motion Results for Open-Channel Flow (From Mavis et al.)

Bed Material	d(mm)	s	u_{dc} (ft/sec)	$\frac{u_{dc}}{\sqrt{(s-1)\,gd}}$	$\frac{\tau_c}{(\gamma_s-\gamma)\,d}$	R_c^*
Sand	0.35	2.64	--	--	0.015	3
Haydite	0.5	1.83	--	--	0.015	4
Sand	0.5	2.64	--	--	0.014	6
Haydite	0.7	1.83	--	--	0.014	7
Sand	0.7	2.64	--	--	0.014	9
Haydite	1.0	1.83	--	--	0.016	12
Sand	1.0	2.64	0.35	0.9	0.016	18
Haydite	1.4	1.83	0.30	0.9	0.017	21
Sand	1.4	2.64	0.42	0.9	0.019	31
Haydite	2.0	1.83	0.36	0.9	0.018	37
Sand	2.0	2.64	0.51	0.9	0.021	57
Sand	2.8	2.64	0.64	0.9	0.022	97
Sand	4.0	2.64	0.77	0.9	0.024	170
Crushed Limestone	4.0	2.60	0.79	1.0	0.026	175
Sand	5.7	2.64	0.98	1.0	0.028	310
Crushed Limestone	5.7	2.60	1.00	1.0	0.029	320

value of $f'(R_c^*)$ would be 0.033, or approximately one-third of the same parameter for White's tests. There is obviously a difference in

what various observers call incipient motion. The writer does not believe that there could be enough difference in judgement between the investigators Mavis et al. and the investigator White to constitute the discrepancy shown in the results. Ho and Tu performed identical experiments independently of one another and achieved tolerable agreement. The writer believes that the flows of White and Mavis et al. were different to the extent that the same bottom velocity u_{dc} for the different experiments produced different fluid-resistance forces. White realized that his incipient-motion parameter was much greater than the ones determined by Shields and others. White explained the difference as being that, for developed flows (or essentially developed) as occur in streams and in long flumes, the turbulence level is greater than for undeveloped flows like his converging flow. Large instantaneous fluctuations in the bed velocity constitute large instantaneous forces. Highly turbulent flows could move the same bed particles with smaller values of u_d than turbulent flows with lesser intensities of turbulence. It is believed that the intensity of turbulence is at least one factor resulting in the disagreement between the results of Mavis et al. and those of White.

Also reported by Mavis et al. are the results of Schaffernak. Schaffernak conducted incipient-motion tests on various grades of material in a channel 100 cm wide. The results to be reported here are for uniform, rounded grains. Mavis et al. reports values of a bottom velocity determined by Schaffernak at incipient-motion conditions. If these values of Schaffernak's so-called bottom velocity are equated to u_{dc} the parameter $u_{dc}/\sqrt{(s-1)\,gd}$ can be computed. There are no values of the angle of repose, Φ, reported. The results of Schaffernak's incipient-motion

tests are listed in Table 4 with the assumption that the kinematic viscosity of the water was $(10^{-5})ft^2/sec$. The specific gravity of the bed material was 2.7. Values of Shields' parameter are computed from Equations (11) and (22).

Table 4. Incipient-Motion Results for Open-Channel Flow (Schaffernak's Data)

Bed Material	d(mm)	u_{dc} (ft/sec)	$\frac{u_{dc}}{\sqrt{(s-1)\ gd}}$	$\frac{\tau_c}{(\gamma_s-\gamma)\ d}$	R_c^*
Gravel	5.0	0.90	1.0	0.026	260
Gravel	12.3	1.32	0.9	0.023	910
Gravel	16.2	1.94	1.1	0.037	1750
Gravel	25.0	2.3	1.1	0.034	2970
Gravel	30.0	2.4	1.0	0.031	4010
Gravel	50.0	3.15	1.0	0.032	8800
Gravel	70.0	3.3	0.9	0.025	12900

The values of $u_{dc}/\sqrt{(s-1)\ gd}$ for Schaffernak are in good agreement with those of Mavis et al. This is not surprising as all of the investigations were conducted in essentially developed turbulent flows. The parameter $u_{dc}/\sqrt{(s-1)\ gd}$ can be assumed to have a constant value of approximately 1.0 for these data when $18 < R_c^* < 12900$. The parameter $f(R_c^*)$ is not known for these data since the angle of repose was not reported. If Φ is assumed to have an average value of 40°, $f(R_c^*) \cong 1.1$.

Oscillatory Flow

For unsteady turbulent boundary layers there is meager information,

if any, available for the boundary shear stress on rough boundaries. Hence the parameter $f'(R_c^*)$ becomes unsuitable for unsteady turbulent boundary layers. On the other hand, there are data available for velocity distributions within and above unsteady turbulent boundary layers occurring above rough boundaries. The suitable parameter for incipient motion of bed particles in an unsteady turbulent flow is Equation (9), $f(R_c^*)$, even though R_c^* cannot be determined. The LHS of Equation (9) can be determined from experimental results. The velocity distribution in an oscillatory turbulent boundary layer can be represented by the results from Kalkanis (12). For a fluid oscillating simple harmonically above a bed the velocity within the turbulent boundary layer is given by Kalkanis

$$\frac{u}{U_m} = \left[1 + f_1^2(y) - 2f_1(y) \cos\left[f_2(y)\right]\right]^{\frac{1}{2}} \sin(\omega t + \theta) \quad (23)$$

in which

$$f_1(y) = \frac{1}{2} \exp\left[- \frac{133\, y\omega}{U_m d\sqrt{\omega/2\nu}}\right] ,$$

$$f_2(y) = \frac{1}{2}\left[\sqrt{\frac{\omega}{2\nu}}\, y \right]^{2/3} ,$$

$$\theta = \tan^{-1}\left[\frac{f_1(y) \sin\left[f_2(y)\right]}{1 - f_1(y) \cos\left[f_2(y)\right]}\right] ,$$

and U_m is the maximum velocity of the flow outside the boundary layer. If the velocity u_d is evaluated as being the maximum during a cycle of oscillation at $y = 0.35d$, Equation (9) becomes

$$\frac{U_{mc}\left[1 + f_1{}^2(0.35d) - 2f_1(0.35d)\cos\left[f_2(0.35d)\right]\right]^{\frac{1}{2}}}{\sqrt{(s-1)\,gd\,[\tan\Phi\cos\alpha + \sin\alpha]}} = f(R_c^*) \quad (24)$$

in which U_{mc} is the value of U_m at incipient motion. The LHS of Equation (24) can be determined from the results of Manohar (7) and those of the writer.

Manohar determined conditions for incipient motion by oscillating a bed of particles simple harmonically under an otherwise quiescent tank of water. The boundary layer was turbulent for the results to be analyzed here. Manohar conducted many tests for each bed material by varying the amplitude and the frequency of oscillation of the bed. He found that, for each bed material, incipient motion occurred at a constant value of the maximum velocity, U_m, of the plate. The velocity distribution for the flow relative to the oscillating plate is given by Equation (23). Since Manohar did not report measured values of the angle of repose of his bed materials the factor $\tan\Phi$ will be omitted from Equation (24). For a horizontal bed Equation (24) is written

$$\frac{u_{dc}}{\sqrt{(s-1)\,gd}} = \frac{U_{mc}\left[1 + f_1{}^2(0.35d) - 2f_1(0.35d)\cos\left[f_2(0.35d)\right]\right]^{\frac{1}{2}}}{\sqrt{(s-1)\,gd}} \quad (25)$$

Values of the LHS of Equation (25) were computed from the test results of each of Manohar's bed materials. He conducted many incipient-motion tests for each bed material by varying both the amplitude and the frequency of oscillation of the plate. The value of $u_{dc}/\sqrt{(s-1)gd}$ is essentially constant for all tests on each bed material. Pertinent characteristics of the bed materials and average values of $u_{dc}/\sqrt{(s-1)gd}$ are listed in Table 5.

Table 5. Incipient-Motion Results for an Oscillatory Turbulent Boundary Layer (Manohar's Data)

Bed Material	d(mm)	s	Number of Tests	U_{mc}(ft/sec)	$\frac{u_{dc}}{\sqrt{(s-1)\ gd}}$
Sand	0.280	2.65	3	0.738	2.2
Glass beads	0.610	2.54	19	1.000	1.9
Sand	0.786	2.63	18	1.072	1.7
Sand	1.006	2.60	15	1.129	1.6
Sand	1.829	2.60	19	1.355	1.5
Sand	1.981	2.63	18	1.380	1.5
Polyvinyl Chloride Pellets	3.17	1.280	13	0.812	1.7
Polystyrene Pellets	3.17	1.052	13	0.295	1.5

The suitability of the parameter $u_{dc}/\sqrt{(s-1)\ gd}$ for turbulent flow is again demonstrated here. This incipient-motion parameter has nearly a constant value for bed particles above 0.8 mm diameter. For unidirectional flow of water, sand grains larger than approximately 0.9 mm diameter also exhibited a constant value of the parameter $u_{dc}/\sqrt{(s-1)gd}$. An average value of $u_{dc}/\sqrt{(s-1)\ gd}$ for $d \gtrsim 0.8$ mm is approximately 1.6 for oscillatory flow. Again it is unfortunate that Manohar did not measure the angle of repose of his materials. If, however, Φ is assumed to be 35° for his sand grains larger than 0.8 mm the average value of the parameter $u_{dc}/\sqrt{(s-1)\ gd\ \tan\Phi}$ is approximately 1.9. It is interesting that the average value of $u_{dc}/\sqrt{(s-1)\ gd\ \tan\Phi}$ for Manohar's larger bed particles compares favorably with the average value of 1.95 for White's

larger sands. Admittedly, values of Φ are assumed for Manohar's sand. But, inasmuch as 35° is a suitable value for Φ for sands of 1.0 mm size and since tan Φ is under the radical, the value of 1.9 for $u_{dc}/\sqrt{(s-1)\ gd\ \tan\Phi}$ is probably fairly accurate. The writer feels that the credible agreement between results of Manohar and White and the unsatisfactory agreement between results of Manohar and Mavis et al. can be attributed to the fact that Manohar's flow possessed very little turbulence, if any, outside the boundary layer. The degree of turbulence in White's convergent turbulent boundary layer and in Manohar's oscillatory turbulent boundary layer was obviously very low. Strictly speaking, if White and Manohar each had the same definition for incipient motion, and if each flow possessed the same level of turbulence, the critical velocity u_{dc} would have to be greater in Manohar's case inasmuch as u_{dc} is really an instantaneous velocity in oscillatory flow. Obviously the instantaneous velocity would have to be greater than just a threshold velocity for the bed particles to be moved a short distance. In any event it is concluded that, for hydraulically rough boundaries

$$\frac{u_{dc}}{\sqrt{(s-1)\ gd\ [\tan\Phi\cos\alpha + \sin\alpha]}} = f(R_c^*) \cong 1.9 \qquad (26)$$

for flows having low degrees of turbulence. For sand particles in water, Equation (26) applies for particles having diameters greater than approximately 0.8 mm.

The writer found that, for incipient motion of the 0.585 mm Ottawa sand in the U-tube, the maximum velocity, U_{mc} = 0.960 ft/sec. The corresponding value of the LHS of Equation (25) is 1.9. This value is in

accord with the results for Manohar's glass beads.

Discussion of Shields' Parameter

Since Shields' parameter, $\tau_c/(\gamma_s-\gamma)d$ is widely recognized as a suitable criterion for incipient motion, it was deemed appropriate to discuss its merit. The writer would prefer the inclusion of the angle of repose in the criterion as he feels that it is a necessary sediment property. However, inasmuch as most investigators do not report values of the angle of repose, Shields' parameter will be discussed instead.

It is apparent that there is a wide disparity in the value of Shields' parameter for a laminar boundary layer (White's data) and for a turbulent boundary layer (Shaffernak's data). There would appear to be some transitional region between the two. This transitional region will be delineated by analyzing the results of Chepil and Zingg.

Both Chepil (17) and, later, Zingg (18) report incipient-motion results for bed material placed in a wind tunnel. Chepil used soils having different sizes and various specific gravities and quartz sands of small sizes. For the soil he reports values of u_c^* and $u_c^*/\sqrt{(\gamma_s/\gamma-1)gd}$. The temperature and density of the air are not reported. However, the writer decided to use $\nu = 1.8(10^{-4})ft^2/sec$ after investigating Chepil's data. Chepil's data for incipient motion of his soil and computed values of R_c^* and $f''(R_c^*)$ are listed in Table 6.

Chepil reports measured values of the air velocity six inches above the bed containing quartz sand. The values of u_c^* are computed from Equation (16), assuming $\nu = 1.8(10^{-4})ft^2/sec$. The results are given in Table 7.

Table 6. Incipient-Motion Results for Air Flow over Soil (Chepil's Data)

d(mm)	Specific Gravity	u_c^* (ft/sec)	$\frac{\tau_c}{(\gamma_s-\gamma)d}$	R_c^*
0.027	2.58	0.82	0.102	0.4
0.075	2.07	0.49	0.017	0.7
0.125	2.09	0.44	0.008	1.0
0.165	1.96	0.57	0.010	1.7
0.215	1.94	0.67	0.010	2.6
0.325	1.91	0.73	0.008	4.3
0.505	1.91	0.90	0.008	8.3
0.710	1.80	1.09	0.010	14
1.010	1.78	1.51	0.012	28
1.595	1.74	1.79	0.012	52
2.500	1.65	2.14	0.012	98

Table 7. Incipient-Motion Results for Air Flow over Quartz Sand (Chepil's Data)

d(mm)	$[u]_{y=6\text{ in}}$ (ft/sec)	$\frac{\tau_c}{(\gamma_s-\gamma)d}$	R_c^*
0.015	3.48	0.304	0.3
0.035	2.11	0.053	0.5
0.075	1.35	0.011	0.6
0.125	1.25	0.006	1.0
0.200	1.63	0.006	2.0

Zingg reports value of τ_c which he obtained both by direct measurement and by resolution from velocity profiles above the bed. He used quartz sand having specific gravity 2.65 as bed material. His results and computed values of R_c^* are reported in Table 8.

All the data analyzed for laminar and turbulent boundary layers for unidirectional flow are presented in the form of Shields' parameter in

Table 8. Incipient-Motion Results for Air Flow over Quartz Sand (Zingg's Data)

d(mm)	τ_c (lb/ft^2)	$\frac{\tau_c}{(\gamma_s-\gamma)d}$	R_c^*
0.200	0.00129	0.012	2.9
0.275	0.00180	0.012	5.0
0.360	0.00250	0.013	7.8
0.505	0.00350	0.013	12.9
0.715	0.00513	0.013	21.8

Figure 2. The solid line on the figure is the one conceived by Shields; the data grouped around the line (blacked-in circles) are those measured by Shields and others and analyzed by Shields. There is a wide discrepancy between results of the various investigators. The results of Chepil and Zingg appear to outline the transitional region between a laminar boundary layer and a turbulent boundary layer. It appears that Shields' parameter approaches a constant value between 0.25 and 0.3 for $R_c^* \lesssim 0.3$. For a turbulent boundary layer there is a considerable disagreement between results of the many investigators. This disagreement has been discussed before as possibly being due to different levels of turbulence intensity.

For Chepil's and Zingg's data the parameter $u_{dc}/\sqrt{(\gamma_s/\gamma-1)gd} = 0.8$ for $R_c^* > 18$. This value is only somewhat less than that of the results of Mavis et al. and of Schaffernak. All of the results for the incipient-motion criterion $u_{dc}/\sqrt{(\gamma_s/\gamma-1)gd}$ are presented in Figure 3 for unidirectional flow.

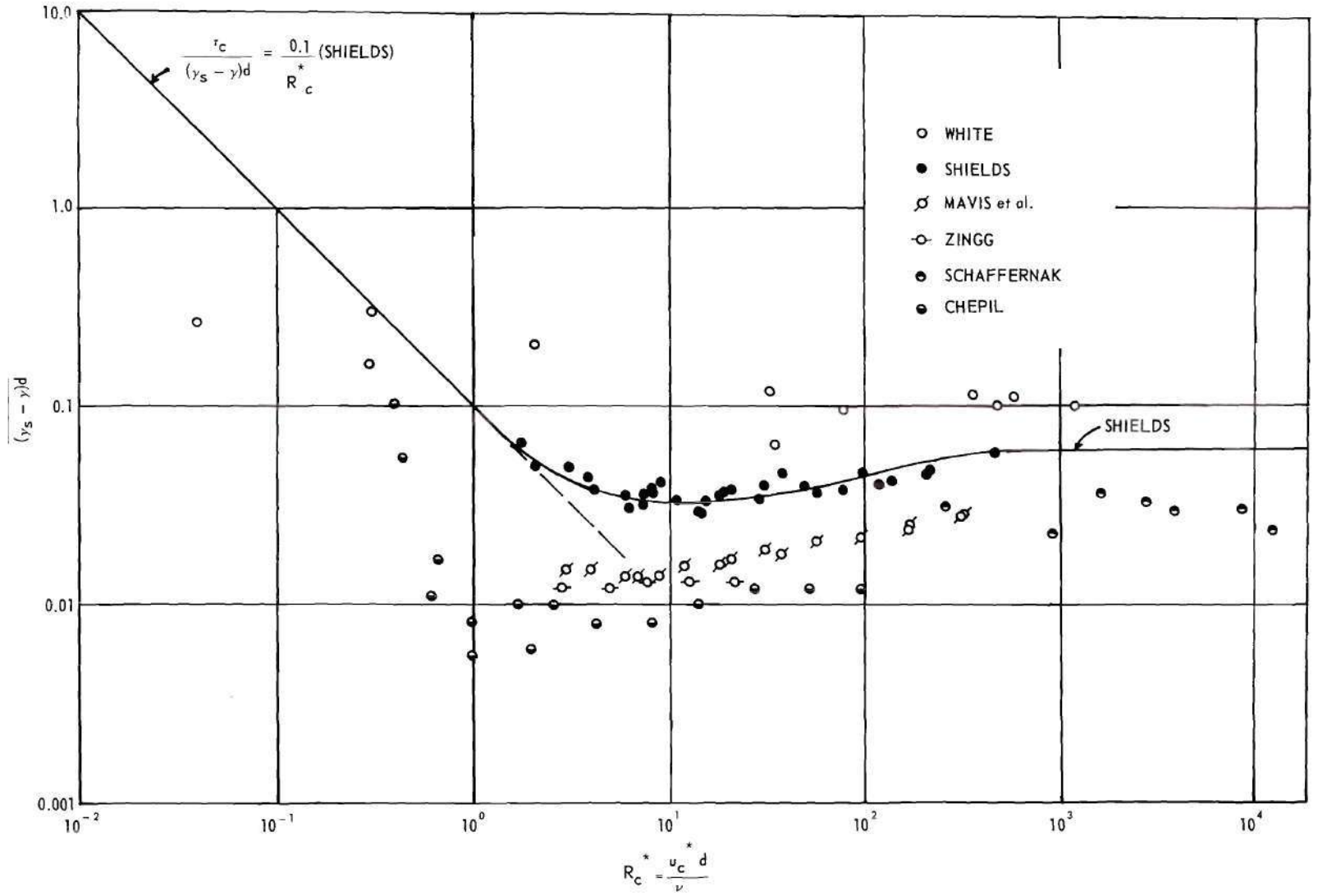

Figure 2. Incipient-Motion Results in Terms of Shields' Parameter (Unidirectional Flow).

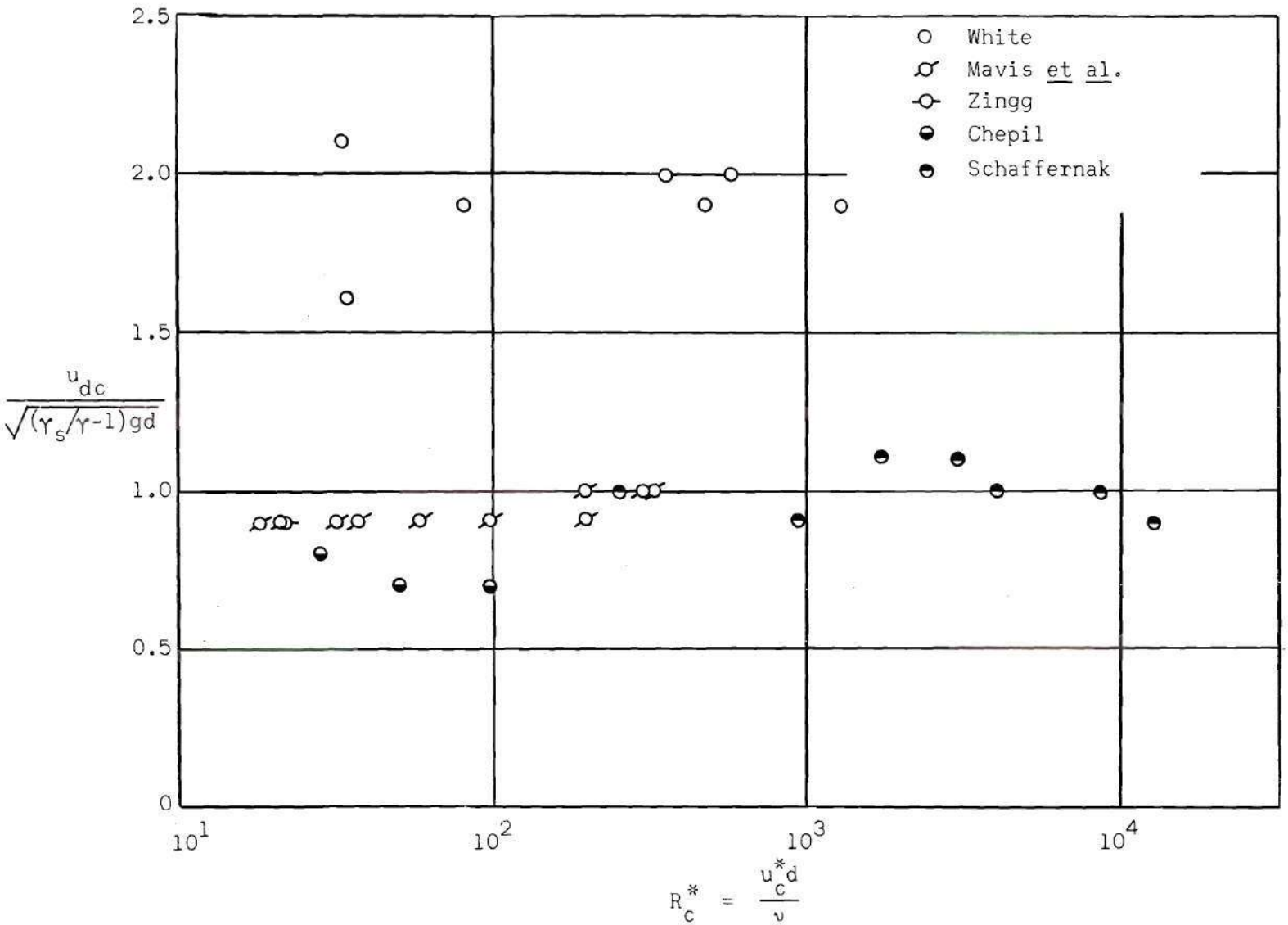

Figure 3. Incipient-Motion Results in Terms of Critical Velocity, u_{dc}, for Unidirectional Flow.

Summary

Several conclusions may be formed from the above analyses. (1) For bed particles in laminar flow or completely immersed in a laminar sublayer for which there is no turbulence, $\tau_c/(\gamma_s-\gamma)d[\tan \Phi \cos \alpha + \sin \alpha] = 0.19$. (2) For turbulent boundary layers for which $R_c^* \gtrsim 18$ the parameter based on a critical velocity $u_{dc}/\sqrt{(s-1)gd\,[\tan \Phi \cos \alpha + \sin \alpha]}$ equals 1.9 for flows having extremely low degrees of turbulence and equals approximately 1.1 for flows having rather high degrees of turbulence. The velocity u_d is determined at a distance of 0.35d from the theoretical wall, which is 0.20 d below the plane tangent to top of the bed particles. The number 1.9 for the critical velocity parameter applies as well to oscillatory flow with a turbulent boundary layer. (3) The parameter based on the critical boundary tractive force, $\tau_c/(\gamma_s-\gamma)d[\tan \Phi \cos \alpha + \sin \alpha]$, and Shields' parameter, $\tau_c/(\gamma_s-\gamma)d$, vary considerably from investigator to investigator. The writer feels that the wide variation indicated on Figure 2 (and Figure 3) is not solely due to differences in judgement between investigators, but somewhat dependent on the level of turbulence present in the main stream above the bed. Since $\tau \propto u_d^2$, large fluctuations in velocity can entail sharp increases in the instantaneous boundary shear stress. Thus, neither the time-average boundary-shear stress nor the time-average value of the bottom velocity, u_d, are reliable indicators for incipient motion.

CHAPTER IV

INVESTIGATION OF THE SEEPAGE FORCE

The seepage force, F_s, is present wherever and whenever there is flow within the permeable bed. In this chapter attention will be directed to the determination of the magnitude of the seepage force, F_s, on the top bed particles for a given flow within the bed.

Static Analysis of Seepage Force

The magnitude of the seepage force within the bed on a mass of bed particles and fluid is easily determined. The seepage force, F_s, per unit volume of bed material and fluid mass is simply the product of the specific weight of the fluid and the piezometric-head gradient in the direction of flow. The piezometric head

$$h = p/\gamma + y$$

in which y is the vertical coordinate and p is the fluid pressure at a point. The components of the seepage force per unit volume in the vertical and horizontal directions are $-\gamma\frac{\partial h}{\partial y}$ and $-\gamma\frac{\partial h}{\partial x}$, respectively, in which x is the horizontal coordinate. The question arises as to whether or not the seepage force on those particles at the top of the bed is equal to the seepage force on particles several layers below the bed. In the usual static analysis of the effect of seepage on the stability of slopes, as performed by Haefeli (19), the seepage force on the top particles is assumed to be equal to that on the particles within the bed.

With reference to Figure 4, a static analysis of the effect of seepage on the angle, α, at which a bed makes with the horizontal will be effected. The direction of seepage flow is at some arbitrary angle, β, with the bed surface and, in the sketch, out of the bed. The bed material is assumed to be completely saturated.

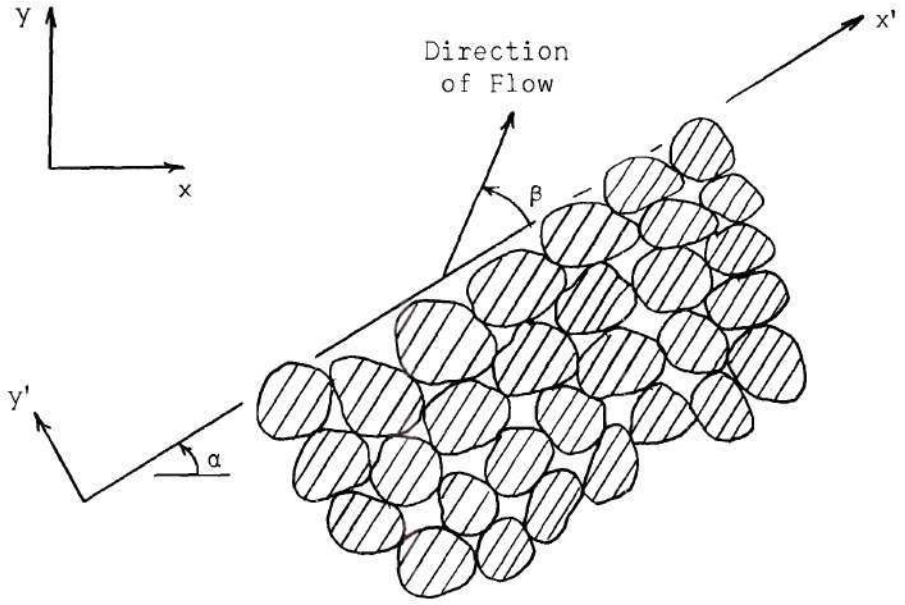

Figure 4. Seepage out of a Bed.

In the following analysis the forces will be considered to be acting on a small incremental volume, $\Delta\forall$, of bed particles and fluid at the surface of the bed. In the direction of flow there is the seepage force, F_s. The other external force is the effective weight force, W. For the critical state of equilibrium (incipient motion), Equation (6) can be written

$$\tan \Phi = \frac{F_s \cos \beta - W \sin \alpha}{F_s \sin \beta - W \cos \alpha} \tag{27}$$

The seepage force on the top layer of bed particles is assumed to be equal to the seepage force on particles several layers down within the bed times what is defined as a flow coefficient, C. The two components of the seepage force per unit volume on bed particles several layers beneath the top layer of particles are simply $-\gamma \left[\partial h/\partial x'\right]_{y'=o}$ and $-\gamma\left[\partial h/\partial y'\right]_{y'=o}$. The flow coefficient, C, would be expected a priori to vary with the angle the seepage flow makes with the bed, β. Each component of the seepage force depicted in Figure 4 is assumed to be associated with a flow coefficient; namely, $C_{\parallel}$ and $C_{\perp}$. These two flow coefficients are not expected to be equal and would be expected to depend on the angle β. Utilizing the flow coefficient concept, Equation (27) can be expressed

$$\tan \Phi = \frac{C_{\parallel} \gamma \Delta \forall \left[\partial h/\partial x'\right]_{y'=o} + (\gamma_s \Delta \forall_s - \gamma \Delta \forall_s) \sin \alpha}{C_{\perp} \gamma \Delta \forall \left[\partial h/\partial y'\right]_{y'=o} + (\gamma_s \Delta \forall_s - \gamma \Delta \forall_s) \cos \alpha}$$

in which γ_s is the specific weight of the bed material, $\Delta \forall_s$ is the incremental volume of solids (bed material) within $\Delta \forall$, and $\Delta \forall_v$ is the volume of voids (fluid) within $\Delta \forall$. The voids ratio is defined as $e = \Delta \forall_v / \Delta \forall_s$. Since $\Delta \forall = \Delta \forall_v + \Delta \forall_s$, the above expression can be reduced to

$$\tan \Phi = \frac{C_{\parallel} (1 + e)\left[\partial h/\partial x'\right]_{y'=o} + (s - 1) \sin \alpha}{C_{\perp} (1 + e)\left[\partial h/\partial y'\right]_{y'=o} + (s - 1) \cos \alpha} \tag{28}$$

in which s is the ratio γ_s/γ. Haefeli assumed the flow coefficients to have the value of unity. There is no reason to accept Haefeli's assumption a priori inasmuch as the flow pattern around the top bed particles is obviously different from that several particles deep. In the following the flow coefficient for flow perpendicular to the bed, $C_\perp$, as well as that for flow parallel to the bed, $C_{||}$, is determined from experimental results.

Experimental Investigation of Flow Coefficient for Flow Perpendicular to the Bed

An experimental program was undertaken for the determination of the magnitude of the flow coefficient for seepage perpendicular to the bed. This flow coefficient, $C_\perp$, is expected to depend upon the geometry of the flow passages within the bed, and might also be expected to differ depending on whether the flow is into or out of the bed. The experimental setup was designed to be a special case of the bed configuration shown in Figure 4. The direction of flow was made to be perpendicular to the bed and reversible. Water was made to flow through a 4 1/2-in diameter clear plastic pipe which contained the bed material. The apparatus was designed such that the pipe could be rotated about its center of gravity. A definitive sketch of the experimental setup is shown in Figure 5; a photograph of the setup is shown in Figure 6. The tubes hanging from the pipe in Figure 6 are connected to piezometers which are placed at 6-in intervals along the pipe. For a given rate of flow of water through the sand the piezometric-head variation within the bed can be measured by means of the simple manometer and gage shown in the right-hand side of the photograph.

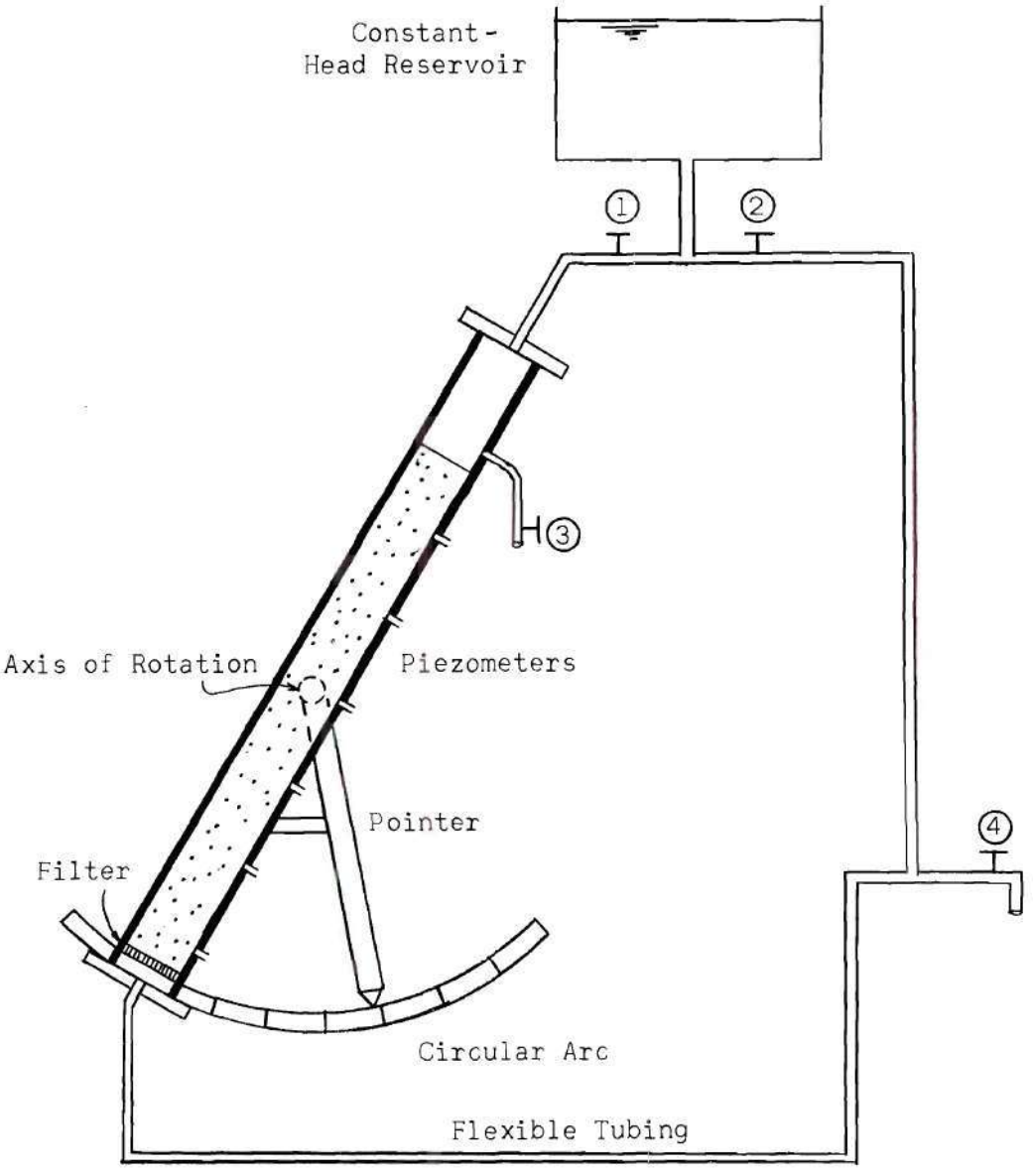

Figure 5. Definitive Sketch of Seepage Test Facility.

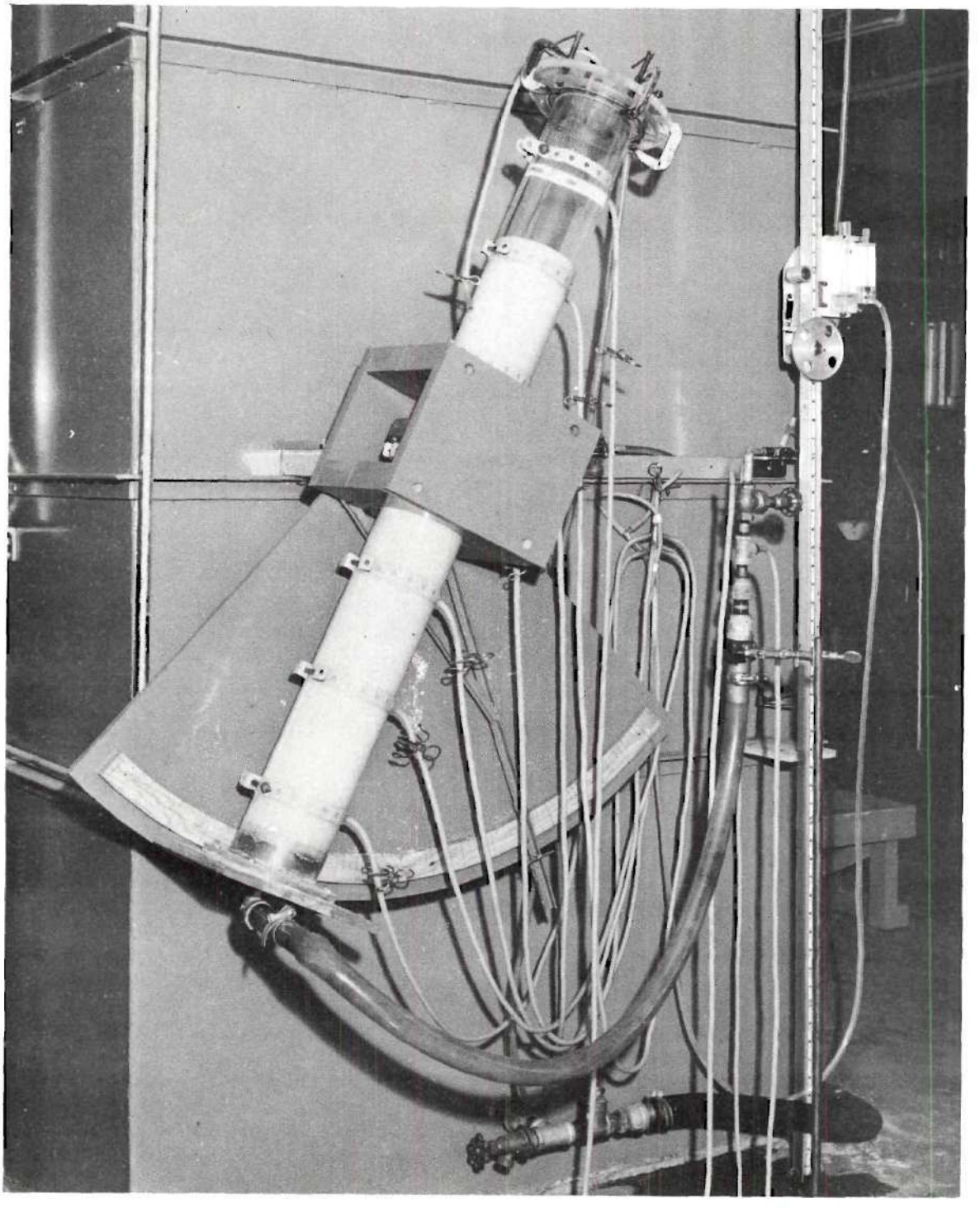

Figure 6. Photograph of Seepage Test Facility.

The bed can be oriented at any angle with the horizontal. The graduated circular scale shown provides for the measurement of the exact angle. In the setup shown the bed material is completely saturated and the water completely fills the space above the bed and the space below the filter. The bed materials used were the glass beads and the Ottawa sand described in Chapter III. The experiment was designed such that the piezometric head within the bed and the angle of the bed could be measured at slope failure. The experimental procedure differed depending upon whether the flow was into the bed or out of the bed. In both cases the bed was first leveled by vibrating the pipe while in the vertical position.

Experimental Procedure for Flow into the Bed

For flow into the bed water was allowed to flow at the maximum rate available such that the bed would be stable for large values of the angle α. Upon closing valves ② and ③, valves ① and ④ were fully opened. The pipe was then rotated to the desired bed angle α. Care had to be taken to reduce vibrations which were found to cause slope failure. At the desired angle α the column was locked in place and, by slowly closing valve ④, the flow was reduced until the slope failed. For this flow rate the piezometric-head variation within the bed was measured. In Figures 7 and 8 is shown the piezometric-head variation within the sand column for the glass beads and Ottawa sand, respectively.

Experimental Procedure for Flow out of the Bed

For flow out of the bed the pipe was rotated to some angle α less than the natural angle of repose, Φ, of the bed material. All valves except ② were initially closed. By slowly opening valve ③ the rate

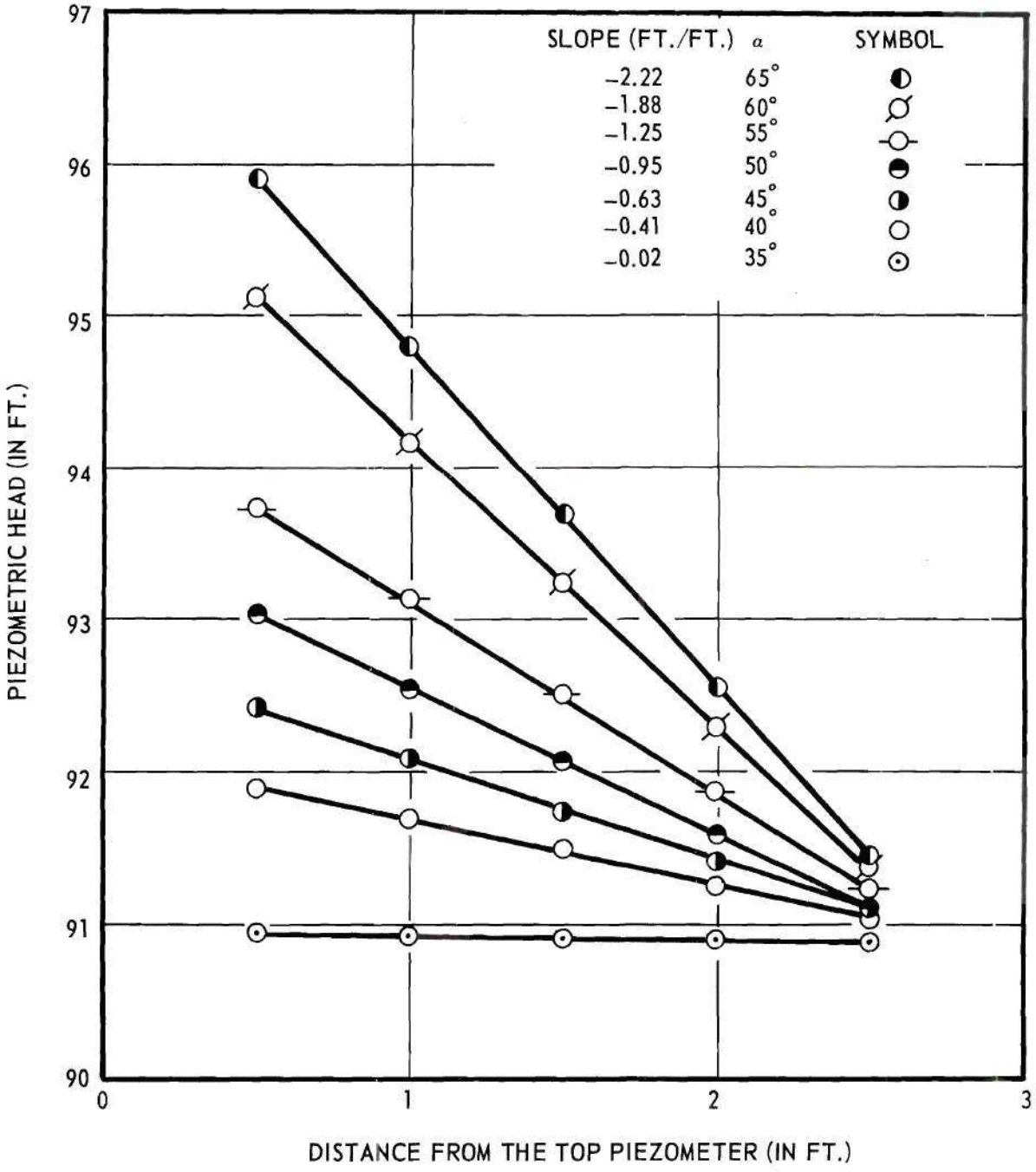

Figure 7. Piezometric-Head Variation for Flow into the Bed (Glass Beads).

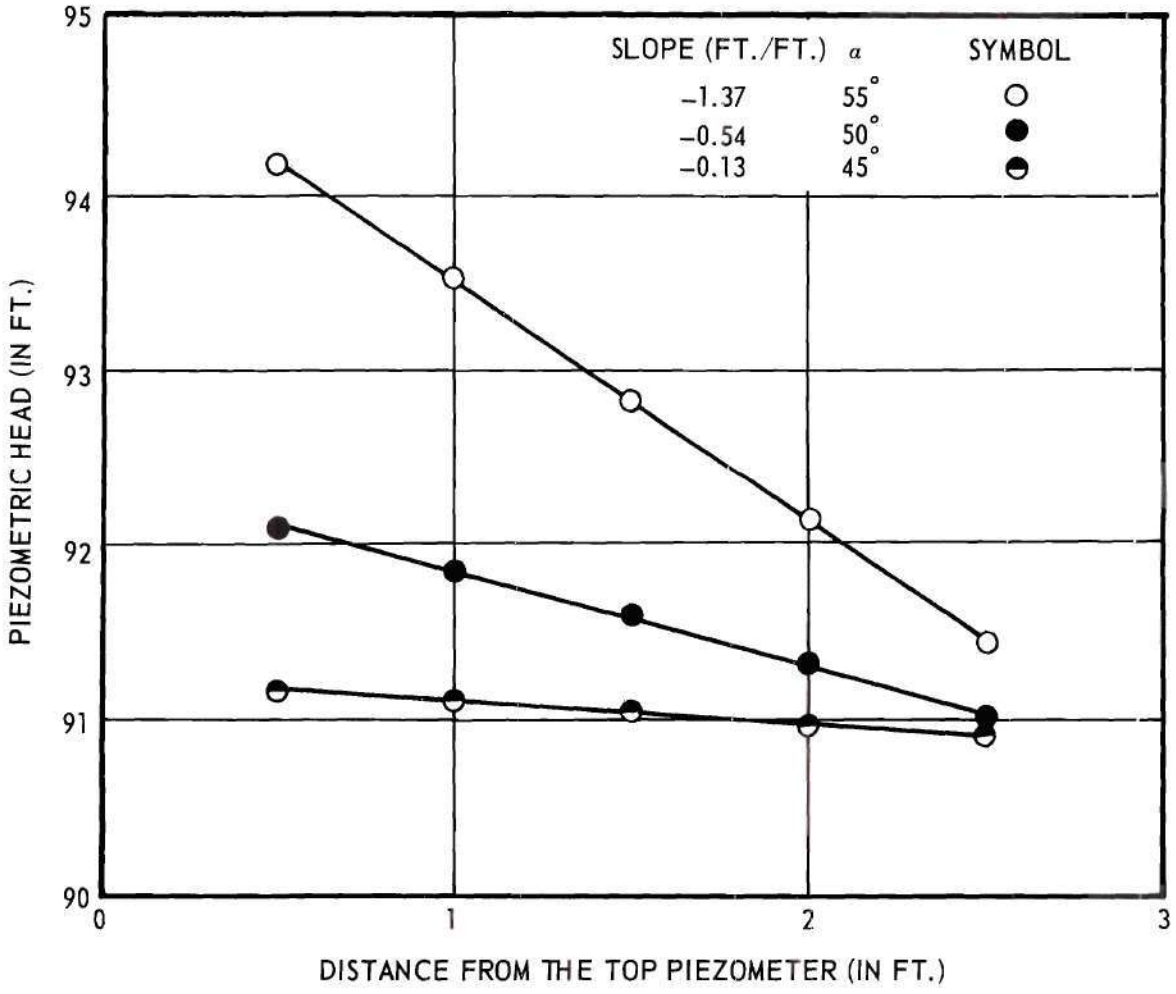

Figure 8. Piezometric-Head Variation for Flow into the Bed (Ottawa Sand).

of flow out of the bed was increased until failure occurred. The piezometric-head variation within the bed was then measured. At the conclusion of all tests the bed was made "quick" in order that the voids ratio could be computed. The results are shown in Figures 9 and 10 for the glass beads and Ottawa sand, respectively.

Discussion of Results

The results were analyzed such that the flow coefficient $C_{\perp}$ could be computed for various angles of the bed, α, and for the two directions of flow. Since the flow was always perpendicular to the bed, Equation (28) can be expressed as

$$C_{\perp} = \frac{(s - 1)(\sin \alpha - \cos \alpha \tan \Phi)}{(1 + e)[\partial h/\partial y']} \qquad (29)$$

in which $[\partial h/\partial y']$, the piezometric-head gradient in the column, is equal to $[\partial h/\partial y']_{y'=o}$, the piezometric-head gradient several layers from the top of the bed.

The voids ratio was 0.47 for the glass beads and 0.57 for the Ottawa sand. The natural angle of repose of the bed materials was obtained by interpolation from a plot of the piezometric-head gradient, $\partial h/\partial y'$, and angle of the bed, α. The natural angle of repose, Φ, corresponds to no seepage flow and was 32.5° and 41° for the glass beads

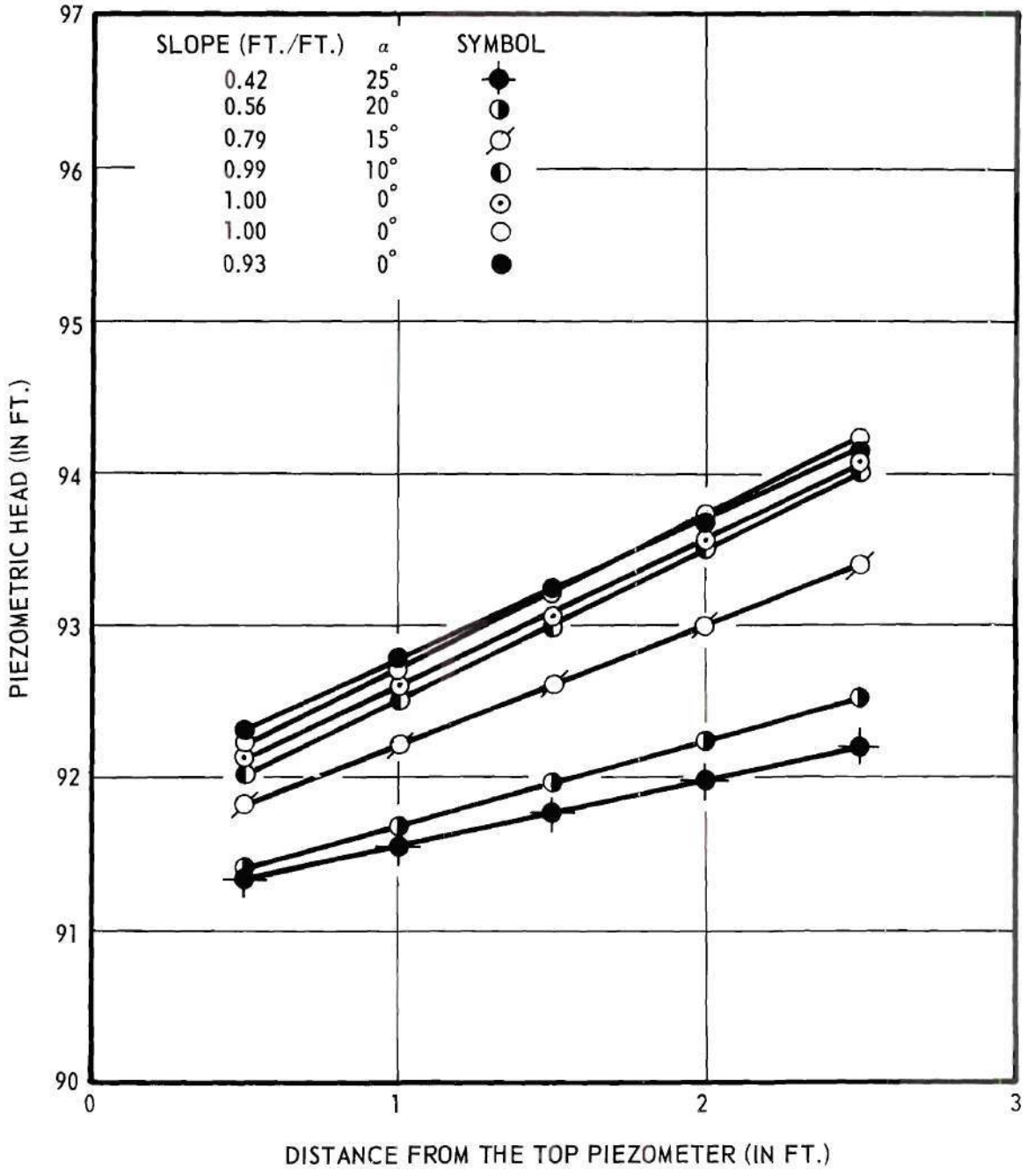

Figure 9. Piezometric-Head Variation for Flow out of the Bed (Glass Beads).

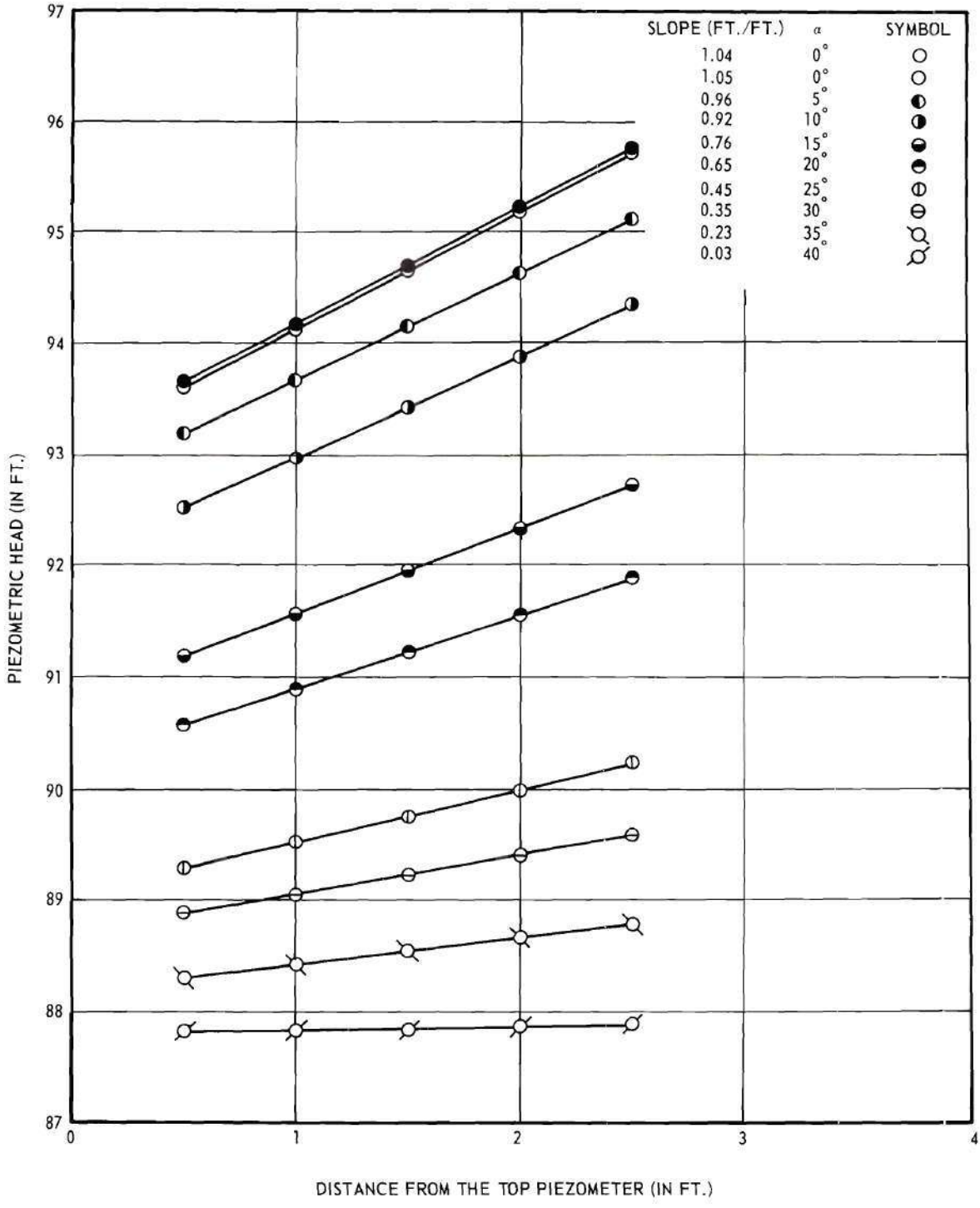

Figure 10. Piezometric-Head Variation for Flow out of the Bed (Ottawa Sand).

and Ottawa sand, respectively.[1]

The results of the seepage tests are shown in Figure 11 in terms of the flow coefficient, $C_\perp$. Computed values of $C_\perp$ for values of the angle α close to Φ are subject to error as the numerator of Equation (29) is proportional to a difference in two terms of the same order of magnitude. Since the data were not considered to possess the degree of accuracy required to produce suitable values of $C_\perp$ for values of α near Φ some of the computed results are not shown on Figure 11. The computed results omitted are for the tests for which α is closest to Φ. It is at once apparent that, for each bed material, the flow coefficient $C_\perp$ is essentially a constant provided that $\alpha < \Phi$. The constant values shown by the horizontal lines on Figure 11 are roughly 0.7 and 0.9 for the glass beads and Ottawa sand, respectively. For values of $\alpha > \Phi$ the flow coefficient $C_\perp$ decreases

---

[1] It should be noted that these values of Φ are considerably greater than the ones measured by pouring and quoted in Chapter III; namely, 24° and 32.5° for the glass beads and Ottawa sand, respectively. As explained by Bernatzik (20), the so-called angle of repose depends upon the relative magnitude of the three normal stresses, as well as upon other parameters. He shows, for example, that the angle Φ for a conically shaped pile of cohesionless material is less than that for a plane slope of the same material. For a conically shape hole within a sand bed the angle of repose Φ is greater than either one of the above cases. These differences are attributable to the relative magnitude of the normal stresses. The angle of repose for any material also depends on how densely the material is packed. The sand column in the seepage tests closely resembles Bernatzik's example of a plane slope. Consequently the angle of repose Φ should be higher for the material when placed in the sand column than when resting on a pile. There are at least three other reasons why Φ should be higher when the bed material is in the column. First, the density of the bed material is greater when located within a compacted bed than when resting on the face of a pile. Second, there is an additional stress on the bed material in the column by virtue of the load transmitted to the walls. Thirdly, the impulse-momentum capacity of particles rolling down the slope of a pile which is being poured reduces the ultimate angle of stability.

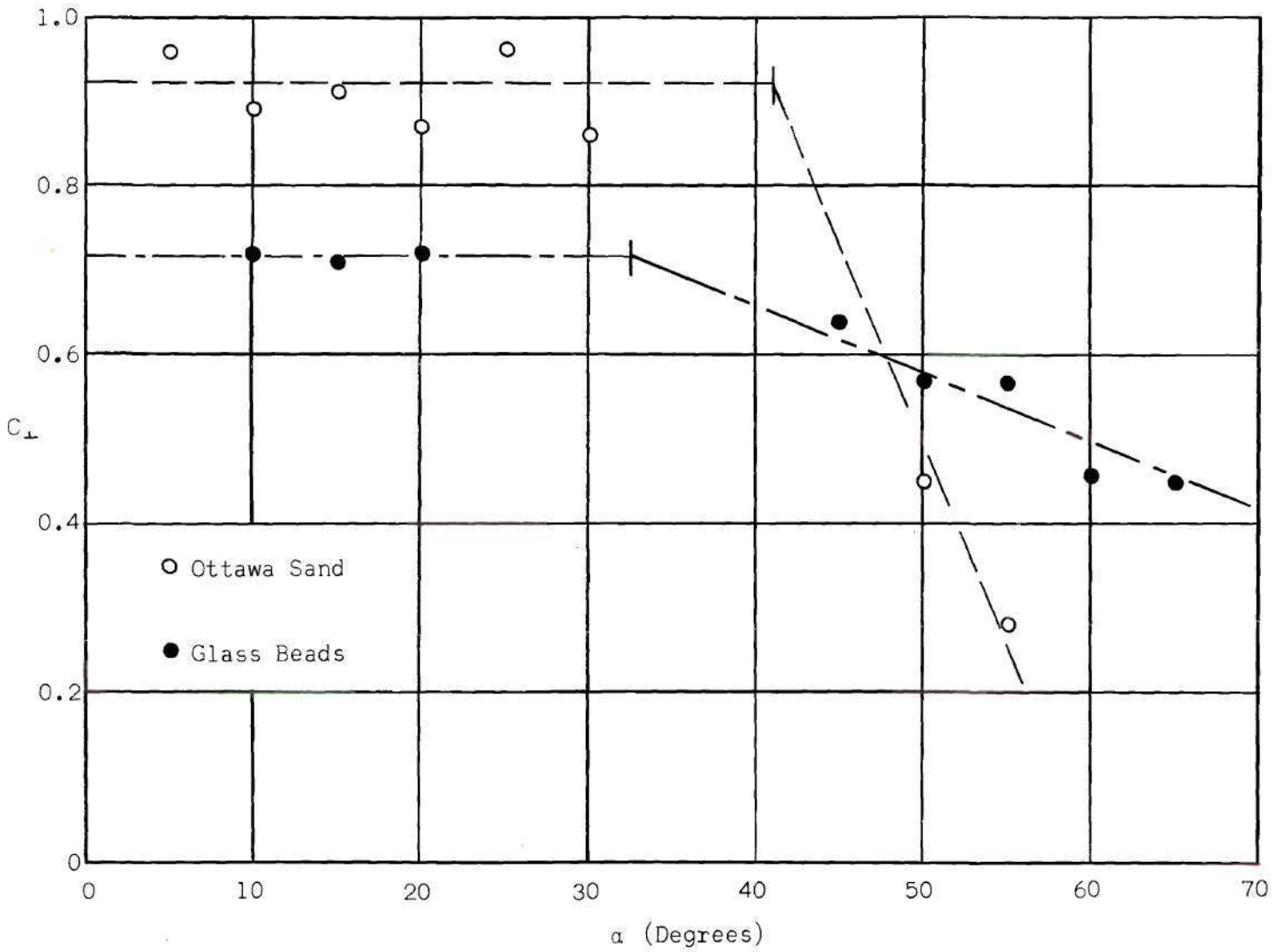

Figure 11. Variation of the Flow Coefficient, $C_\perp$, with Angle of Bed (Writer's Data).

radically. The following discussion and crude analysis are developed in an attempt to explain the radical decrease of the flow coefficient for values of $\alpha > \Phi$.

After each run the column was vibrated in order to re-level the bed. There were always a number of single bed particles which protruded out of the essentially plane bed. For seepage flow out of the bed ($\alpha < \Phi$) the reduction or absence of the seepage force on these particles does not create instability of the bed. On the other hand, for seepage flow into the bed ($\alpha > \Phi$) the reduction or absence of the seepage force on these particles can create instability of the bed. This instability was apparent from observation of avalanches set off by a single grain or a series of grains. For some tests with $\alpha > \Phi$ only a portion of the bed would undergo failure for a given value of the piezometric-head gradient, $\partial h/\partial y'$, through the mechanism of an avalanche. The remaining portion would frequently remain stable for a large decrease in $\partial h/\partial y'$. The fact that the flow coefficient $C_\perp$ decreased at a greater rate for the Ottawa sand than for the glass beads can be explained by a crude analysis based on the impulse-momentum principle. The impulse that a rolling particle can impart to another particle is proportional to the particle's momentum, $M_s V_t$, in which M_s is the mass of the particle and V_t is considered to be the terminal velocity of the particle rolling down the bed. The terminal velocity V_t is determined on the basis that the drag force is proportional to the effective weight force down the plane. The drag force for the glass beads and for the Ottawa sand is proportional to $\mu V_t d$ for the Reynolds numbers involved here, Eagleson and Dean (1). Hence

$$(\gamma_s-\gamma)\, d^3 \sin\alpha \propto \mu\, V_t d$$

Therefore the momentum, m, of the particle

$$m \propto \frac{\rho(\gamma_s - \gamma)\, d^5 \sin\alpha}{\mu}$$

Since the variables ρ, $\gamma_s-\gamma$, and μ were essentially constant for all tests for both bed materials, the momentum

$$m \propto d^5 \sin\alpha$$

This rough analysis demonstrates the functional dependence of the momentum on the particle diameter, d, and the angle of the bed, α. The mean diameter of the Ottawa sand is nearly twice that of the glass beads. Hence the momentum of a sand grain could be expected to be 32 times that of a glass bead for the same angle α. The lower values of the flow coefficient $C_\perp$ for the sand than for the glass beads may be influenced by the greater momentum of the sand grains. The dependence of the angle α on the flow coefficient is shown by Figure 11.

It is concluded that the data for $\alpha > \Phi$ do not truly represent the phenomenon desired. The sole purpose of these tests was to ascertain the magnitude of the seepage force, F_s, for flow out of and into the bed. The flow coefficient $C_\perp$ has been defined as the ratio of the seepage force on the top layer of particles to that on particles several layers beneath the bed. Obviously there is a difference in flow-passage geometry between grains at the bed and between those down within the bed. Moreover it might be expected <u>a priori</u> that, for a given rate of flow

through a given bed, the flow coefficient depends on whether the flow is out of or into the bed. It has been shown analytically and experimentally by McNown et al. (21) and analytically by Keller (22) that, for laminar flow through narrow curved passages, the majority of the total viscous resistance on the boundaries occurs at the location of minimum pore area. In other words the pressure gradient required to maintain a certain flow rate through a narrow passage depends mainly upon the minimum passage area and not so much upon the shape of the remainder of the passage. McNown et al. investigated laminar flow between a sphere and a cylindrical tube. They concluded that, for large values of the ratio of the diameter of the sphere, d, to the diameter of the cylinder, D, the pressure gradient across the sphere could be determined by assuming that the majority of the viscous shear on the sphere occurred in the equatorial region of the sphere. Their analytical development was confirmed by experiment. Keller studied viscous flow between a row of cylinders and formed the same conclusion. Using the conclusions of the above investigators it is concluded that, for laminar flow in porous media, the seepage force depends only upon the geometry of the narrow passages between pores and not upon the direction of flow. The flow coefficient, $C_{\perp}$, as defined should have a constant value for a given bed configuration and should not depend upon whether the seepage flow is into or out of the bed. The latter statement may not hold true for large flow rates for which the flow separates from the boundary of the particles. For boundary-layer separation the flow coefficient would conceivably depend on the direction of flow. For the test results taken with the glass beads and the Ottawa sand the flow was definitely laminar.

It is concluded that the flow coefficient $C_\perp$ is 0.7 for the glass beads and 0.9 for the Ottawa sand. The difference in the values are thought to be due to the fact that the nearly spherical glass beads have different flow passages than the well-rounded Ottawa sand grains. In order to establish further qualifications as to the magnitude of $C_\perp$, results of another investigator are analyzed in the following.

Analysis of Results of Bernatzik for Perpendicular Flow

Bernatzik (23) conducted the same type of seepage tests as the writer. He used sand as the bed material and water as the fluid. His test container was in the form of a rectangular cylinder having cross-sectional dimensions of 19.8 cm by 20.4 cm and a length of 40 cm. His bed material was quartz sand, having a mean diameter of nearly 0.2 mm and having a specific gravity of 2.67. He mounted his container on an axle whereby the bed could be brought to any desired slope. Tests were conducted for flow into the bed and for flow out of the bed. Bernatzik used the same quantity of sand for all tests. In preparing the test sample he vibrated this quantity into place in the test container such that it always occupied the same height, 18 cm. The voids ratio remained constant at 0.67. He conducted the seepage tests in essentially the same manner as the writer.

Bernatzik's results are delineated on Figure 12 in terms of the flow coefficient, $C_\perp$, versus angle of the bed, α. He was able to vary α from 0° to 180° in 10° intervals. The angle of repose was 42°. For values of α of 40° and 50° the flow coefficient is not given inasmuch as great accuracy of results is needed for bed angles near the angle of

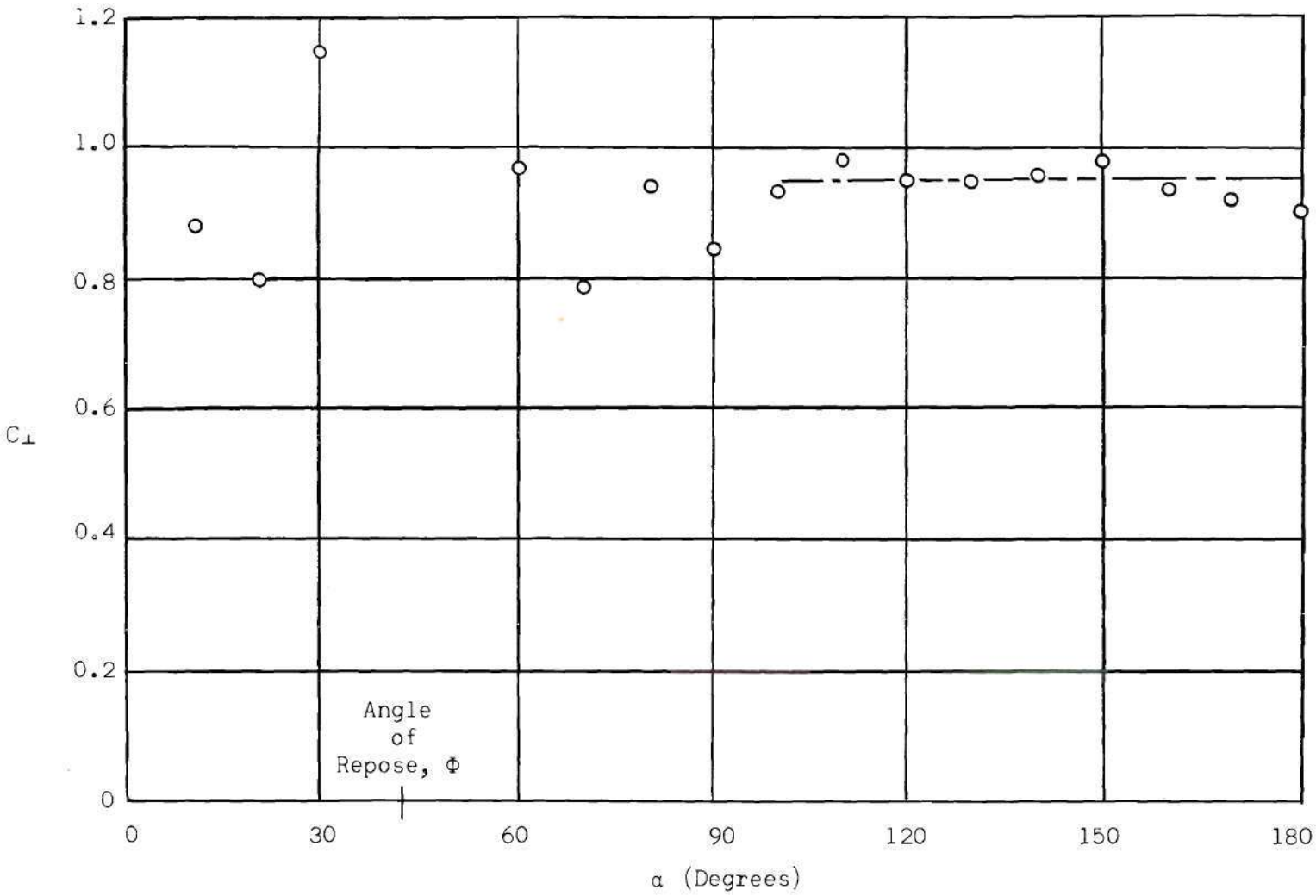

Figure 12. Variation of the Flow Coefficient, $C_\perp$, with Angle of Bed (Bernatzik's Data).

repose. The results given in Figure 12 are from Bernatzik's published results. He states that at least three tests were run at each bed angle and that test results which deviated greatly from the mean were eliminated. The results he published are apparently the end result of many experiments and of some discretionary action on his part.

The flow coefficient computed from Bernatzik's results varies considerably for $0° < \alpha < 90°$ but remains nearly constant for $90° < \alpha < 180°$. He states that, with flow out of the bed, that is for $\alpha < \Phi$, the bed would frequently fail by rupture (quick condition) rather than by the normal sliding process. The scatter of the data for $\Phi < \alpha < 90°$ may well be due to the dislodging effect discussed earlier. For $\alpha > 90°$ any individual bed particle which does not receive sufficient seepage force to hold it stable will fall freely through the water and hence will not dislodge any other particle by rolling. In other words, there is no problem from rolling for $\alpha > 90°$. The absence of the rolling effect may be the reason that Bernatzik's data are quite consistent for $\alpha > 90°$. The average value of the flow coefficient, $C_{\perp}$, is 0.95 for $100° < \alpha < 180°$. The maximum deviation from this average value is five percent.

Bernatzik states that he also ran identical tests on sands of other sizes. He found that the results were essentially unaltered except that there was an influence of grain size on the scatter of the data. In the following the flow coefficient for parallel flow is investigated.

Analysis of Results of Havlicek for Parallel Flow

Havlicek (24) investigated the effect of the seepage force on the

stability of slopes. He conducted experiments for water flowing through a saturated sand mass. The sand grains had a specific gravity of 2.65. He measured the angle of repose of dry sand by tilting a sand bed until failure occurred. The test that Havlicek conducted is that for seepage flow parallel to the bed. The test arrangement he used is shown in Figure 13.

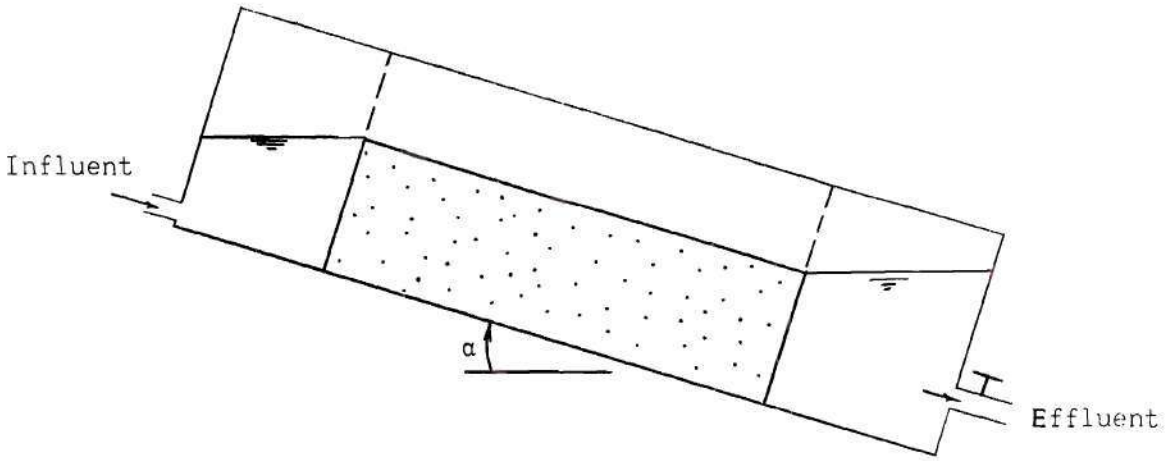

Figure 13. Definitive Sketch of Havlicek's Tilting Flume.

The sand was placed in a tilting flume so that the streamlines would be parallel to the bed. For a given flow rate he would increase the angle α until the first movement of grains. Havlicek's results will now be analyzed using this angle α as the failure angle. The condition for incipient motion, Equation (28), is applicable here. The flow coefficient for flow parallel to the bed

$$C_{II} = \frac{(s - 1)}{(1 + e)} \left[\frac{\cos \alpha \tan \Phi - \sin \alpha}{\left[\frac{\partial h}{\partial y'}\right]_{y'=o} \tan \Phi + \left[\frac{\partial h}{\partial x'}\right]_{y'=o}} \right] \qquad (30)$$

Inasmuch as the streamlines are parallel to the bed, the piezometric-head gradient normal to the bed is zero, that is

$$\left[\frac{\partial h}{\partial y'}\right]_{y'=o} = 0$$

Since the pressure is constant at the bed (atmospheric) the piezometric head at $y' = 0$ is simply equal to the vertical coordinate, y. The piezometric-head gradient parallel to the bed is equal throughout the bed. At the bed

$$\left[\frac{\partial h}{\partial x'}\right]_{y'=o} = \left[\frac{\partial y}{\partial x'}\right]_{y'=o} = \sin \alpha$$

The flow coefficient

$$C_{\parallel} = \frac{(s - 1)}{(1 + e)} \left[\cot \alpha \tan \Phi - 1\right] \qquad (31)$$

in which α is the bed angle at incipient motion. The results of Havlicek's tests are given in Table 9. The sands had the same voids ratio for the seepage tests as they did for the angle of repose tests. The maximum and minimum values of α found by Havlicek and the corresponding maximum and minimum computed values of the flow coefficient, $C_{\parallel}$, are listed for each sand. The value of the flow coefficient, $C_{\parallel}$, is essentially constant for each sand but it varies considerably from one sand to another. The reason for the discrepancy of the values of $C_{\parallel}$ from sand to sand is not apparent. The average value of $C_{\parallel}$ in Table 9 is 0.97. It may be simply fortuitous that this average value of $C_{\parallel}$ agrees with the value of $C_{\perp}$ from the results of Bernatzik.

Table 9. Results of Havlicek's Parallel Seepage Tests

Sand	Φ (avg.)	e	α_{min}	α_{max}	$(C_{\parallel})_{min}$	$(C_{\parallel})_{max}$
I	37.6°	0.60	18.2°	18.5°	1.39	1.34
II	39.9°	0.53	20.2°	22.5°	1.36	1.10
III (Loose)	36.0°	0.60	22.7°	23.2°	0.76	0.72
III (Dense)	37.8°	0.48	27.7°	27.7°	0.53	0.53

Summary

The results presented in this chapter are fairly conclusive as to the magnitude of the seepage force at the bed. The flow coefficient, which is defined as the ratio of the seepage force on the top layer of bed particles to that on bed particles several layers within the bed, has been determined from results of two different seepage flows. From the results of the writer the flow coefficient, $C_{\perp}$, is concluded to be 0.7 for the glass beads and 0.9 for the Ottawa sand. From Bernatzik's results the writer concludes $C_{\perp}$ to be 0.95. The average value of the flow coefficient, $C_{\parallel}$, from Havlicek's tests is 0.97. For sand for which β is either 0° or 90°, the value of C appears to be in the vicinity of 0.9 to 1.0. In the remainder of this treatise $C_{\perp}$ will be assumed to have the value 0.9. The seepage force at the bed can be evaluated for any seepage flow perpendicular to or parallel with the bed as long as the piezometric-head gradient is known. For seepage flow through sand which obeys Darcy's Law the piezometric head within the bed satisfies Laplace's equation

$$\frac{\partial^2 h}{\partial x^2} + \frac{\partial^2 h}{\partial y^2} = 0 \qquad (32)$$

The solution to Equation (32) and the appropriate boundary conditions gives the piezometric-head variation within the bed. The seepage force per unit volume at the surface of the bed is simply C times the piezometric-head gradient at the bed which can be computed from the solution to Equation (32). Hence the solution to Laplace's equation provides the necessary information for the magnitude of the seepage force for many seepage flows. For seepage flows neither perpendicular to nor parallel with the bed the flow coefficient, C, is not known. For engineering purposes the writer would recommend using $C = 0.9$ for all values of the angle β.

CHAPTER V

EFFECT OF SEEPAGE FLOW ON INCIPIENT MOTION

The effect of the permeable bed on incipient motion can only be ascertained by considering both the fluid-resistance force analyzed in Chapter III and the seepage force analyzed in Chapter IV. Incipient motion can be predicted by utilizing Equation (6). In this chapter an experimental result on the effect of flow out of a bed on incipient motion is discussed. Experimental results of others on the altering of the flow near a porous boundary undergoing fluid injection or suction are also discussed.

Incipient-Motion Test with Seepage

The U-tube described in the Appendix was the facility used for investigating the effect of seepage flow on incipient motion. The only type of test conducted was for seepage out of the bed into an oscillatory flow.

The effect of seepage out of the bed on incipient motion was studied by subjecting an isolated portion of the bed in the U-tube to an upward flow of water. This was effected by means of a 4 1/2-in ID transparent plastic pipe which protrudes through the center of the floor of the test section. The vertical pipe is 4 ft long terminating 1/4 in below the top of the sand bed. Water was pumped through the pipe filled with the bed material and into the bed by means of a small pump. The vertical piezometric-

head variation in the pipe was measured by means of seven piezometers, which are spaced on 6-in centers along the pipe, and a differential manometer. A schematic drawing of the experimental setup is shown in Figure 14.

Incipient-motion tests with seepage out of the bed were conducted by pumping water upward through the bed while the U-tube was in operation. The amplitude of oscillation in the test section was set at a value less than that for which incipient motion occurred with no seepage. The piezometric-head gradient at the bed was gradually increased by increasing the flow rate through the pump. As the gradient was increased the bed material immediately above the end of pipe was observed for any movement by means of a telescope. The bed material used was the glass beads described in Chapter III. For the test results presented here the total amplitude of oscillation, $2a = 6.50$ in. It was observed that, only for the vertical piezometric-head gradient slightly less than that required to give a fluidized bed, did any motion at all occur. For that gradient a few bed particles would roll over and then come to rest until the horizontal water motion reversed in direction. The particles never did translate, even up to a gradient equivalent to a fluidized state of the bed material in the column. There was no translation of bed particles because the seepage force was greatly reduced once a particle rolled out of its recess. The particle would then roll back on the return motion and repeat the same sequence of events. The seepage force becomes negligible once a bed particle rocks only slightly out of its recess. The conclusion is that the seepage force for flow out of a bed does not aid incipient motion. Although the test was conducted for oscillatory flow the conclusion should

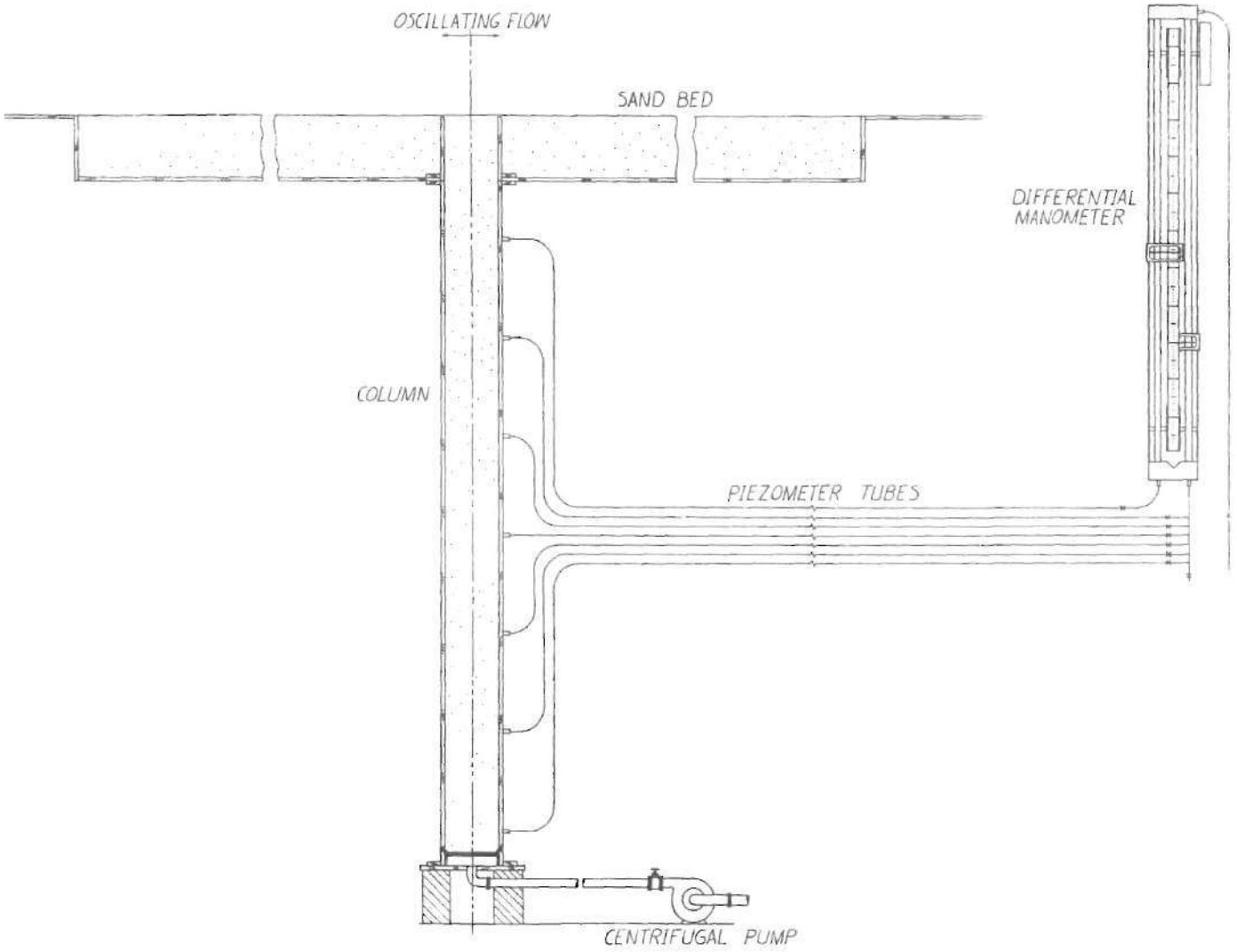

Figure 14. Schematic Diagram of Uplift Facility.

apply as well for unidirectional flow as a particle only has to rock slightly to lose the seepage force. For flow out of a bed the seepage force should not be included in the incipient-motion criterion. Hence either Equation (9) or (10) applies. It will be shown in the following, however, that seepage out of a bed can affect incipient motion by altering the flow characteristics at and adjacent to the bed.

At the time of the testing it was thought that the same experimental setup could not be used to determine the effect of flow into the bed on incipient motion. With the pump reversed the bed particles immediately above the end of the pipe experience a downward force. In order to overcome this force the amplitude of oscillation in the U-tube would most likely have to be increased above that required for incipient motion with no suction. For such amplitudes the remainder of the bed would be in motion, with the likelihood of the formation of ripples. For this reason tests were not conducted for flow into the bed.

Incipient-Motion Criteria with Seepage

The condition for incipient motion can now be ascertained by coupling the results of the analysis of the fluid-resistance force and of the seepage force into the incipient-motion criterion, Equation (6). For seepage flow out of the bed the seepage force shall not be included in Equation (6) inasmuch as this force can not aid incipient motion.

Seepage out of the Bed (Injection)

For vertical seepage flow out of a bed the incipient-motion criterion for laminar flow over a horizontal bed is

$$\frac{\tau_{cs}}{(\gamma_s-\gamma)\ d\ \tan\Phi} = 0.19 \qquad (33)$$

in which τ_{cs} is the critical boundary shear stress with seepage. For turbulent flow the parameter based on the bottom velocity, Equation (9)

$$\frac{u_{dcs}}{\sqrt{(s - 1)\ gd\ \tan \Phi}} = 1.1 \text{ to } 1.9 ,$$

depending on the intensity of turbulence within the flow. The value 1.1 is used for flows having high intensities of turbulence whereas the value 1.9 is used for flows having low intensities of turbulence. The value of the above parameter would be expected to lie between 1.1 and 1.9 for flows having intermediate intensities of turbulence.

Seepage into the Bed (Suction)

The seepage force should be included in incipient-motion criteria for flow into a bed. Equation (14) and (29) are introduced into Equation (6) for laminar flow. For laminar flow over a horizontal bed for which the seepage velocity is perpendicular to the bed

$$\frac{\tau_{cs}}{\left[(\gamma_s - \gamma) + 0.9\ (1 + e)\ \gamma\left[\frac{\partial h}{\partial y}\right]_{y=o}\right] d\ \tan \Phi} = 0.19 \qquad (34)$$

For turbulent flow over a horizontal bed Equation (9) and (29) are introduced into Equation (6), producing

$$\frac{u_{dcs}}{\sqrt{\left[(s - 1) + 0.9\ (1 + e)\left[\frac{\partial h}{\partial y}\right]_{y=o}\right] gd\ \tan \Phi}} = 1.1 \text{ to } 1.9 \qquad (35)$$

For any given problem the piezometric-head variation within the bed can be determined from Equation (32), provided that Darcy's Law is satisfied.

In the following the effect of injection and suction on the boundary-shear stress and velocity distribution is discussed.

Change in Flow Characteristics by Seepage

The boundary-layer characteristics are obviously altered by the flow out of or into a bed. The boundary shear stress is usually decreased by injection and increased by suction as compared to that for an impermeable boundary. Suction is known to enhance stability of a laminar boundary layer, thus delaying transition. Only when transition is prevented is the boundary shear stress with suction less than that with an impermeable wall. Injection is known to enhance transition of laminar boundary layers. The increase in boundary shear stress brought about by transition could conceivably aid incipient motion for seepage out of a bed.

Seepage out of the Bed

There is some information available on the effect of injection on the boundary shear stress and velocity distribution above smooth and rough walls. The main impetus behind research on fluid injection has been the need for more knowledge on the mechanism of transpiration cooling.

Turcotte (25) developed a theory for the laminar sublayer for fluid injection into an incompressible turbulent boundary layer. For small flow rates of seepage he found the following relationship to apply for smooth boundaries

$$\frac{\tau_s}{\tau} = 1 - 13.9 \frac{v_s}{u^*} \qquad (36)$$

in which τ_s is the boundary shear stress with injection and v_s is the

injection (seepage) velocity. The shear velocity, u^*, is that based on the boundary shear stress, τ, without seepage. Equation (36) definitely shows that injection reduces the boundary shear stress. Moreover it may be concluded that injection (seepage out of the bed) can hinder incipient motion if the boundary shear stress is reduced. For seepage flow which obeys Darcy's Law the seepage velocity at the bed

$$v_s = \kappa \left[\frac{\partial h}{\partial y}\right]_{y=o} \tag{37}$$

in which κ is the coefficient of permeability. For laminar flow through porous media Todd(26) shows that the coefficient of permeability can be approximated by

$$\kappa = \frac{\gamma d^2}{2000\ \mu} \tag{38}$$

Using the fact that, at incipient motion without seepage, $\tau = \tau_c$, and $u^* = u_c^*$, Equation (36) can be rewritten with the aid of Equations (14), (37), and (38)

$$\frac{\tau_s}{\tau_c} = 1 - \frac{0.0159\ \gamma\ d^{\frac{3}{2}} \left[\frac{\partial h}{\partial y}\right]_{y=o}}{\mu \sqrt{(s-1)\ g \tan \Phi}} \tag{39}$$

Furthermore, if $\gamma = 62.4\ \text{lb/ft}^3$, $\mu = 2.1\ (10^{-5})\ \frac{\text{lb-sec}}{\text{ft}^2}$, $\Phi = 25°$, and $s = 2.65$

$$\frac{\tau_s}{\tau_c} = 1 - 1.79\ d^{\frac{3}{2}} \left[\frac{\partial h}{\partial y}\right]_{y=o} ;\quad d \text{ in mm}$$

Values of τ_s/τ_c are tabulated in Table 10 for the conditions stated above.

Table 10. Reduction of Boundary Shear Stress With Flow out of a Smooth Boundary

$\left[\frac{\partial h}{\partial y}\right]_{y=o}$	$\frac{\tau_s}{\tau_c}$					
d(mm) =	0.05	0.10	0.15	0.20	0.25	0.30
0	1.00	1.00	1.00	1.00	1.00	1.00
0.2	1.00	0.99	0.98	0.97	0.96	0.94
0.4	0.99	0.98	0.96	0.94	0.91	0.88
0.6	0.99	0.97	0.94	0.90	0.87	0.82
0.8	0.98	0.95	0.92	0.87	0.82	0.77
1.0	0.98	0.94	0.90	0.84	0.78	0.71

For the assumed conditions of a hydraulically smooth boundary, Equation (39) should apply for $d \lesssim 0.3$ mm.

The foregoing analysis shows that the boundary shear stress can be reduced as much as 30 per cent by seepage out of a hydraulically smooth bed. For small values of the permeability and/or of the vertical piezometric-head gradient, however, seepage has little or no effect on the critical boundary shear stress.

Eckert *et al.* (27) have investigated the effect of air injection through porous rough surfaces on flow in channels. The porous materials they used had equivalent sand roughnesses of 0.11 mm, 0.21 mm, 0.31 mm, and 0.55 mm. The actual roughnesses were found to be nearly equal to the equivalent sand roughnesses. They determined the variation of the Darcy-Weisbach resistance coefficient, f_s, for each roughness for various values of the ratio of the injection velocity, v_s, to the average

channel velocity, $\bar{V}_s$. Values of the ratio of f_s, the resistance coefficient with seepage, to that without seepage, f, are tabulated in Table 11 for the two largest surface materials.

Table 11. Reduction of Darcy-Weisbach Resistance Coefficient with Flow out of a Rough Surface

$\frac{v_s}{\bar{V}_s}$	$\frac{f_s}{f}$	
d(mm)	0.31	0.55
0	1.00	1.00
0.001	0.86	0.83
0.002	0.73	0.70
0.003	0.61	0.60
0.004	0.49	0.50
0.005	0.39	0.41
0.006	0.30	0.33
0.007	0.22	0.27
0.008	0.15	0.21
0.009	0.09	0.17
0.010	0.04	0.13

Seepage into the Bed

Aerodynamicists have been concerned with suction in their studies of boundary-layer control. Excepting the case for which suction prevents boundary-layer transition the boundary shear stress is increased by

increasing amounts of suction, that is seepage into a porous bed. Incipient motion can be aided or hindered, depending upon the relative magnitudes of the boundary shear stress and the vertical piezometric-head gradient in Equation (34) or (35). Most of the investigations on suction have been for flow over flat plates or over airfoils. However, there have been some studies on the effects of suction on flow through smooth pipes.

Burnage (28) investigated the effect of sucking air through a porous cylindrical pipe on the pressure drop along the pipe and on the velocity distribution. He presents results on the increase of the local skin-friction coefficient with increasing rates of suction. Strictly speaking, because of the continual loss of fluid through the pipe wall, the flow within the pipe never fully develops. Nevertheless, the results obtained by Burnage for the most distant downstream station will be presented here in order that an idea may be attained as to the order-of-magnitude effect of suction on the increase in the boundary shear stress. Burnage shows graphically the variation of the local skin-friction coefficient with seepage, C_{fs}, with increasing rates of suction. At a station 74 pipe diameters downstream from the entrance the following expression holds

$$\frac{C_{fs}}{C_f} = 1 + 346 \frac{v_s}{\overline{V}_o} \tag{40}$$

in which C_f is the local skin-friction coefficient without suction, v_s is again the seepage velocity through the wall, and $\overline{V}_o$ is the mean velocity at the entrance to the tube. From Burnage's results one can also formulate that

$$\frac{C_{fs}}{C_f} = 1 + 310 \frac{v_s}{\bar{V}_s}, \quad \frac{v_s}{\bar{V}_s} \lesssim 2(10^{-3}) \tag{41}$$

in which $\bar{V}_s$ is the mean velocity at the measuring station, in this case 74 pipe diameters from the entrance to the pipe. For all tests conducted by Burnage the Reynolds number based on $\bar{V}_o$ was 40,800. From Equations (40) and (41) it is apparent that a ratio of seepage velocity to main stream velocity of 0.003 constitutes a doubling of the local drag coefficient. Burnage's results should be applied only to hydraulically smooth boundaries and only for $v_s/\bar{V}_o \lesssim 3.2\ (10^{-3})$ since his tests were restricted to these conditions.

There are meager data available on the effect of suction through porous rough surfaces on the boundary-layer flow characteristics. It has been shown by Dutton (29) that, for increasing rates of suction, the velocity profiles become more nearly uniform and that the level of turbulence intensity is markedly reduced. The boundary shear stress is increased by suction provided that transition is not prevented. There are no general functional relationships, to the writer's knowledge, for local skin-friction coefficients and velocity distributions for suction through rough porous surfaces.

Summary

In ascertaining the effect of a permeable bed on incipient motion of bed particles it is apparent that not only does the seepage force have to be considered, but also the alteration of the boundary-layer characteristics by the flow out of or into the bed. The seepage force does not aid incipient motion for flow out of a bed inasmuch as it disappears once a

bed particle rocks. The boundary shear stress is reduced for flow out of a bed and increased for flow into a bed; these statements hold true provided that boundary-layer transition is not enhanced by seepage out of the bed or prevented by seepage into the bed. Except when transition is caused by injection, seepage flow out of a permeable bed can only hinder, not aid, incipient motion. Seepage flow into a permeable bed can either hinder or enhance incipient motion, depending upon the relative magnitude of the boundary shear stress and the piezometric-head gradient at the bed.

The information presented in this chapter on the effect of seepage on boundary shear stress is to be used in two practical examples for which the seepage force is present. In the following the problems of seepage flow into and out of a sea bed under gravity waves and of seepage into canal beds are investigated as regards incipient motion.

CHAPTER VI

APPLICATION OF INCIPIENT-MOTION CRITERIA TO BED PARTICLES UNDER WATER WAVES

Wave-induced seepage flow under an ocean floor is subject to theoretical analysis provided that the characteristics of the waves are known. It is well known that water flows into the sand bed beneath a wave crest and out of the bed beneath a wave trough. The question arises as to what effect does this seepage flow have on incipient motion at the bed. For known wave shapes the piezometric-head variation within the bed can be determined from Laplace's equation, provided that Darcy's Law is satisfied. The effect of the seepage out of or into the bed on the boundary-layer characteristics will be estimated from the analysis presented in Chapter V. The analysis will be effected for both simple-harmonic and cnoidal waves.

Piezometric-Head Variation within the Bed under Oscillatory Waves

The piezometric-head variation within the sea bed must be known in order that the seepage force at the bed can be determined. In this analysis the seepage flow within the bed is assumed to obey Darcy's Law. The piezometric head thus satisfies Laplace's equation, Equation (32). A boundary-value problem then arises for the solution to

$$\frac{\partial^2 h}{\partial x^2} + \frac{\partial^2 h}{\partial y^2} = 0$$

and the appropriate boundary conditions. The boundary conditions can be explained with reference to Figure 15, in which the coordinate system is moving with the wave train. The wave height from trough to crest is H, the depth of water for the undisturbed state is D, the wavelength is L, the horizontal coordinate is x, and the vertical coordinate is y. In order to solve for the piezometric-head variation within the bed the pressure variation on the horizontal sea bed must be known. For assumed types of waves the pressure variation on the bed can be obtained from classical irrotational flow theory. The boundary conditions for the problem can be stated as

$$
\begin{aligned}
&y = 0 \;:\; h(x) = h_o(x) && ;\; 0 < x < L/2 \\
&y = -\infty :\; \partial h/\partial y = 0 && ;\; 0 < x < L/2 \\
&x = 0 \;;\; \partial h/\partial x = 0 && ;\; -\infty < y < 0 \\
&x = L/2 ;\; \partial h/\partial x = 0 && ;\; -\infty < y < 0
\end{aligned}
$$

The first condition gives the imposed periodic piezometric-head variation on the bed, $h_o(x)$. The second condition ensures that the vertical seepage velocity becomes zero at an infinite distance beneath the bed. The last two conditions make the vertical lines under the wave crest and wave trough streamlines.

The technique of separation of variables will be applied to Laplace's equation. A product solution

$$h(x,y) = X(x) \cdot Y(y)$$

is assumed. Upon differentiating and substituting, Laplace's equation becomes

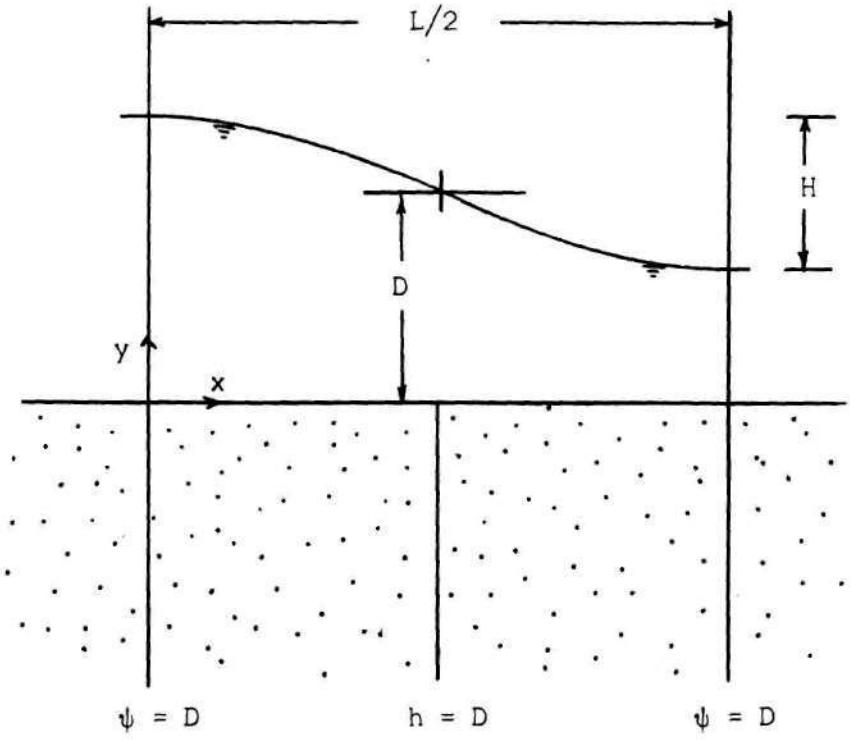

Figure 15. Definitive Sketch for Wave Parameters.

$$\frac{X''}{X} + \frac{Y''}{Y} = 0 , \tag{42}$$

in which X" and Y" denote $\frac{d^2X(x)}{dx^2}$ and $\frac{d^2Y(y)}{dy^2}$, respectively. Equation (42) can be rewritten as

$$\frac{X''}{X} = -\frac{Y''}{Y} = -\lambda^2$$

in which λ is a constant. Hence, two, linear, total differential equations evolve

$$\frac{d^2X}{dx^2} + \lambda^2 X = 0 , \tag{43a}$$

and

$$\frac{d^2Y}{dy^2} - \lambda^2 Y = 0 , \tag{43b}$$

from which solutions

$$X(x) = a_1 \cos \lambda x + a_2 \sin \lambda x ,$$

and

$$Y(y) = a_3 \exp (\lambda y) + a_4 \exp (-\lambda y)$$

exist, in which a_1, a_2, a_3, and a_4 are constants. The boundary condition

$$\left[\frac{\partial h}{\partial x} \right]_{x=o} = 0$$

requires that

$$\frac{\partial}{\partial x} [X(x)Y(y)] = [- \lambda a_1 \sin \lambda x + \lambda a_2 \cos \lambda x] \cdot [Y(y)] = 0$$

or

$$X'(0) = \lambda a_2 = 0$$

Hence, $a_2 = 0$. The boundary condition

$$\left[\frac{\partial h}{\partial x} \right]_{x=L/2} = 0 = -\lambda a_1 \sin \frac{\lambda L}{2}$$

yields

$$\frac{\lambda L}{2} = n\pi, \quad \text{or} \quad \lambda_n = \frac{2n\pi}{L} .$$

The eigenvalues of the problem are $2n\pi/L$.

The condition of

$$\lim_{y \to -\infty} \left[\frac{\partial h}{\partial y}\right] = 0$$

results in $a_4 = 0$. A particular solution of the type

$$h(x, y) = A_o + \sum_{n=1}^{\infty} A_n \cos(2n\pi x/L) \exp(2n\pi y/L) \tag{44}$$

exists. The A's are determined from the given piezometric-head variation at the sea bed, and are the Euler coefficients for a Fourier cosine series.

$$A_o = \frac{1}{L} \int_o^L h_o(x)\, dx \tag{45a}$$

$$A_n = \frac{2}{L} \int_o^L h_o(x) \cos(2n\pi x/L)\, dx; \quad n = 1,2,3,... \tag{45b}$$

Simple-Harmonic Waves

For waves of small amplitude, the piezometric-head variation at the sea bottom can be obtained from wave theory, Lamb (30), in the form

$$h_o(x) = \frac{H}{2 \cosh(2\pi D/L)} \cos(2\pi x/L) + D$$

Thus

$$h = \frac{H}{2 \cosh (2\pi D/L)} \left[\cos(2\pi x/L) \exp(2\pi y/L)\right] + D \qquad (46)$$

from the method described above.

The stream function ψ, can be obtained by integrating

$$\psi = - \int \left(\frac{\partial h}{\partial x} \right) dy + \text{const.} \qquad (47)$$

Upon carrying out the integration

$$\psi = \frac{H}{2 \cosh (2\pi D/L)} \left[\sin (2\pi x/L) \exp (2\pi y/L)\right] + D \qquad (48)$$

These solutions, Equations (46) and (48), have been previously obtained for a finite strip, Putnam (31). Figure 16 is a graphical presentation of the solution for the semi-infinite strip. The vertical piezometric-head gradient variation at the bed

$$\left[\frac{\partial h}{\partial y} \right]_{y=o} = \frac{\pi}{\cosh 2\pi D/L} \frac{H}{L} \cos 2\pi x/L \qquad (49)$$

Bed particles under the wave crest experience the maximum downward seepage force whereas ones under the wave trough experience the maximum upward seepage force.

Cnoidal Waves

For finite-amplitude waves having $D/L < 0.1$, the simple-harmonic wave profile does not adequately describe the wave shape. These finite-amplitude, shallow-water waves are generally called cnoidal waves and are represented by elliptic functions. For cnoidal waves of the first

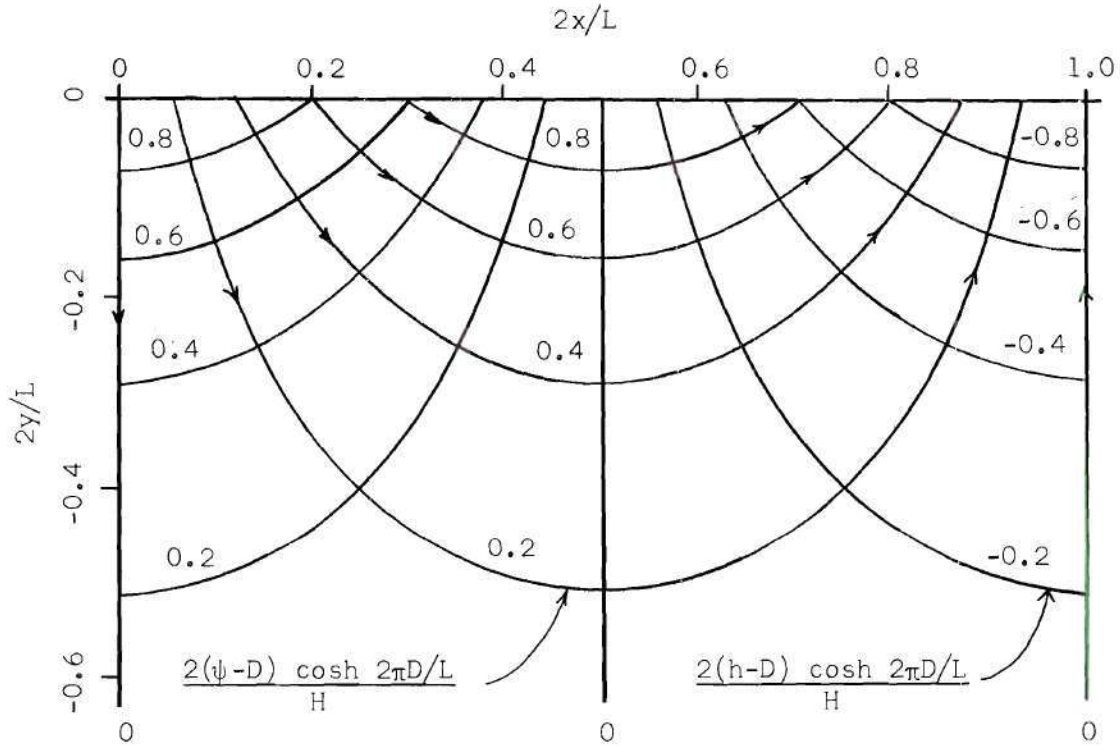

Figure 16. Potential Pattern in the Bed under a Simple-Harmonic Wave.

approximation, the piezometric head at the sea bottom is given by the hydrostatic relationship, Wiegel (32)

$$h_o(x) = y_t + H\ cn^2 \left[2\ K(k)\ \frac{x}{L}\ ,\ k \right] \qquad (50)$$

in which y_t is the vertical distance from the sea bottom to the wave trough, H is the wave amplitude from trough to crest, cn is the Jacobian elliptic function akin to the cosine function, and $K(k)$ is the complete elliptic integral of the first kind with modulus k. Since herein k is a real number with a range $0 \leq k \leq 1$, the cn function has a single period of $4K(k)$. This means that the cn^2 function has a

period of $2K(k)$. For convenience the parameter $K(k)$ will be denoted by simply K. The wavelength, L, is given by

$$L = \left[\frac{16D^3}{3H} \right]^{1/2} kK \tag{51}$$

in which D is the depth of water for the undisturbed state. As Equation (50) is periodic and continuous everywhere, the boundary condition at the bed can easily be represented by a Fourier series. From Jacobi (33),

$$cn^2 \left[2K \frac{x}{L}, k\right] = \frac{1}{k^2} \left[\frac{E}{K} + k^2 - 1 \right] + \frac{2\pi^2}{k^2K^2} \sum_{n=1}^{\infty} \frac{nq^n}{1-q^{2n}} \cos(2n\pi x/L) \tag{52}$$

in which $E = E(k)$ is the complete elliptic integral of the second kind with modulus k and

$$q = \exp(-\pi K'/K) \tag{53}$$

in which q is referred to as Jacobi's nome. $K' = K(k')$ is the associated complete elliptic integral of the first kind and k' is the complementary modulus. Since $q < 1$, the series in Equation (52) can be shown to be both absolutely and uniformly convergent by use of the Weierstrass M-test, Copson (34).

By using Equations (50) and (52) along with Equations (45a) and (45b), the solution for the piezometric head in the bed is represented by

$$h = y_t + \frac{H}{k^2} \left[\frac{E}{K} + k^2 - 1 \right] + \frac{2\pi^2 H}{k^2K^2} \sum_{n=1}^{\infty} \frac{nq^n}{1-q^{2n}} \cos(2n\pi x/L)\exp(2n\pi y/L) \tag{54}$$

Differentiating Equation (54) to obtain the vertical piezometric-head gradient at the bed

$$\left[\frac{\partial h}{\partial y}\right]_{y=o} = \frac{4\pi^3}{k^2K^2}\frac{H}{L}\sum_{n=1}^{\infty}\frac{n^2q^n}{1-q^{2n}}\cos(2n\pi x/L) \tag{55}$$

For bed particles under the wave crest

$$\left[\frac{\partial h}{\partial y}\right]_{\substack{y=o,\\ x=o}} = \frac{4\pi^3}{k^2K^2}\frac{H}{L}\sum_{n=1}^{\infty}\frac{n^2q^n}{1-q^{2n}} \tag{56}$$

and, under the wave trough

$$\left[\frac{\partial h}{\partial y}\right]_{\substack{y=o,\\ x=L/2}} = \frac{4\pi^3}{k^2K^2}\frac{H}{L}\sum_{n=1}^{\infty}\frac{n^2q^n}{1-q^{2n}}\cos n\pi \tag{57}$$

In evaluating the infinite series in Equations (56) and (57), the following procedure is followed. The series in Equation (56) is expressed as an approximation

$$\sum_{n=1}^{\infty}\frac{n^2q^n}{1-q^{2n}} \simeq \sum_{n=1}^{m}\frac{n^2q^n}{1-q^{2n}} + \sum_{m}^{\infty} n^2q^n \tag{58}$$

in which m is an integer large enough such that

$$\sum_{n=m}^{\infty} n^2q^n \cong \sum_{n=m}^{\infty}\frac{n^2q^n}{1-q^{2n}}$$

The value of m depends upon the magnitude of the modulus k and upon the degree of accuracy required in the summation. Likewise, the series in

Equation (57) can be expressed as

$$\sum_{n=1}^{\infty} \frac{n^2 q^n}{1-q^{2n}} \cos n\pi \cong \sum_{n=1}^{m} \frac{n^2 q^n}{1-q^{2n}} \cos n\pi + \sum_{m}^{\infty} n^2 q^n \cos n\pi \qquad (59)$$

The sum of the following infinite series further facilitated the evaluation of Equations (56) and (57). From Jolley (35)

$$\sum_{n=1}^{\infty} n^2 q^n = \frac{q(1+q)}{(1-q)^3}$$

and

$$\sum_{n=1}^{\infty} n^2 q^n \cos n\pi = -\frac{q(1-q)}{(1+q)^3}$$

Hence Equation (56) becomes

$$\left[\frac{\partial h}{\partial y}\right]_{\substack{y=o,\\ x=o}} = \frac{4\pi^3}{k^2K^2} \frac{H}{L} \left[\sum_{n=1}^{m} \frac{n^2 q^{3n}}{1-q^{2n}} + \frac{q(1+q)}{(1-q)^3} \right] \qquad (60)$$

Equation (57) becomes

$$\left[\frac{\partial h}{\partial y}\right]_{\substack{y=o,\\ x=L/2}} = \frac{4\pi^3}{k^2K^2} \frac{H}{L} \left[\sum_{n=1}^{m} \frac{n^2 q^{3n}}{1-q^{2n}} \cos n\pi - \frac{q(1-q)}{(1+q)^3} \right] \qquad (61)$$

The infinite series in Equations (56) and (57) were evaluated by utilizing Equations (60) and (61). The finite series in Equations (60) and (61) were evaluated by using the facilities of the Rich Electronic Computer Center. In Table 12 are listed values of the infinite series in Equations

(56) and (57) times the quantity $4\pi^3/k^2K^2$ (these products are $[\partial h/\partial y]_{y=o}/(H/L)$ for bed particles under the wave crest and wave trough, respectively).

Table 12. Values of Jacobian Elliptic Functions and of Two Infinite Series

			$\frac{[\partial h/\partial y]_{y=o}}{H/L}$	
k^2	K	q	Under Wave Crest	Under Wave Trough
0.500000	1.85408	0.043214	3.71980	-2.63370
0.600000	1.94957	0.057020	3.91932	-2.48618
0.700000	2.07536	0.074690	4.18507	-2.30767
0.800000	2.25721	0.099274	4.57419	-2.07822
0.900000	2.57809	0.140173	5.27170	-1.74353
0.950000	2.90834	0.179316	5.99901	-1.47477
0.970000	3.15588	0.206880	6.54773	-1.31309
0.990000	3.69564	0.262196	7.74837	-1.04847
0.999000	4.84113	0.360738	10.29234	-0.72777
0.999900	5.99159	0.438831	12.83133	-0.56118
0.999990	7.14277	0.501134	15.35932	-0.45997
0.999999	8.29405	0.551573	17.87953	-0.39109

It is readily apparent from Table 12 that, for a given value of H/L, the bed particles beneath a cnoidal wave crest experience a larger seepage force than ones beneath a wave trough. This difference is caused by the fact that the wave crests are highly peaked whereas the wave troughs are quite flat. The peakedness and the flatness become more and more pronounced as k^2 increases. In order to further illustrate these characteristics several cnoidal wave profiles will be presented. From Wiegel (32)

the cnoidal wave shape

$$\eta = H\, cn^2\,(2Kx/L) \tag{62}$$

in which η is the vertical distance from the elevation of the wave trough to the free surface. The cnoidal wave shapes are shown in Figure 17 for four values of the modulus squared, k^2. This figure clearly illustrates the asymmetry of a cnoidal wave.

The Effect of Seepage Flow on Incipient Motion

The problem of ascertaining the degree to which seepage out of or into a sea bed affects incipient motion is quite complicated. Only directly beneath the wave crest and the wave trough is the seepage velocity normal to the bed. The degree to which the seepage alters the flow characteristics near the bed is not known. Seepage into the bed may prevent boundary-layer transition whereas seepage out of the bed may augment it. In the following some calculations are effected in order to give an order-of-magnitude effect of seepage on incipient motion under oscillatory waves.

Simple-Harmonic Waves

Order-of-magnitude effects of seepage flow on incipient motion will be determined by considering only those bed particles under the wave trough and the wave crest. At these two locations the seepage flow is perpendicular to the bed and the horizontal velocity of the water outside the boundary layer is a maximum. Incipient motion would be expected to occur at these locations.

Bed Particles Beneath Wave Trough. Provided that boundary-layer

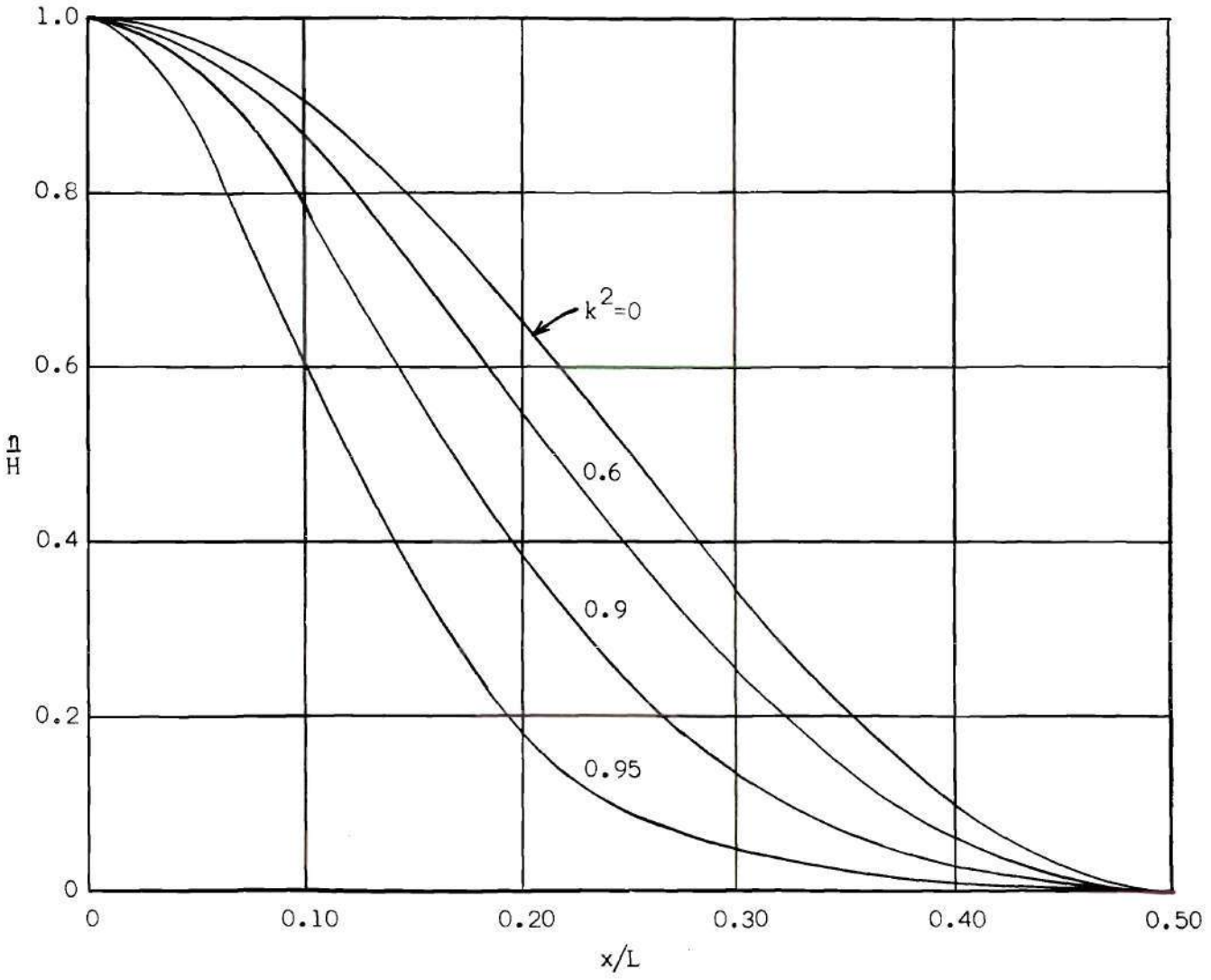

Figure 17. Various Cnoidal Wave Profiles.

transition is not caused by injection, seepage out of the bed can only hinder incipient motion. The seepage force can not aid incipient motion and, therefore, is not included in the incipient-motion criterion. The degree to which flow out of the bed beneath a wave trough hinders incipient motion depends upon the degree to which the flow characteristics at the bed are altered. The effect of seepage on incipient motion is ascertained by comparing the flow characteristics at the bed with seepage with those for which there is no seepage. The physical case of no seepage could be visualized as several sand layers resting on an impermeable bed.

For bed particles immersed in a laminar boundary layer the reduction in the boundary shear stress by seepage is determined by using the results of Table 10. In order that the ratio τ_s/τ_c can be determined, realistic values of the vertical piezometric-head gradient at the bed, $[\partial h/\partial y]_{y=o}$, must be known. The maximum value of $[\partial h/\partial y]_{y=o}$ for which the bed is not in motion is limited by the condition of incipient motion. Realistic possible values of $[\partial h/\partial y]_{y=o}$ are estimated from computed values of the wave parameters corresponding to incipient motion without seepage. This procedure is used because values of $[\partial h/\partial y]_{y=o}$ at incipient motion are not known, and can only be estimated. As found by Manohar (7) and by the writer, incipient motion occurs in a laminar boundary layer for bed particles having a specific gravity of approximately 2.5 and having a mean diameter less than about 0.3 mm. For incipient motion of bed particles immersed in a laminar boundary layer, Equation (14) can be expressed in terms of wave parameters as

$$\frac{H_c \sqrt{\mu}\ \sqrt{\rho}}{T^{3/2}\ (\gamma_s-\gamma)\ d\ \tan\Phi\ \sinh 2\pi D/L} = 0.024 \qquad (63)$$

The wave celerity of a simple-harmonic wave

$$c = \frac{L}{T} = \sqrt{\frac{gL}{2\pi} \tanh 2\pi D/L} \tag{64}$$

Introducing the wave period, T, into Equation (63)

$$\frac{H_c}{L} = \frac{0.15\ (s-1)\ d \tan \Phi \cosh 2\pi D/L}{\sqrt{\nu T}} \tag{65}$$

Assuming $s = 2.60$ (quartz sand in sea water) and $\Phi = 25°$ (sands less than 0.3 mm)

$$\frac{H_c}{L} = \frac{0.115\ d \cosh 2\pi D/L}{\sqrt{\nu T}}$$

For $\nu = (10^{-5})$ ft^2/sec, $D/L = 0.10$, and for several realistic values of the wave period T, computed values of H_c/L are listed in Table 13.

Table 13. Values of H_c/L at Incipient Motion Without Seepage for a Laminar Boundary Layer

	$\frac{H_c}{L}$		
T(sec)	d(mm) = 0.1	0.2	0.3
6	0.019	0.038	0.057
8	0.015	0.030	0.045
10	0.015	0.029	0.042
12	0.012	0.025	0.038

The maximum value of H_c/L for incipient motion without seepage is 0.057. The corresponding maximum vertical piezometric-head gradient, which would occur for a permeable bed under the same wave, is computed from Equation (49)

$$\left[\frac{\partial h}{\partial y}\right]_{\substack{y=o,\\ x=o}} = -\left[\frac{\partial h}{\partial y}\right]_{\substack{y=o,\\ x=L/2}} = \left[\frac{\partial h}{\partial y}\right]_o = \frac{\pi}{\cosh 2\pi D/L}\,\frac{H}{L} \qquad (66)$$

For bed particles immersed in a laminar boundary layer the corresponding maximum value of $[\partial h/\partial y]_o$ is, from $H_c/L = 0.057$ and Equation (66), 0.14. According to Table 10, the maximum decrease in the boundary shear stress for $[\partial h/\partial y]_o = 0.14$ is 4 per cent, that is $\tau_s/\tau_c = 0.96$. This analysis shows that the effect of seepage on incipient motion is not significant for a laminar boundary layer.

For bed particles immersed in a turbulent boundary layer at incipient motion, a similar analysis can be effected. In this case the effect of the seepage on the alteration of the flow characteristics above the bed is determined by using the results given in Table 11 for the reduction of the Darcy-Weisbach resistance coefficient for flow out of a rough surface. In order that the ratio f_s/f can be determined, the velocity ratio $v_s/\bar{V}_s$ must be known. The mean channel velocity, $\bar{V}_s$, will be equated to U_m, the velocity outside the boundary layer without seepage, in order that some order-of-magnitude calculations may be made. The seepage velocity, v_s, depends on the permeability, κ, and the vertical piezometric-head gradient, $[\partial h/\partial y]_o$. Realistic values of $[\partial h/\partial y]_o$ must be known in order that values of f_s/f can be determined from Table 11. The ratio f_s/f will be determined by entering Table 11

with the ratio v_s/U_{mc}, in which U_{mc} is the critical maximum velocity outside the boundary layer. Outside the boundary layer the bottom velocity is obtained from irrotational flow theory, Lamb (30), to be

$$u = \frac{\pi H}{T \sinh 2\pi D/L} \cos 2\pi x/L \qquad (67)$$

in which T is the wave period. Considering only those bed particles beneath the wave crest and wave trough

$$|u|_{x=o} = |u|_{x=L/2} = U_m = \frac{\pi H}{T \sinh 2\pi D/L} \qquad (68)$$

Realistic values of H_c/L for which there is no seepage, and corresponding values of $[\partial h/\partial y]_o$ based on this H_c/L, are computed for various ratios of D/L and for particular bed-particle characteristics. The criterion for incipient motion developed in Chapter III for oscillatory flow for which there was no seepage

$$\frac{u_{dc}}{\sqrt{(s-1)\ gd \tan \Phi}} = 1.9$$

It was found that, in analyzing Manohar's incipient-motion results for the oscillating plate, the velocity u_d was nearly always 0.6 times U_m, the maximum velocity of the oscillating plate. For incipient motion without seepage

$$\frac{U_{mc}}{\sqrt{(s-1)\ gd \tan \Phi}} = 3.2 \qquad (69)$$

In terms of wave parameters

$$\frac{H_c}{T \sinh 2\pi D/L \sqrt{(s-1)\ gd \tan \Phi}} = 1.0 \qquad (70)$$

Utilizing the wave period T from Equation (64)

$$H_c/L = 2.5 \sqrt{(d/D)(s-1) \tan \Phi} \sqrt{(D/L) \tan 2\pi\ D/L} \cosh 2\pi\ D/L \qquad (71)$$

for $\Phi = 35°$ and $s = 2.60$

$$H_c/L = 2.7 \sqrt{d/D}\ \sqrt{(D/L) \tanh 2\pi\ D/L} \cosh 2\pi\ D/L$$

Tabulated below are values of H_c/L for various values of D/d and D/L.

Table 14. Values of H_c/L at Incipient Motion Without Seepage for a Turbulent Boundary Layer

	$\frac{H_c}{L}$		
D/L	D/d = 100	1000	10000
0.04	0.028	0.008	0.003
0.06	0.042	0.013	0.004
0.08	0.058	0.018	0.006
0.10	0.076	0.024	0.008

The maximum value of H_c/L is 0.076. For seepage under the same wave, the corresponding maximum value of $[\partial h/\partial y]_o$ is 0.20. Now that maximum realistic values of $[\partial h/\partial y]_o$ are known, the ratio f_s/f can be determined from Table 11 by utilizing v_s/U_{mc}. Using Equations (37), (38), and (69)

$$\frac{v_s}{U_{mc}} = 1.5(10^{-4}) \frac{\gamma d^{3/2} [\partial h/\partial y]_o}{\mu \sqrt{(s-1)\, g \tan \Phi}} \qquad (72)$$

If, for example, $\gamma = 62.4$ lb/ft^3, $s = 2.60$, $\mu = 2.1(10^{-5})$ $\frac{\text{lb-sec}}{\text{ft}^2}$, and $\Phi = 35^o$

$$\frac{v_s}{U_{mc}} = 0.0143\, d^{3/2} \left[\frac{\partial h}{\partial y}\right]_o \; ; \quad d \text{ in mm}$$

For a maximum value of $[\partial h/\partial y]_o$ of 0.2

$$\frac{v_s}{U_{mc}} = 0.00286\, d^{3/2} \; ; \; d \text{ in mm}$$

For $d = 0.31$ mm, $v_s/U_{mc} = 0.0005$, and, from Table 11, $f_s/f = 0.9$. For $d = 0.55$ mm, $v_s/U_{mc} = 0.0012$, and $f_s/f = 0.8$. The ratio v_s/U_{mc} increases with increasing sand size and, consequently, f_s/f decreases. The boundary shear stress with seepage, τ_s, continually decreases, all other quantities held constant, as the sand size is increased. Seepage out of the wave trough apparently has more of an effect on incipient motion with a turbulent boundary layer than with a laminar boundary layer.

The effect on seepage on incipient motion of bed particles beneath the wave trough depends on the permeability of the sand or, in other words, the size of the sand grains. For sand grains for which incipient motion occurs in a laminar boundary layer ($d \lesssim 0.3$ mm), the effect of seepage is probably insignificant. For sand grains for which incipient motion occurs in a turbulent boundary layer ($d \gtrsim 0.3$ mm) the effect of seepage may be significant. The hindrance of the seepage flow under the

wave trough on incipient motion becomes more and more pronounced for larger and larger bed particles.

Bed Particles Beneath Wave Crest. Seepage into the bed may aid or hinder incipient motion, depending on the relative magnitude of the boundary shear stress, τ_s, and the vertical piezometric-head gradient, $[\partial h/\partial y]_o$. The seepage force must be included in any incipient-motion criterion.

For incipient motion of bed particles immersed in a laminar boundary layer with seepage, Equation (34) applies for bed particles beneath the wave crest

$$\frac{\tau_{cs}}{\left[(\gamma_s-\gamma) + 0.9\ (1+e)\ \gamma[\partial h/\partial y]_o\right] d\ \tan\Phi} = 0.19$$

For no seepage

$$\frac{\tau_c}{(\gamma_s-\gamma)\ d\ \tan\Phi} = 0.19$$

In comparing the case of seepage to the case of no seepage the ratio τ_{cs}/τ_c is meaningful for the same bed particles. The ratio

$$\frac{\tau_{cs}}{\tau_c} = 1 + 0.9\ \frac{(1+e)}{(s-1)}\left[\frac{\partial h}{\partial y}\right]_o \qquad (73)$$

A realistic value of $(1+e)/(s-1)$ is unity. If the maximum possible value of $[\partial h/\partial y]_o = 0.14$ is used

$$\frac{\tau_{cs}}{\tau_c} = 1.13$$

This calculation means that, if $\tau_s/\tau_c < 1.13$, seepage may hinder incipient motion. If $\tau_s/\tau_c > 1.13$ seepage aids incipient motion for all conditions listed in Table 13. For any given wave the quantity τ_s is not easily found. The value of τ_s would have to come from a solution to the Navier-Stokes equations with seepage included. Hunt (36) obtained a solution for the flow within the bed under small-amplitude water waves by satisfying all the viscous boundary conditions. His interest was the damping effect of the bed, not the boundary-shear variation. The technique utilized by Hunt could conceivably be applied to the determination of τ_s. At the present the boundary shear stress variation with seepage is not known.

For bed particles immersed in a turbulent boundary layer Equation (35) would apply. Inasmuch as no data are available on the effect of suction on an oscillatory turbulent boundary layer, even order-of-magnitude effects of seepage on incipient motion are difficult to determine. However, for extremely large amounts of suction -- which correspond in this instance to large values of the permeability as $[\partial h/\partial y]_o$ at incipient motion is limited in magnitude -- the boundary layer is negligibly thin. This condition will exist for large diameter sand grains as the permeability $\kappa \propto d^2$. For negligibly thin boundary layers $u_{dcs} = U_{mcs}$. At incipient motion with seepage, Equation (35) may be written

$$\frac{U_{mcs}}{\sqrt{\left[(s-1) + 0.9\ (1+e)\ \left[\frac{\partial h}{\partial y}\right]_o\right] gd \tan \Phi}} = 1.9 \qquad (74)$$

At incipient motion without seepage, Equation (69) applies. Combining

Equations (69) and (74)

$$\frac{U_{mcs}}{U_{mc}} = 0.6 \sqrt{1 + 0.9 \frac{(1+e)}{(s-1)} \left[\frac{\partial h}{\partial y}\right]_o} \qquad (75)$$

If the maximum value of $[\partial h/\partial y]_o$ of 0.20 is used, and if $(1+e)/(s-1) = 1$,

$$\frac{U_{mcs}}{U_{mc}} = 0.65$$

According to this analysis the maximum bottom velocity outside the boundary layer with seepage need be only 0.65 times that without seepage to move the same bed particles.

These approximate analyses have shown that seepage into the bed under a wave crest may either enhance or delay incipient motion of bed particles. For very small sand particles, for which the suction velocity is small, the seepage force likely hinders incipient motion. On the other hand, for extremely large sand particles for which the suction velocity is sizeable, incipient motion is most probably enhanced, as the boundary shear stress is greatly increased by the seepage.

Cnoidal Waves

It would be expected that seepage flow induced by cnoidal waves would have, because of their asymmetric shape, a greater effect on incipient motion than simple-harmonic waves. The vertical piezometric-head gradient at the bed is greater under the sharp wave crests than under the flat wave troughs. For finite-amplitude, shallow-water waves the vertical piezometric-head gradient at the bed deviates considerably from that produced by a simple-harmonic wave. The piezometric-head gradient is considerably larger under the wave crest, and considerably smaller

under the wave trough, for a cnoidal wave than for a simple-harmonic wave. For sand sizes in the realistic range, however, incipient motion occurs long before waves reach finite-amplitude size. The cnoidal waves for which incipient motion occurs are normally of small amplitude and are quite similar in shape to simple-harmonic waves.

Calculations may be performed which show that, for incipient motion of sands of realistic size, the wave characteristics of the cnoidal wave and simple-harmonic wave are nearly identical. Small amplitude cnoidal waves correspond to small values of the elliptic modulus, k, Equation (51)

$$H = \frac{16}{3} k^2 K^2 \frac{D^3}{L^2}$$

It can be shown that, for shallow-water waves, as $k^2 \rightarrow 0$, values of the properties of the cnoidal wave approach those of the simple-harmonic wave. For example, the maximum bottom velocity under a cnoidal wave, which occurs at the crest, is, from Keller (37)

$$U_m = \sqrt{gD} \frac{H}{D} \left[1 - \frac{1}{k^2} \left[\frac{E}{K} - (1 - k^2) \right] \right] \qquad (76)$$

From Laitone (38), the following expansion holds for small values of k^2

$$\frac{E}{K} = 1 - \frac{1}{2} k^2 - \frac{1}{16} k^4 \ldots \qquad (77)$$

Therefore, in the limit

$$\lim_{k^2 \rightarrow o} U_m = \frac{1}{2} \sqrt{gD} \frac{H}{D}$$

For a simple-harmonic wave of small amplitude in shallow water the wave celerity $c = \sqrt{gD}$. As the ratio D/L approaches zero, the bottom velocity for a simple-harmonic wave, Equation (68), becomes

$$\lim_{D/L \to o} U_m = \frac{\pi H}{2\pi (D/L) T} = \frac{Hc}{2D} = \frac{1}{2} \sqrt{gD} \frac{H}{D}$$

Thus it is proven that, for small amplitude waves in shallow water, cnoidal theory and simple-harmonic theory give essentially the same results.

Inasmuch as the analysis here is nearly qualitative in nature and since the cnoidal wave and simple-harmonic wave are nearly identical for the conditions considered here, no calculations are presented for the effect of seepage on incipient motion of bed particles under cnoidal waves.

Summary

The effect of the seepage force on the sea bed on incipient motion of the top layer of bed particles has been demonstrated. The seepage flow out of the bed under a wave trough can aid incipient motion if and only if boundary layer transition occurs. Except for the case of transition of the boundary layer the seepage out of the bed under a wave trough delays incipient motion of those bed particles inasmuch as the boundary shear stress is reduced by injection. For a laminar boundary layer the boundary shear stress would not be expected to be decreased much more than 4 per cent by seepage out of the bed. For a turbulent boundary layer the Darcy-Weisbach resistance coefficient could be expected to be reduced more than 20 per cent by seepage out of the bed. For large sand grains and hence greater permeabilities the reduction in boundary shear stress may

be more than 20 per cent. The seepage flow into the sea bed under a wave crest may aid or hinder incipient motion, depending upon the relative magnitude of the boundary shear stress and the vertical piezometric-head gradient at the bed. For a laminar boundary layer the boundary shear stress under the wave crest has to be increased more than 13 per cent by seepage in order to aid incipient motion. For a turbulent boundary layer the increase in boundary shear stress by the suction of the water into the bed is probably great enough to aid incipient motion, especially for large sand grains.

For large sand grains seepage out of the bed hinders, whereas seepage into the bed aids, incipient motion. The reason for this fact is that the piezometric-head gradient is independent of the permeability of the sand whereas the boundary shear stress is considerably influenced by the permeability of the sand. For very small sand grains for which the permeability and hence the seepage velocity is quite small, seepage out of the bed has no effect on incipient motion and seepage into the bed hinders incipient motion only to a slight degree.

In reality, the permeable bed under water waves most likely has no discernible effect on incipient motion since the boundary shear stress and the piezometric-head gradient both depend on the same quantity, the wave amplitude, H. In the following chapter an example of seepage into a bed for which the boundary shear stress and piezometric-head gradient depend on independent quantities is investigated.

CHAPTER VII

APPLICATION OF INCIPIENT-MOTION CRITERIA TO BED PARTICLES ON A CANAL BED

The seepage of water through stream beds or irrigation canal beds is another example for which the seepage force may affect incipient sediment motion. It is well known that, after flood waters subside, stream banks may slough off due to the high ground-water level, thereby decreasing the stability of the banks. The problem to be considered here is not one of slope instability of a mass of bed material but one of incipient motion of the uppermost layer of bed particles; namely, those on the bottom of a stream bed or irrigation canal bed. Obviously the elevation of the ground-water table with respect to the free surface in the stream or canal is quite important as to the magnitude and direction of the seepage force at the bed. The seepage flow may, of course, be out of or into the bed. The permeability of the bed is quite important as regards the effect of the seepage on the boundary shear stress.

In the following the piezometric-head gradient at the bed is given for seepage flow out of a trapezoidal and out of an infinitely wide canal. The effect of the seepage force on incipient motion is discussed for those two canal shapes.

Piezometric-Head Gradient for Seepage Flow out of Canals

The magnitude of the vertical piezometric-head gradient along the

bottom of any canal bed depends upon the geometry of the canal and upon the difference in elevation of the free surface of the water in the canal and the ground-water table. The geometric shapes to be considered here are a trapezoidal canal and an infinitely wide canal. The elevation of the ground-water table is assumed to be an infinite distance, at least mathematically, below the canal.

Trapezoidal Canal

The boundary-value problem for seepage from a trapezoidal canal to the ground-water table level at infinity has been solved by Wedernikov (39). His main interest was the gross quantity of flow rather than the point-by-point variation in seepage velocity, or piezometric-head gradient. However he did present values of the piezometric-head gradient at the bed for one trapezoidal canal. The variation of the piezometric-head gradient is shown in Figure 18 for the trapezoidal canal for which Wedernikov gives a solution.

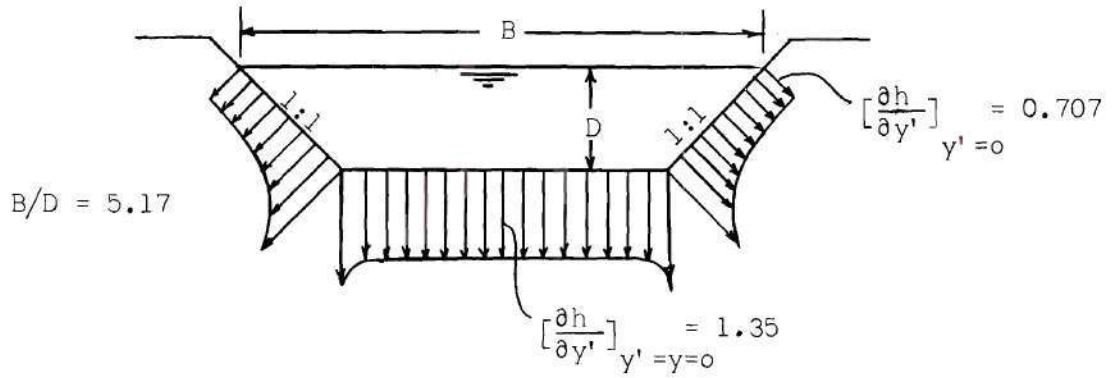

Figure 18. Variation of Piezometric-Head Gradient on Trapezoidal Canal Bed and Banks.

The vertical piezometric-head gradient is 1.35 at the center of the bottom of the canal bed. For canals wider than $B/D = 5.17$ the vertical piezometric-head gradient at the center of the bed is less than 1.35.

Infinitely Wide Canal

For any canal that can be considered infinitely wide the piezometric-head gradient at the bed approaches unity.

The Effect of Seepage Flow on Incipient Motion

The seepage force on the bed particles for the two canals investigated is quite large compared to that on bed particles beneath a wave. The seepage force and the flow quantities are independent for the canals; whereas the seepage force and the flow quantities for the waves depend upon the same quantity, the wave amplitude. It would be expected then, that a permeable bed would play more of a role on incipient motion of bed particles lying on a canal bed than for the same particles resting on a sea bed. The seepage force per unit volume depends only on the piezometric-head gradient for a given fluid, and is independent of the permeability of the bed material. On the other hand, however, the boundary shear stress is very dependent on the permeability of the bed material. The permeability of the bed material, and hence for a given fluid the grain size of the bed material, is a very important variable as regards the effect of a permeable bed on incipient motion.

For very fine bed materials incipient motion occurs for the bed particles immersed in a laminar sublayer. If there were no seepage, Equation (14) applies

$$\frac{\tau_c}{(\gamma_s-\gamma)\ d\ \tan\Phi} = 0.19$$

For the case of incipient motion for which there is seepage, Equation (34) is applicable

$$\frac{\tau_{cs}}{\left[(\gamma_s-\gamma) + 0.9\ (1+e)\ \gamma\left[\frac{\partial h}{\partial y}\right]_{y=o}\right] d\ \tan\Phi} = 0.19$$

The ratio of the two boundary shear stresses

$$\frac{\tau_{cs}}{\tau_c} = 1 + 0.9\ \frac{(1+e)}{(s-1)}\left[\frac{\partial h}{\partial y}\right]_{y=o} \qquad (78)$$

A realistic value of the ratio $(1 + e)/(s - 1)$ is unity. Hence Equation (78) reduces to

$$\frac{\tau_{cs}}{\tau_c} = 1 + 0.9\left[\frac{\partial h}{\partial y}\right]_{y=o}$$

For those bed particles at the centerline of the trapezoidal canal investigated herein, τ_{cs}/τ_c must be 2.2 or greater for incipient motion with seepage to occur. For the infinitely wide canal, $\tau_{cs}/\tau_c = 1.9$. In order that incipient motion occurs with seepage the boundary shear stress has to be roughly twice that for incipient motion without seepage. For extremely small bed particles the seepage velocity, v_s, is negligible. In this case the boundary shear stress is essentially independent of seepage. Equation (41) will be used in order to determine roughly what size bed particles are necessary to have a considerable retarding effect on incipient motion. Equation (41) is

$$\frac{C_{fs}}{C_f} = 1 + 310 \frac{v_s}{\bar{V}_s}$$

The seepage velocity is, from Equations (37) and (38)

$$v_s = \frac{\gamma d^2}{2000 \mu} \left[\frac{\partial h}{\partial y}\right]_{y=o} \tag{79}$$

The mean velocity, $\bar{V}_s$, in the canal will be computed on the basis of a formula given by Keulegan (40) for smooth channels

$$\frac{\bar{V}}{u^*} = 3.3 + 5.75 \log_{10} \frac{u^* y_o}{\nu} \tag{80}$$

Although Keulegan developed Equation (80) for an impervious boundary it will be utilized here for the case of small seepage flow rates. For small bed particles the velocity distribution in the canal would not be expected to be altered by seepage. At the condition of incipient motion Equation (80) becomes

$$\bar{V}_{cs} = u^*_{cs} \left[3.3 + 5.75 \log_{10} \frac{u^*_{cs} y_o}{\nu}\right] \tag{81}$$

in which u^*_{cs} is the critical shear velocity with seepage. Upon introducing Equations (79) and (81) into Equation (41)

$$\frac{C_{fs}}{C_f} = 1 + \frac{0.155 \gamma d^2 \left[\frac{\partial h}{\partial y}\right]_{y=o}}{\mu u^*_{cs} \left[3.3 + 5.75 \log_{10} \frac{u^*_{cs} y_o}{\nu}\right]}$$

Using the incipient-motion condition for bed particles in a laminar sublayer, Equation (34), along with the fact that $u^*_{cs} = \sqrt{\tau_{cs}/\rho}$

$$\frac{C_{fs}}{C_f} = 1 + \frac{0.355\,\gamma d^2 \left[\frac{\partial h}{\partial y}\right]_{y=o}}{\mu \sqrt{\left[(s-1) + 0.9\,(1+e)\left[\frac{\partial h}{\partial y}\right]_{y=o}\right] gd \tan\Phi}\left[3.3 + 5.75 \log_{10} \frac{u^*_{cs} y_o}{\nu}\right]}$$

The characteristics of the bed material are assumed to be as follows: $s = 2.65$, $e = 0.6$, and $\Phi = 25°$. For the water: $\gamma = 62.4$ lb/ft^3, $\mu = 2.3\,(10^{-5})$ lb-sec/ft^2. Hence

$$\frac{C_{fs}}{C_f} = 1 + \frac{46.8 d^{3/2} \left[\frac{\partial h}{\partial y}\right]_{y=o}}{\sqrt{1.65 + 1.44\left[\frac{\partial h}{\partial y}\right]_{y=o}}\left[3.3 + 5.75 \log_{10} \frac{u^*_{cs} y_o}{\nu}\right]} \quad ; \quad d \text{ in mm}$$

For the trapezoidal canal, for which $\left[\partial h/\partial y\right]_{y=o} = 1.35$

$$\frac{C_{fs}}{C_f} = 1 + \frac{33.2\, d^{3/2}}{1.7 + 5.75 \log_{10}\left[\frac{\sqrt{gd}\; y_o}{\nu}\right]} \quad ; \quad d \text{ in mm}$$

For the infinitely wide canal, for which $\left[\partial h/\partial y\right]_{y=o} = 1$

$$\frac{C_{fs}}{C_f} = 1 + \frac{26.6 d^{3/2}}{1.7 + 5.75 \log_{10}\left[\frac{\sqrt{gd}\; y_o}{\nu}\right]} \quad ; \quad d \text{ in mm}$$

Listed in Table 15 are values of C_{fs}/C_f for the infinitely wide canal and for realistic values of d and the parameter $\sqrt{gd}\; y_o/\nu$. For small bed particles the seepage velocity does not measurably increase the skin-friction coefficient. It may be concluded that, for small bed particles (say $d \lesssim 0.2$ mm), the seepage force plays a significant role in inhibiting

Table 15. Values of C_{fs}/C_f at Incipient Motion of Bed Particles Comprising a Smooth Boundary

$\frac{\sqrt{gd}\ y_o}{\nu}$	$\frac{C_{fs}}{C_f}$				
d(mm) =	0.01	0.05	0.10	0.20	0.30
10^3	1.001	1.02	1.04	1.13	1.23
10^4	1.001	1.01	1.03	1.10	1.18
10^5	1.001	1.01	1.03	1.08	1.14

incipient motion. This statement is true provided that of course, the ground-water table is significantly below the free surface in the canal. The seepage force is of the same order of magnitude and, for bed particles of realistic density and packing,is nearly equal to the effective weight force of the bed particles. For vertical piezometric-head gradients at the bed of unity the seepage force may be considered to essentially double the effective weight force.

The seepage force per unit volume of bed material and water is independent of the permeability of the bed material. But, for a given piezometric-head gradient, the boundary shear stress increases as the permeability of the bed material increases. The permeability varies as the bed particle diameter squared, $\kappa \propto d^2$. As the bed particle size increases more and more above the small sizes considered above, the inhibiting effect of a permeable bed on incipient motion becomes less and less. There is most probably a bed particle diameter above which the permeable bed enhances incipient motion.

For large bed particles and the corresponding high seepage flow rates the velocity distribution in the canal can be considered to be nearly uniform. The turbulence level in the canal has been markedly reduced by suction. The incipient-motion condition in this case is Equation (35)

$$\frac{u_{dcs}}{\sqrt{\left[(s - 1) + 0.9\ (1 + e)\ \left[\frac{\partial h}{\partial y}\right]_{y=o}\right] gd \tan \Phi}} = 1.9$$

in which u_{dcs} is the critical bottom velocity. For a nearly uniform velocity distribution $u_{ds} = \bar{V}_s$, the mean canal velocity. In the same canal without seepage, the turbulence level would likely be much higher and the incipient-motion condition should be

$$\frac{u_{dc}}{\sqrt{(s - 1)\ gd \tan \Phi}} = 1.1$$

From Rouse (41), the mean velocity for two-dimensional flow

$$\frac{\bar{V}}{u_d} = 0.71 + 0.68 \log_{10} \frac{y_o}{d} \qquad (82)$$

For the corresponding conditions of incipient motion with seepage and without seepage

$$\frac{\bar{V}_{cs}}{\bar{V}_c} = \frac{1.72\sqrt{1 + 0.9\ \frac{(s - 1)}{(1 + e)}\ \left[\frac{\partial h}{\partial y}\right]_{y=o}}}{\left[0.71 + 0.68 \log_{10} \frac{y_o}{d}\right]} \qquad (83)$$

For $(s - 1)/(1 + e) = 1$

$$\frac{\bar{V}_{cs}}{\bar{V}_c} = \frac{2.55}{[0.71 + 0.68 \log_{10} \frac{y_o}{d}]}$$

for the trapezoidal canal and

$$\frac{\bar{V}_{cs}}{\bar{V}_c} = \frac{2.37}{[0.71 + 0.68 \log_{10} \frac{y_o}{d}]}$$

for the infinitely wide canal. Values of $\bar{V}_{cs}/\bar{V}_c$ are tabulated below for the infinitely wide canal for various realistic values of y_o/d.

Table 16. Values of $\bar{V}_{cs}/\bar{V}_c$ at Incipient Motion for Large Bed Particles in an Infinitely Wide Canal

$\frac{y_o}{d}$	$\frac{\bar{V}_{cs}}{\bar{V}_c}$
10^2	1.14
10^3	0.86
10^4	0.69

It is evident from Table 16 that, in terms of ths mean velocity in the canal, there is a condition for which the seepage into the bed aids incipient motion. That is, for $\bar{V}_{cs}/\bar{V}_c < 1$, the increase in the motivating force (drag force) on the bed particles overbalances the increase in the resisting force (caused by seepage force) on the same particles. Although the preceding analysis is admittedly crude it is believed that there is in reality a condition for which seepage out of a canal enhances incipient motion.

Summary

For the ground-water table considerably below the free surface in a canal the seepage force on bed particles is roughly equal in magnitude to the effective weight force on those particles. For very small bed particles ($d \lesssim 0.2$ mm) the seepage force plays a decided role in inhibiting incipient motion. For quite large bed particles the seepage into the bed may even aid incipient motion since the boundary shear stress is considerably increased by the effect of suction.

CHAPTER VIII

CONCLUSIONS

From this investigation the following statements and conclusions are considered pertinent:

1. For laminar flow over an impermeable bed, incipient motion occurs if

$$\frac{\mu \left[\frac{\partial u}{\partial y}\right]_{y=o}}{(\gamma_s - \gamma)\, d \tan \Phi} \gtrsim 0.19$$

This criterion is valid for both unidirectional and oscillatory flows.

2. For a turbulent boundary layer any incipient-motion criterion should contain some knowledge about the nature and intensity of the turbulent fluctuations in the vicinity of the bed. For $R_c^* \gtrsim 18$ the incipient-motion criterion $u_{dc}/\sqrt{(s-1)\, gd \tan \Phi}$ is essentially a constant, having the value 1.1 for flows having high intensities of turbulence and 1.9 for flows having low intensities of turbulence. For oscillatory flow over bed particles for which $d \gtrsim 0.8$ mm,

$$\frac{U_{mc}}{\sqrt{(s - 1)\, gd \tan \Phi}} = 3.2.$$

3. Shields' parameter, $\tau_c/(\gamma_s - \gamma)d$, varies widely from investigator to investigator.

4. The seepage force on the uppermost layer of bed particles is a constant times the seepage force on bed particles several layers beneath

the top layer. This constant is called a flow coefficient, C, and depends on the shape and packing of the bed particles. The flow coefficient for flow perpendicular to the bed, $C_{\perp}$, is independent of the direction of the flow provided that Darcy's Law is satisfied. The value of $C_{\perp}$ is 0.7 for spherical glass beads and between 0.9 and 0.95 for uniform, well-rounded sand. For any given seepage flow perpendicular to the bed the seepage force at the bed may be determined by using the value of $C_{\perp}$ and the value of the piezometric-head gradient at the bed, which is determined from the solution to Laplace's equation. For seepage flow parallel to the bed the flow coefficient, $C_{\parallel}$, is 0.97.

5. Experiment shows that, for flow out of a bed, the seepage force does not aid incipient motion.

6. Seepage flow out of or into a permeable bed can have a considerable influence on the flow characteristics above the bed. Seepage out of a bed may enhance boundary-layer transition whereas seepage into a bed may delay transition.

7. Except for the cases for which transition is enhanced or delayed, seepage decreases the boundary shear stress for flow out of the bed and increases it for flow into the bed. The change in the boundary shear stress brought about by seepage surely has to be considered in formulating any incipient-motion criterion.

8. Except for the case of boundary-layer transition being enhanced, seepage flow out of a bed can only hinder or delay incipient motion inasmuch as the boundary shear stress is reduced by the seepage and the seepage force can not aid incipient motion (conclusion 5).

9. Seepage flow into a porous bed can either hinder or aid incipient

motion, depending upon the relative magnitudes of the boundary shear stress and the seepage force.

10. For the application of the incipient-motion criteria to the case of seepage in the ocean bed caused by water waves, the following is inferred:

a. For small bed particles, the effect of seepage on incipient motion is essentially negligible.

b. For fairly large bed particles the seepage flow out of the bed under a wave trough can reduce the boundary shear stress upwards of 20 per cent. This reduction delays incipient motion. For large bed particles under the wave crest, the seepage flow may or may not hinder incipient motion.

c. The overall effect of seepage on incipient motion of bed particles under water waves is probably minor as both the motivating force (the boundary shear) and the force aiding resistance (the seepage force) vary with the same parameter, the wave amplitude, H.

11. For the application of the incipient-motion criteria to the case of seepage into a canal bed, the following is concluded (slope stability as a mass is excluded):

a. For rather small bed particles ($d \lesssim 0.2$ mm) the seepage force plays a significant role in inhibiting incipient motion whenever the ground-water table is significantly below the free surface in the canal.

b. For bed particles having diameters larger than 0.2 mm the inhibiting effect of seepage on incipient motion becomes less and less.

c. For very large bed particles the seepage through the bed may even aid incipient motion inasmuch as the boundary shear stress is considerably increased by the suction.

CHAPTER IX

RECOMMENDATIONS

From the experience obtained in performing this investigation, the writer suggests that any future investigator consider the following recommendations:

1. Conduct incipient-motion studies for an impermeable bed for varying degrees of intensities of turbulence. In conducting such studies the investigator should, if physically possible, measure the angle of repose of the bed material in situ. The intensity of turbulence should be varied systematically such that its effect on incipient motion could be delineated.

2. Investigate further the magnitude and variation of the flow coefficient. The value of the flow coefficient should be determined for nonuniform bed particles. The tests should be conducted using containers of various sizes in order that the scale effect could be ascertained.

APPENDIX

DESCRIPTION OF AND CALIBRATION OF U-TUBE FACILITY

NOMENCLATURE

Symbol	Quantity	Dimensions (F, L, T)
a	amplitude of displacement of water in test section of U-tube	L
A	cross-sectional area of the vertical legs of the U-tube	L^2
A_a, A_c	cross-sectional areas of streamtube	L^2
A_o, A_n	Euler coefficients of Fourier cosine series	L
B_n	Euler coefficients of Fourier sine series	L
c	damping coefficient for U-tube	FTL^{-1}
C_1, C_2	arbitrary constants	L
k	equivalent spring constant	FL^{-1}
ℓ	length of contracted area of streamtube	L
M	effective mass of water in U-tube	FT^2L^{-1}
n	integer	none
p	air pressure on free surface in U-tube	FL^{-2}
p_o	maximum air pressure on free surface in U-tube	FL^{-2}
r_o	radius of lower cylindrical insert in U-tube	L
s	displacement of water in test section of U-tube prior to separation	L
t	time	T
t_s	time elapsed until initiation of separation	T
T	period of oscillation in U-tube	T
u	velocity of water in test section of U-tube	LT^{-1}
V	velocity of fluid in streamtube	LT^{-1}

x	horizontal coordinate	L
z	displacement of free surface in U-tube	L
$\dot{z}$	velocity of free surface in U-tube	LT^{-1}
$\ddot{z}$	acceleration of free surface in U-tube	LT^{-2}
γ	specific weight of water	FL^{-3}
δ	logarithmic decrement for damping in U-tube	none

LIST OF TABLES

LIST OF ILLUSTRATIONS

CHAPTER I

DESCRIPTION OF EQUIPMENT

In order to study scour on the sea bed resulting from wave action, the decision was made to model only the mass of the water adjacent to the bed. The water motion at a fixed point close to the bed under a first-order Stokian wave is simple harmonic and is parallel to the bed. A large U-tube with forced oscillation of the water was designed in order to model the water motion under a wave.

U-Tube

The description of this large U-tube is facilitated by referring to Figure 1. The vertical legs of the U-tube are in two rectangular steel tanks (A) at the ends of the horizontal leg which is the test section (B). Forced oscillation of the water mass is achieved by blowing air into the West vertical leg as the water surface is falling and then exhausting this air as the water surface is rising.

The vertical legs of the U-tube are formed within the rectangular steel tanks which are 3 ft by 4 ft in cross section, by streamlined inserts (C). The water passage in each vertical leg is 1 ft by 4 ft in cross section inasmuch as the water surface is never allowed to fall to the curved section of the upper insert (C). In all tests the equilibrium water level was established 48-1/2 in above the top of the test section (B).

The horizontal leg of the U-tube is the test section which is 1 ft (vertical) by 4 ft (horizontal) in cross section and which is 10 ft long.

The central portion of the floor is depressed in order to form a container for the erodible bed material. The erodible bed (D) is 6 ft long by 4 ft wide by 4 in deep. The walls of the test section are fabricated of 1/2-in clear plastic and are framed on the exterior with steel angles and channels. The test section rests upon three prefabricated steel trusses which span from steel tank (A) to steel tank. A 3-ft square flush-mounted door is located in the center of the roof in order to be able to place the bed material and models. Three stopcocks are located in this door such that a 5/16-in diameter rod can be inserted vertically downward into the test section while the equipment is operating. The stopcocks are placed on a line midway between the vertical legs and are located 16-1/8 in, 31-5/8 in, and 39-7/8 in from the South wall of the test section. These openings are hereafter referred to as ports A, B, and C, respectively.

The water in the U-tube is made to oscillate at the resonant frequency. The output of a centrifugal blower is discharged continuously into the air space above the water surface of the West vertical leg. A seven-in diameter, pneumatically powered, exhaust valve (E) in the top of West vertical leg is opened upon receipt of the signal that the minimum water level in this leg is attained.

The feedback mechanism by which the exhaust valve is sequence-operated at the resonant frequency is as follows. The float (F) in the East vertical leg is attached by a light flexible cable to a steel rod(G) which moves vertically past the direction-sensing switch (H). The direction-sensing switch (H) is a lever-operated microswitch. A permanent magnet on the end of the microswitch operating lever is in contact

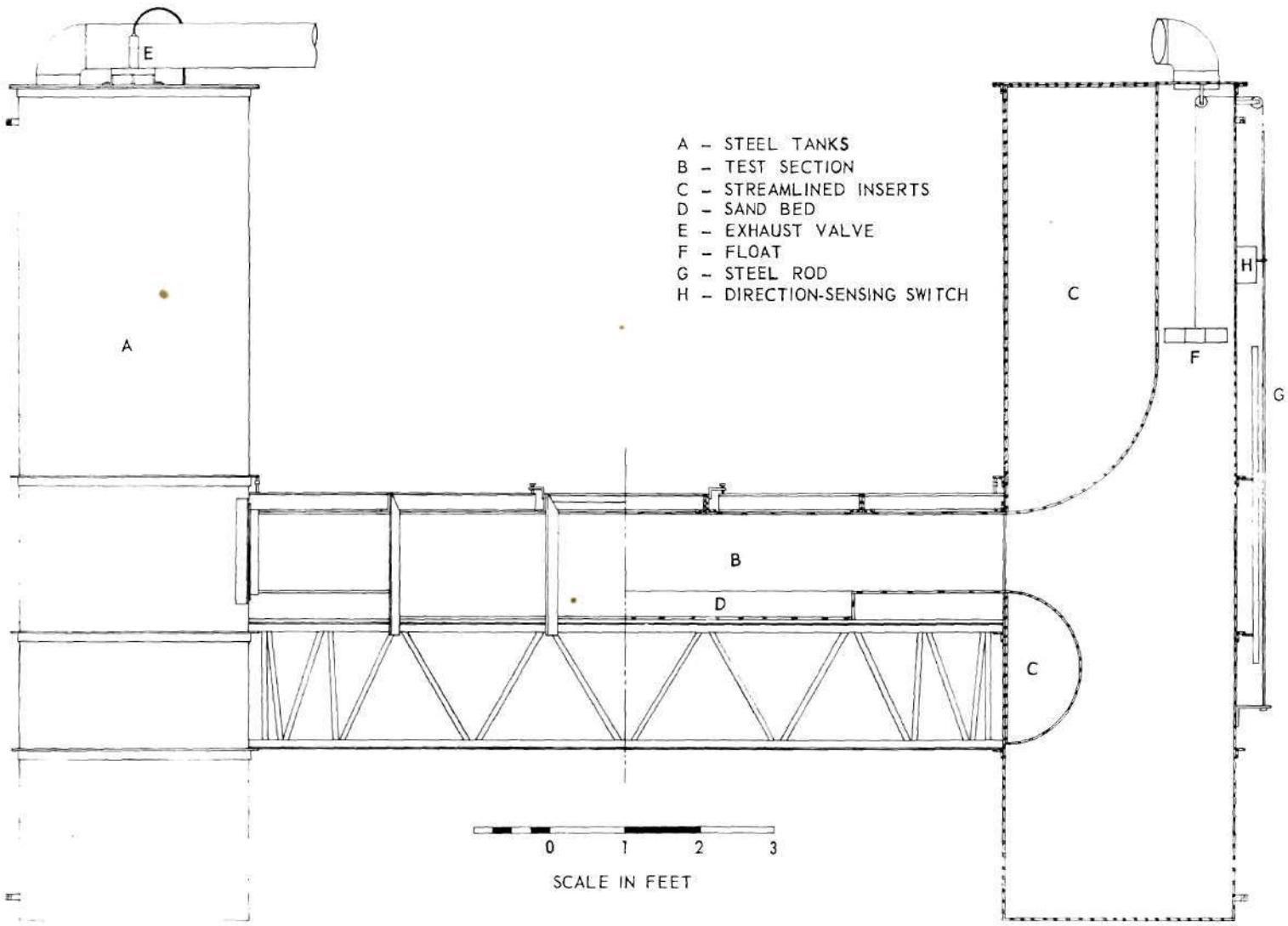

Figure 1. Side Elevation and Cross Section of U-Tube.

with the steel rod (G) which, in turn, follows the motion of the float (F). Whenever the steel rod (G) is rising the switch (H) is closed and whenever the steel rod (G) is falling the switch (H) is open. When the steel rod (G) changes direction and starts to rise, a circuit is closed which, in turn, actuates a single-cycle timer. This timer makes one revolution in 2 seconds and then stops. A second microswitch is contained within the timer. By means of an adjustable cam this second microswitch can be made to open or close at any time within the two-second interval. A solenoid valve which operates the pneumatic piston on the exhaust valve is in the circuit with the timer microswitch. The timer microswitch is set such that the exhaust valve opens when the timer starts and such that the exhaust valve remains open for a half period. The feedback mechanism described above insures that the water is oscillated at resonant frequency with the result that the frequency of oscillation can not be controlled.

On the other hand, the amplitude of the oscillation can be controlled by means of a bleed-off valve in the air duct leading from the centrifugal blower to the West vertical leg. A dial gage is attached to the bleed-off valve in order that the valve position and hence amplitude of oscillation can be readily established. For the determination of amplitude a scale is fixed parallel to the steel rod (G). A pointer on the steel rod passes over the face of the fixed scale.

The photograph, Figure 2, shows the South wall of test section. The amplitude scale is clearly shown on the East or nearer tank.

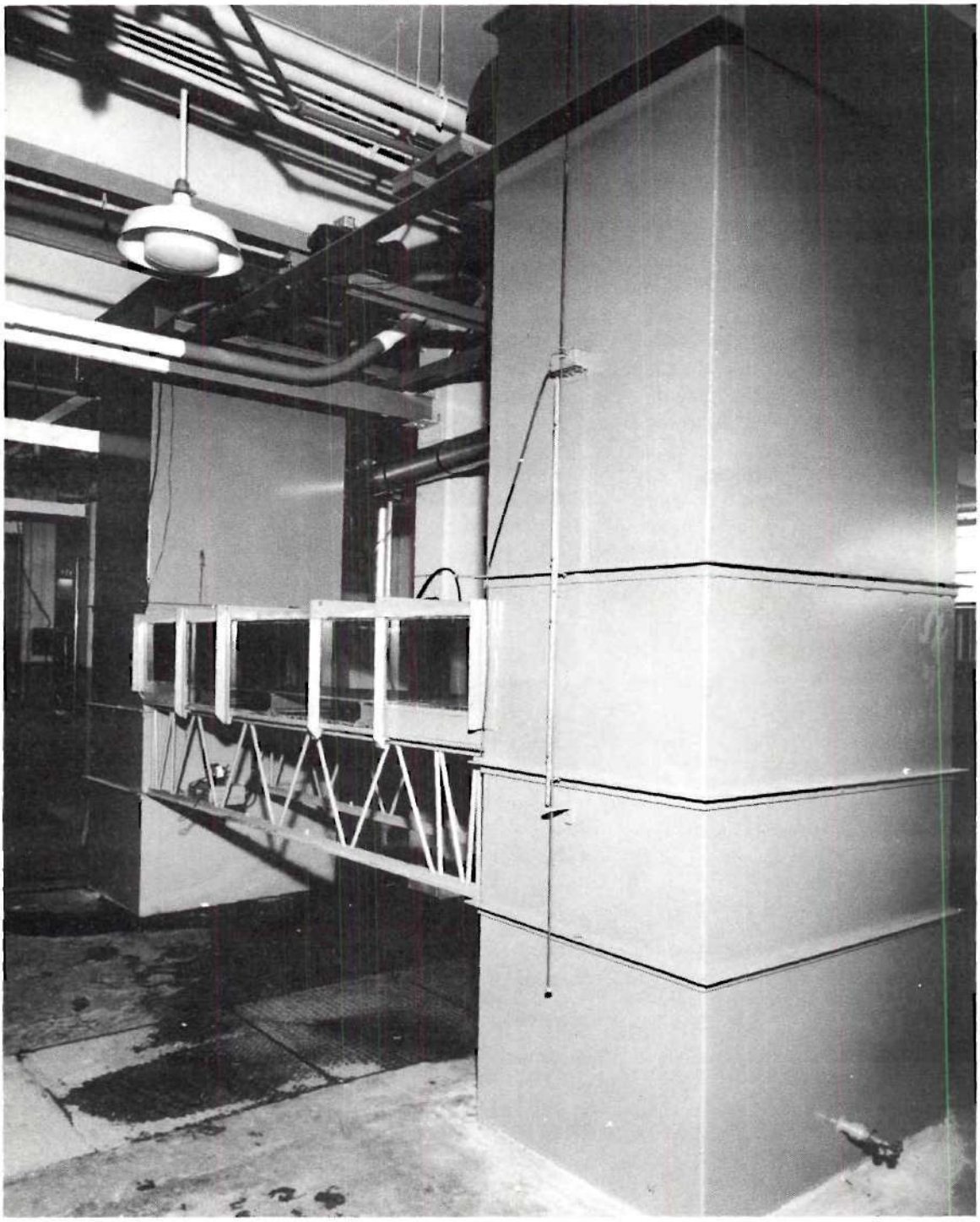

Figure 2. Photograph of U-Tube.

CHAPTER II

CALIBRATION OF EQUIPMENT

The equipment calibration tests were in two categories as follows: (1) determination of the characteristics of the apparatus as a whole and (2) determination of the flow characteristics within the test section. The calibration program was executed without erodible material on the bed of the test section. Temporary flooring, consisting of cement-asbestos sheets bolted to 3-in steel I beams, was used to bridge the depression in the central portion of the floor of the test section.

Overall Characteristics

Calibration tests were made (1) to determine resistance to motion of the entire U-tube, (2) to determine the amplitude as a function of the position of the bleed-off valve, and (3) to determine the period of oscillation as a function of amplitude.

Resistance to Motion

The resistance to motion was determined by experimentally measuring the water-surface amplitude during free oscillation and by utilizing the amplitude-decay data to compute an equivalent linear damping coefficient for the system. The differential equation for free oscillation of the system is

$$M\ddot{z} + c\dot{z} + 2\gamma\ Az = 0 \qquad (1)$$

in which M is the mass, c is a viscous damping coefficient, γ is the specific weight of water, A is the cross-sectional area of the vertical legs of the U-tube, z is the water-surface displacement in the West tank from equilibrium, $\dot{z}$ is the velocity, and $\ddot{z}$ is the acceleration. The product $2\gamma A$ corresponds to the spring constant k of vibration theory. The mass, M, of the oscillating system is unknown because of the effect of enlarged sections of the U-tube in the flow passages joining the horizontal leg to the two vertical legs. The solution of Equation (1) is

$$z = e^{-\frac{c}{2M}t}\left(C_1 \cos\frac{2\pi t}{T} + C_2 \sin\frac{2\pi t}{T}\right) \tag{2}$$

in which T is the damped natural period.

The damped natural period is

$$T = \frac{2\pi}{\sqrt{\frac{2\gamma A}{M} - \frac{c^2}{4M^2}}} \tag{3}$$

Since this system has small resistance, c, and large mass, M, the damped natural period, T, can be taken as

$$T = \frac{2\pi}{\sqrt{\frac{2\gamma A}{M}}} \tag{4}$$

The free-oscillation experiment was performed in the following manner. The bleed-off valve was closed and the centrifugal blower was started. When maximum amplitude was attained the blower was turned off. An observer stationed at the float scale observed and recorded the maximum

values; simultaneously the period was obtained by transmitting the pulse from the direction-sensing microswitch to the marking input device of a Sanborn recorder. When the microswitch circuit was closed the stylus on the recorder oscillated. A built-in timer in the circuit displayed one-second marks on the oscillogram. From this record the period, T, was determined to be 3.56 seconds.

Utilizing the experimentally determined value of T as 3.56 seconds, the mass of the oscillating system is calculated from Equation (4) as being 158 slugs.

The attenuation of the amplitude during free oscillation can be utilized for the determination of the damping coefficient, c, as follows. From Equation (2) the ratio of successive maxima is

$$\frac{z_n}{z_{n+1}} = e^{\frac{cT}{2M}} \tag{5}$$

or in logarithmic form

$$\delta = \log_e \left(\frac{z_n}{z_{n+1}}\right) = \frac{cT}{2M} \tag{6}$$

in which δ is the logarithmic decrement. Thus if the logarithms of the amplitude are plotted as a function of cycles, the slope of the curve is δ.

The attenuation of the amplitude during free oscillation was measured for n = 1 to n = 27. A semi-logarithmic plot of successive peaks of amplitude against number of cycles is presented in Figure 3. For amplitudes less than 5 inches the slope is constant meaning that the damping

is truly viscous. The value of the logarithmic decrement, δ, as a function of amplitude is presented in Figure 4.

Amplitude Calibration

Amplitude calibration consisted simply of observing the amplitude on the float scale at various settings of the bleed-off valve in the air duct to the West tank. The results are shown in Figure 5.

Period Calibration

Period calibration was obtained simultaneously with the amplitude calibration by superposing the on-off cycle of the direction-sensing switch on the timing marker circuit of a Sanborn recorder. As shown in Figure 6 the period remains constant at 3.59 seconds for a total amplitude less than 11 in. The period increases slightly with amplitudes greater than 11 in attaining a value of 3.73 seconds at a total amplitude of 34 in. By virtue of the feedback system of forcing the oscillation, the periods shown in Figure 6 must be the resonant periods.

The explanation for the observed increase in the resonant period for total amplitudes greater than 11 in is that the flow separated from the lower insert (C) for those amplitudes. Upon referring to Equation (4), it is evident that an increase in resonant period can result only from a greater effective mass. When separation occurs in the boundary layer a dead zone results which reduces the flow area in that vicinity. This reduced flow area can be shown to increase the effective mass, M, in the U-tube.

In order to show that a reduced flow area does result in an increased effective mass, a simpler flow system than the one present in the

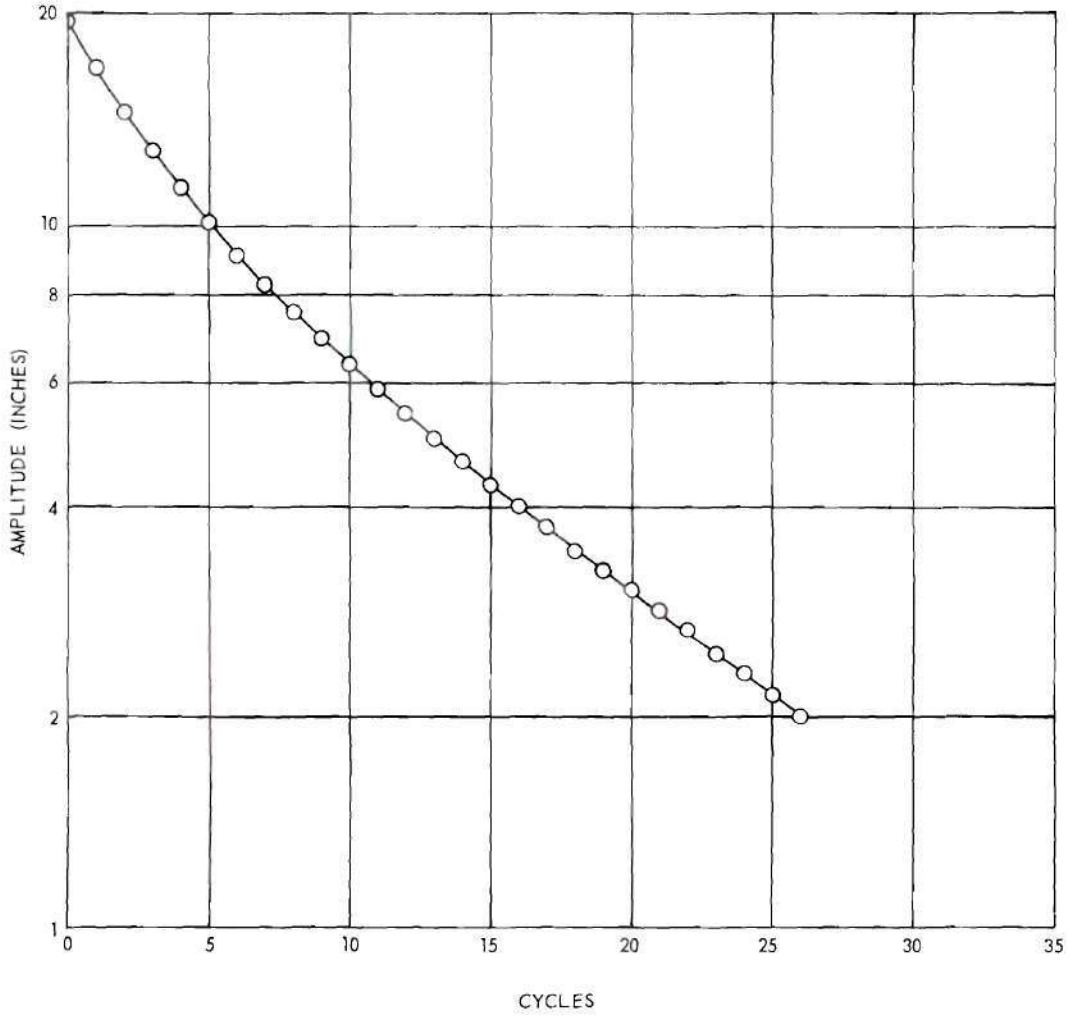

Figure 3. Attenuation of Float Amplitude During Free Oscillation.

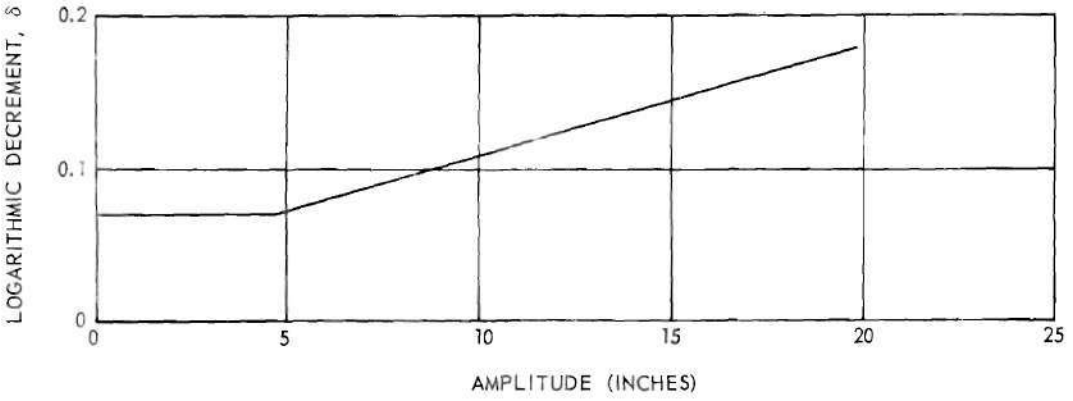

Figure 4. Logarithmic Decrement as a Function of Float Amplitude.

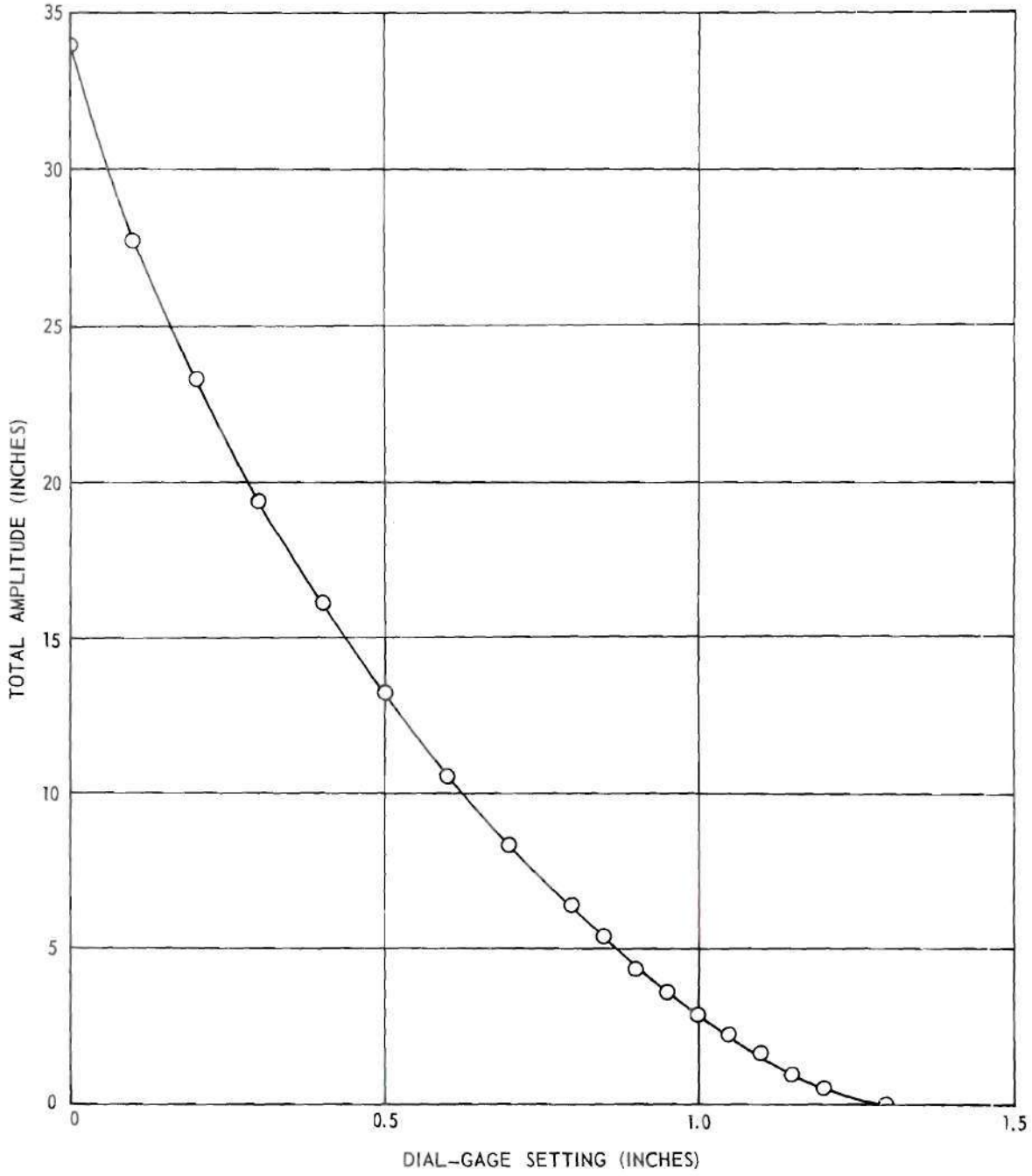

Figure 5. Total Float Amplitude as a Function of Position of Bleed-Off Valve.

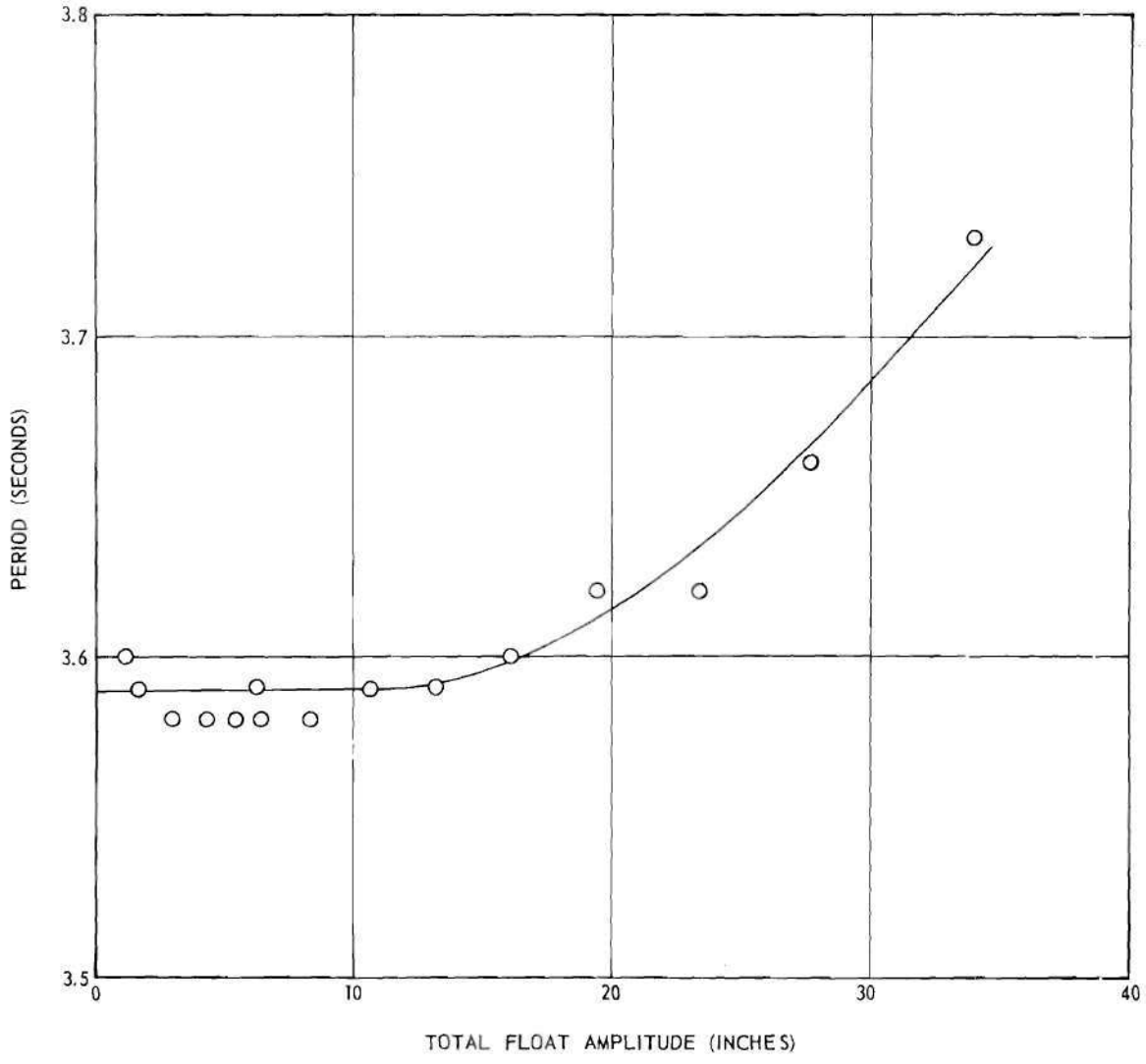

Figure 6. Resonant Period as a Function of Total Float Amplitude.

U-tube will be analyzed. An analogous system consisting of a liquid accelerating from left to right through a contracted-area streamtube will be utilized. In Figure 7 is shown the streamtube, which has a contraction between two cross sections of equal size. The cross sections to be used later are marked a, b, c, d, e, and f. Sections b and c, and d and e, are just to the left or right of the changes in cross-sectional area.

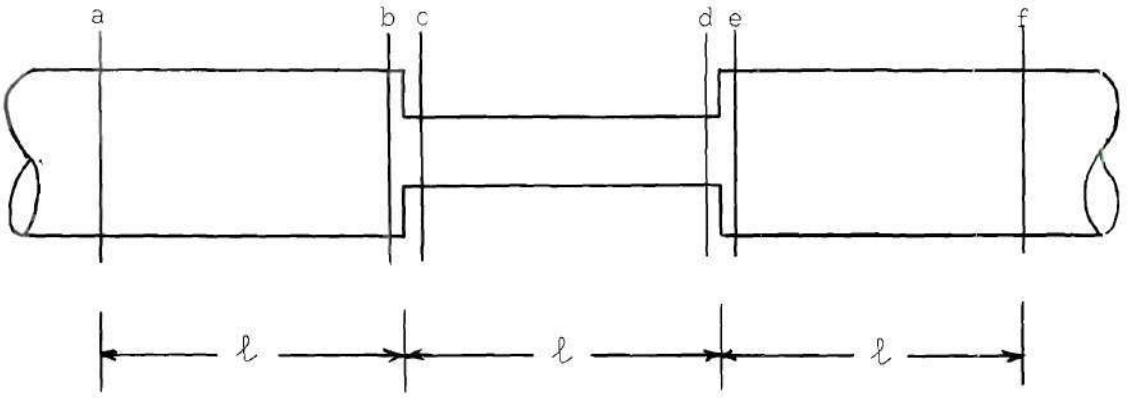

Figure 7. Contracted-Area Streamtube.

The appropriate equation for the total acceleration within the streamtube is

$$\int_a^f \frac{\partial V}{\partial t}\, dx + \tfrac{1}{2} \int_a^f \frac{\partial}{\partial x} (V^2) dx \qquad (7)$$

in which x is the horizontal coordinate, and V is the velocity. The integration over the entire length is obtained by breaking the streamtube into three regions and ignoring the nonuniformity of the flow at the junctions

of these regions

$$\int \frac{\partial V}{\partial t}\, dx = \int_a^b \frac{\partial V}{\partial t}\, dx + \int_c^d \frac{\partial V}{\partial t}\, dx + \int_e^f \frac{\partial V}{\partial t}\, dx$$

and

$$\tfrac{1}{2} \int \frac{\partial}{\partial x} (V^2) dx = \tfrac{1}{2} \int_a^b d(V^2) + \tfrac{1}{2} \int_c^d d(V^2) + \tfrac{1}{2} \int_e^f d(V^2)$$

By utilizing the equation of continuity, Equation (7) becomes

$$\int_a^f \frac{\partial V}{\partial t}\, dx + \tfrac{1}{2} \int_a^f \frac{\partial}{\partial x} (V^2) dx = (2 + A_a/A_c)\, \ell\, \frac{\partial V_a}{\partial t} \qquad (8)$$

in which the subscripts a and c refer to their respective cross sections. The factor $(2 + A_a/A_c)$ is greater than 3 as A_a is larger than A_c, meaning that the streamtube having a contracted area of length ℓ has a greater effective mass than one having in its place an uncontracted area of the same length. Separation of the flow in the U-tube would reduce the flow area and thus would increase the effective mass.

The initiation of separation within the U-tube can be determined qualitatively by investigating the flow within the boundary layer behind a cylinder. Schlichting* discusses two cases of the initiation of separation behind a cylindrical body which is moved (a) impulsively and (b)

*Schlichting, H., Boundary Layer Theory, trans. by J. Kestin, McGraw Hill, 4th ed., 1960, pp 212-221.

with a constant acceleration. Initiation of separation is expressed as the ratio s/r_o in which s is the distance traveled from rest and r_o is the radius of the cylinder. Analytical results are 0.351 for the impulsive motion and 0.52 for the constant acceleration. Simple-harmonic motion in the U-tube should exhibit separation from the cylindrical insert at some comparable value of s/r_o. For simple-harmonic motion the velocity, u, in the test section is given by

$$u = \frac{2a\pi}{T} \sin \frac{2\pi t}{T}$$

in which 2a is the total amplitude of the fluid motion. The distance, s, traveled by the fluid until separation occurs, is

$$s = \int_o^{t_s} u\,dt$$

in which t_s is time elapsed until initiation of separation. Hence

$$\frac{s}{r_o} = \frac{a}{r_o} \left(1 - \cos \frac{2\pi t_s}{T}\right) \qquad (9)$$

As separation is expected to occur from the lower cylindrical insert for which r_o is 1 ft

$$s = a \left(1 - \cos \frac{2\pi t_s}{T}\right) \qquad (10)$$

The minimum total amplitude, 2a, for which separation will just commence

($t_s = T/2$) is 4.51 in for $s/r_o = 0.351$ and 6.29 in for $s/r_o = 0.52$. For larger amplitudes initiation of separation begins increasingly sooner than $t_s = T/2$, meaning that the extent of the reduced flow area in the U-tube increases with amplitude, which would result in increasing effective mass. Since the resonant period is proportional to the square root of the effective mass, this tendency is clearly demonstrated in Figure 6.

Another indication of the flow-pattern change is that the value of the logarithmic decrement δ began to change at a comparable amplitude at which the period change was noted. The comparison of Figures 4 and 6 clearly demonstrates this point. The gross resistance characteristics of the U-tube would also be dependent upon the duration and growth of separation zones from the lower cylindrical inserts.

Test-Section Characteristics

The flow characteristics within the test section were experimentally determined in order (1) to ascertain whether the actual motion was the desired motion (simple harmonic) and (2) to determine whether a system of baffles would be required to attain uniform velocity distribution. This portion of the calibration program was accomplished by recording, on 16 mm motion-picture film, the position of nearly neutrally buoyant particles during the fall from the top to the bottom of the test section. The (polyethylene spheres) particles were 1/4 in in diameter into which a small hole was drilled. The void in the particle was filled with caulking compound until a fall velocity of about 0.06 fps was attained. These particles were inserted into the test section through the ports installed

in the roof after the desired amplitude was established. All runs in this series of tests were made with a float amplitude of 13.7 in. Several runs were made at each of the three ports in the roof.

The procedure during a run was as follows. The bleed-off valve was set for the desired float amplitude (Figure 5). The blower was turned on. A 1/4-in diameter graduated rod was inserted through the stopcock in the roof. A photograph of this rod was obtained by means of the motion-picture camera. The graduated rod was withdrawn. A particle was forced through the stopcock. As soon as the particle entered the test section the camera was started. The camera was allowed to run until this particle fell to the bottom of the test section.

The particle trajectories were obtained by projecting the film record onto a white sheet of paper and marking the particle position thereon. A stop-motion projector was utilized. The scale was established by projecting the image of the graduated rod onto the paper. Elapsed time was established by utilizing the period shown in Figure 6. The assumption was made that the time increment between each frame of the film strip was constant.

For descriptive purposes only a time-lapse photograph of a falling particle is shown in Figure 8.

Analysis of the Motion

The desired motion within the test section is simple harmonic; but, since the external force (air pressure on the water surface) is not applied in a simple-harmonic manner, the question arises as to the nature and magnitude of the deviation of the actual motion from the desired motion.

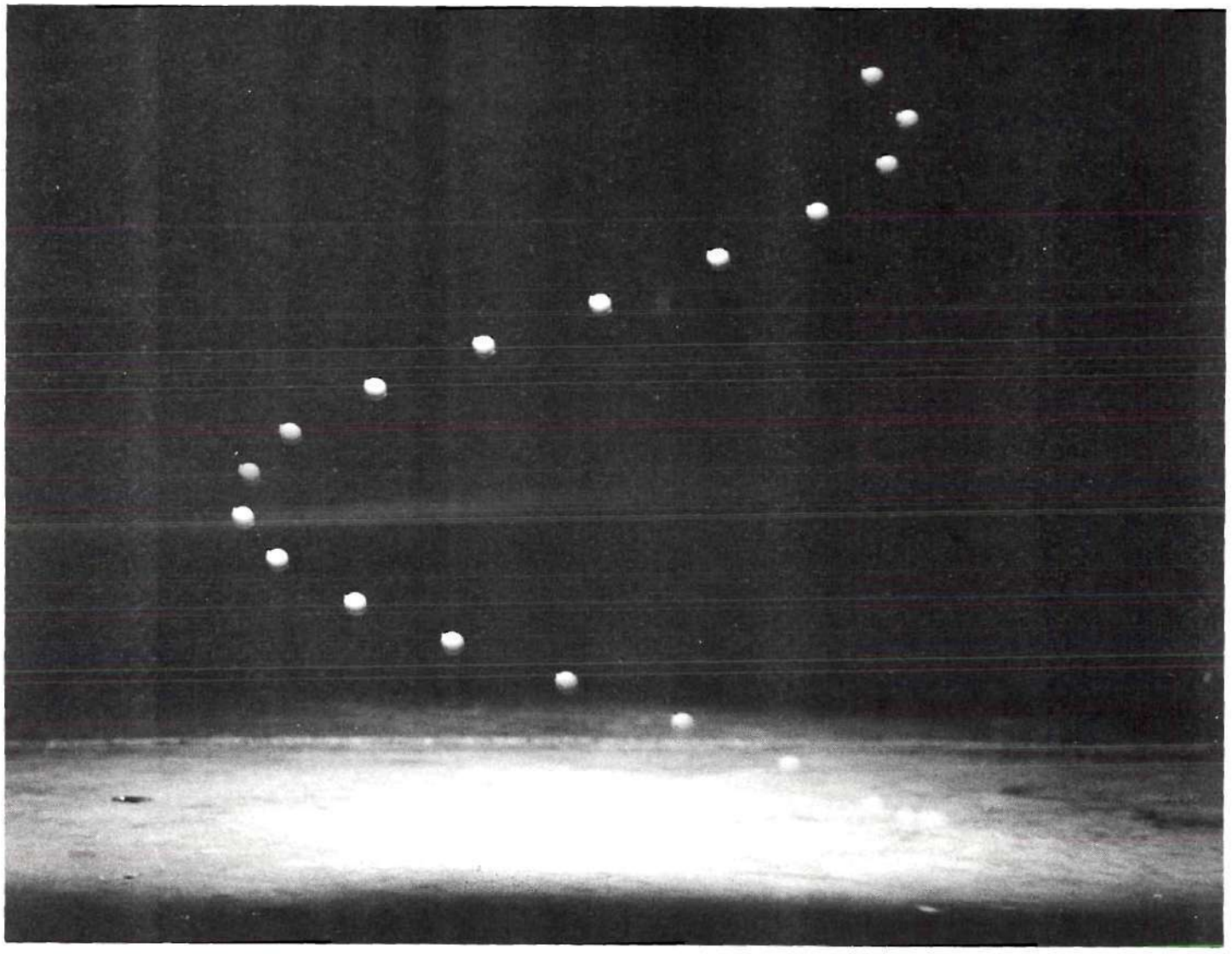

Figure 8. Time-Lapse Photograph of a Falling Particle.

Theoretical Analysis. Utilizing the damping factor determined previously (Figure 4) and assuming the external force on the U-tube is a square-wave function of time, a theoretical solution for the motion in the test section can be obtained. The external force is the pressure in the West vertical leg multiplied by the horizontal cross-sectional area of that leg or pA. The blower can be assumed to apply a constant pressure p_o during the time the exhaust valve is closed. During the time the exhaust valve is open the pressure, p, can be taken as atmospheric. Because of the feedback scheme of operating the exhaust valve, the external force is periodic at the resonant period. The external force, pA, is illustrated in Figure 9.

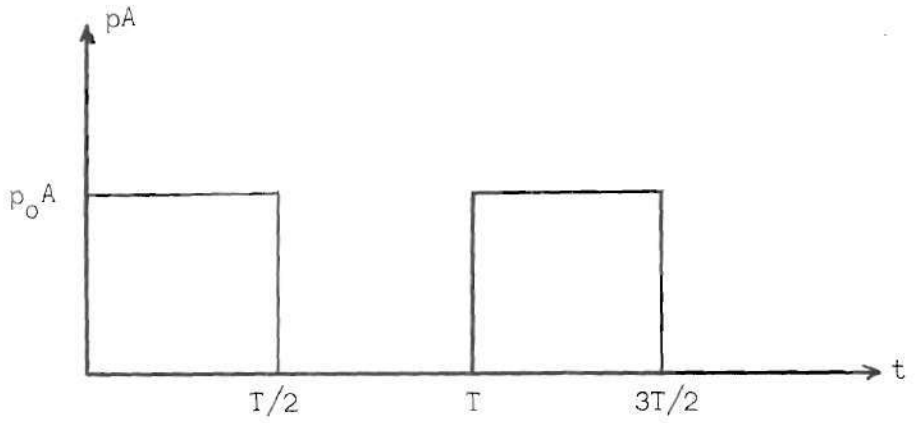

Figure 9. External Force on the U-Tube.

The differential equation of motion is

$$M\ddot{z} + c\dot{z} + 2\gamma Az = -pA \tag{11}$$

The steady-state solution can be represented by a Fourier series

$$z = A_o + \sum_{n=1}^{\infty} \left(A_n \cos \frac{2\pi nt}{T} + B_n \sin \frac{2\pi nt}{T} \right) \tag{12}$$

in which A_o, A_n, and B_n are the Euler coefficients which satisfy Equation (11). The resulting coefficients are

$$A_n = 0 \qquad ; \quad n = 0,2,4,\ldots$$

$$B_n = 0 \qquad ; \quad n = 2,4,6,\ldots$$

$$\frac{A_n}{p_o/\gamma} = \frac{\delta}{\pi^2(n^2 - 1)^2 + \delta^2 n^2} \qquad ; \quad n = 1,3,5,\ldots$$

and

$$\frac{B_n}{p_o/\gamma} = \frac{\pi(n^2 - 1)}{n[\pi^2(n^2 - 1)^2 + \delta^2 n^2]} \qquad ; \quad n = 1,3,5,\ldots$$

Substituting the pertinent coefficients into Equation (12),

$$\frac{z}{p_o/\gamma} = \sum_{n=1,3,5,\ldots}^{\infty} \frac{1}{[\pi^2(n^2 - 1)^2 + \delta^2 n^2]} \left[\delta \cos \frac{2n\pi t}{T} + \frac{\pi(n^2 - 1)}{n} \sin \frac{2n\pi t}{T} \right] \tag{13}$$

The Fourier coefficients were computed for an amplitude of 13.7 in, corresponding to the amplitude of the falling-particle runs. The value of

δ of 0.0895 is obtained from Figure 4. Equation (13) reduces to two terms upon substitution of the particular value of δ.

$$\frac{z}{p_o/\gamma} = 11.17 \cos \frac{2\pi t}{T} + 0.01 \sin \frac{6\pi t}{T} \qquad (13a)$$

The relative magnitude of the coefficients is indicative that the motion will be almost simple harmonic.

Analysis of Experimental Results. The particle trajectories of four half-cycles were analyzed harmonically using Runge's scheme with 24 data points in a half-cycle. The other half of the cycle was made equal in magnitude and sign to the first. The coefficients of a cosine series for the four are listed in Table 1 as a function of vertical position in the test section. The absence of sine terms resulted because of the particular origin chosen for the analysis. The vertical position, y, is measured downward from the roof and was taken as the mean value of y at the extreme positions during that half-cycle.

Table 1. Coefficients of Cosine Terms from Harmonic Analysis

y(inches)	B_o(inches)	B_1(inches)	B_2(inches)	B_3(inches)	B_4(inches)
3.20	0.02	6.39	-0.06	0.01	-0.01
3.77	-0.01	6.40	-0.04	0	-0.02
8.10	0.01	6.80	0.02	0.04	-0.01
8.85	0.08	6.54	0.06	0	-0.01

This analysis was done only for particles which were inserted in Port A. The results from the motion of these were so favorable that no more harmonic analyses were deemed necessary. These data verify that simple-harmonic motion did exist in the test section as predicted, Equation (13a).

Velocity Distribution in the Test Section

Since the motion within the test section has been shown to be simple harmonic, the kinematic features of the motion at a point are simply functions of the amplitude at that point and the period. In other words,

$$x = a \cos \frac{2\pi t}{T} \tag{14}$$

$$u = -\frac{2a\pi}{T} \sin \frac{2\pi t}{T} \tag{14a}$$

and

$$\frac{Du}{Dt} = -\frac{2a\pi^2}{T^2} \cos \frac{2\pi t}{T} \tag{14b}$$

Since the nearly neutrally buoyant particles follow the fluid motion, the difference in the extreme positions of the particles as determined from the film strip is the total amplitude. The ratio of particle amplitude to float amplitude is shown in Figure 10 as a function of distance from the roof at the three lateral positions across the test section. The solid circles denote that the particle had an east-to-west direction of motion; conversely, the open circles denote a west-to-east direction. Ports A and B are located at the third points across the

test section. The results shown in Figure 10 indicate that the velocity distribution is uniform and that the amplitude of fluid motion is equal to the amplitude of the float in the central portion of the test section. Nearer the wall at Port C the fluid motion has a greater amplitude and has a drift from east to west. Since incipient motion is to be studied in the central portion between Ports A and B, no system of baffles is required. Thus the fluid velocity in the central portion of the test section is determined from Equation (14a) in which 2a is the total float amplitude and T is given in Figure 6.

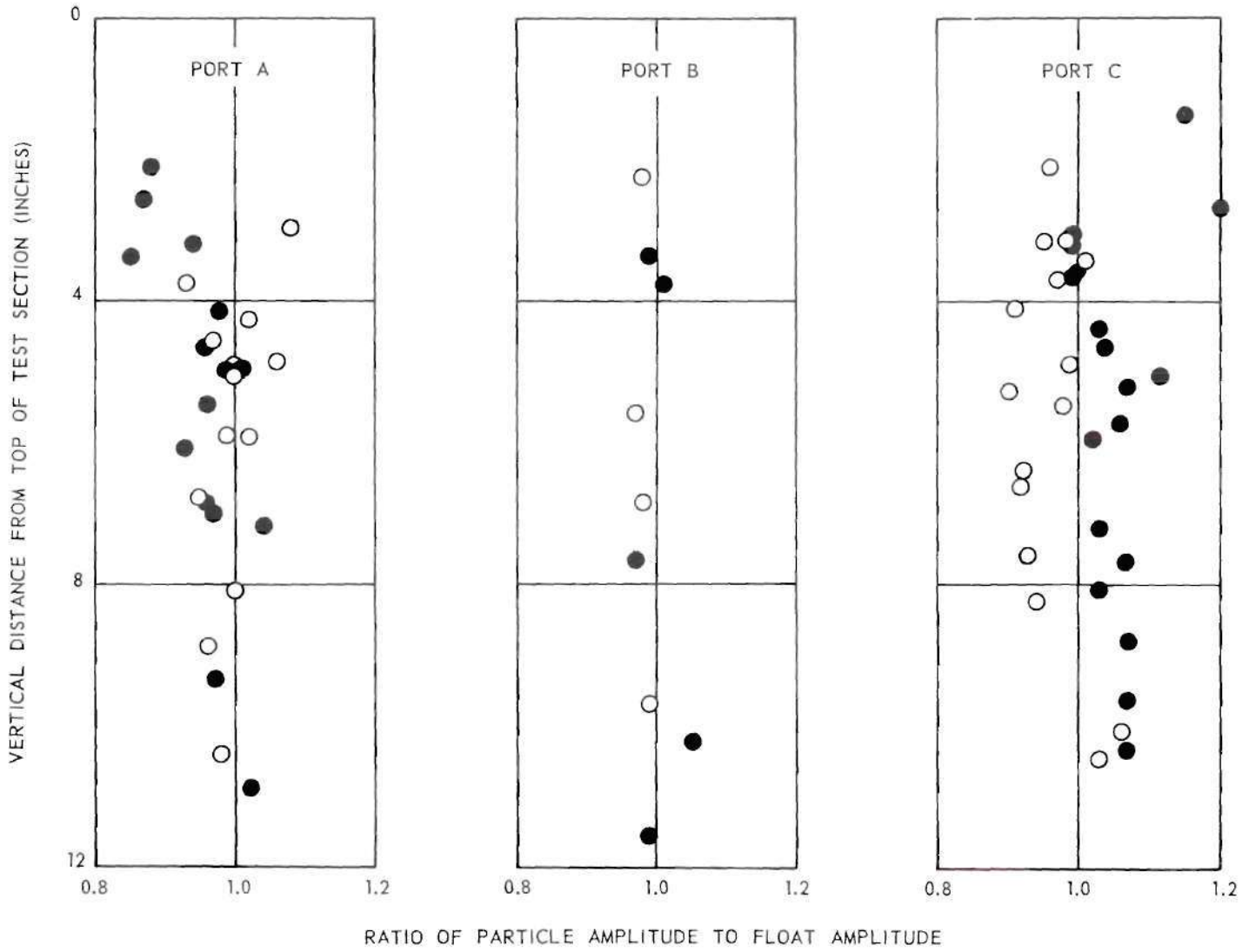

Figure 10. Ratio of Particle Amplitude to Float Amplitude within the Test Section.

REFERENCES

1. Eagleson, P. S. and R. G. Dean, "Wave-Induced Motion of Bottom Sediment Particles," Transactions of American Society of Civil Engineers, Vol. 126, Part I, 1961, pp. 1162-1189.

2. Simons, D. B., "Forces of Wave Motion Which Affect Canal Stability," Colorado State University, Fort Collins, Colorado, 1955 (unpublished).

3. Posey, C. J., "Scour at Bridge Piers (2. Protection of Threatened Piers)," Civil Engineering (New York), Vol. 33, No. 5, May 1963, pp. 48-49.

4. Lane, E. W., "Some Principles of Design of Stable Channels in Erodible Material," Fourth Meeting, International Association for Hydraulic Research, Bombay, 1951, pp. 463-479.

5. Shields, A., "Anwendung der Aehnlichkeitsmechanik und der Turbulenzforschung auf die Geschiebebewegung," Mitteilungen der Preusschen Versuchanstalt für Wasserbau and Schiffbau, Berlin, Vol. 26, 1936. (Translation in Engineering Societies Library, New York).

6. White, C. M., "The Equilibrium of Grains on the Bed of a Stream," Proceedings of the Royal Society of London, Vol. 174 A, 1940, pp. 322-334.

7. Manohar, M., "Mechanics of Bottom Sediment Movement Due to Wave Action," U. S. Dept. of the Army, Beach Erosion Board Tech. Memo. No. 75, 1955, 121 pp.

8. Schlichting, H., Boundary Layer Theory, McGraw-Hill, 4th Ed., New York, 1960, p. 75.

9. Ibid., p. 509.

10. Einstein, H. A. and El-Sayed Ahmed El-Samni, "Hydrodynamic Forces on a Rough Wall," Reviews of Modern Physics, Vol. 21, No. 3, July 1949, pp. 520-524.

11. Iwagaki, Y. and Y. Tsuchiya, "An Analysis of the Stable Cross Section of a Stream Channel," Disaster Prevention Research Institute Bulletin No. 29, March, 1959, 27 pp.

12. Kalkanis, George, "Transportation of Bed Material Due to Wave Action," University of California, Hydraulic Engineering Laboratory, Technical Report HEL-2-4, February 1963, 114 pp.

13. Nikuradse, J., "Laws of Flow in Rough Pipes," translated as Tech. Memo. 1292, National Advisory Committee for Aeronautics, Washington, D. C., 1950.

14. Rouse, H., Elementary Mechanics of Fluids, John Wiley and Sons, New York, 1957, p. 194.

15. Rotta, J., "Das in Wandnähe gültige Geschwindigkeitsgesetz turbulenter Strömungen," Ingenieur Archiv, Vol. 18, 1950, pp. 277-280.

16. Mavis, F., C. Ho and Y. Tu, "The Transportation of Detritus by Flowing Water - I," Bulletin 5, University of Iowa Studies in Engineering, Iowa City, Iowa, March 1935, 53 pp.

17. Chepil, W. S., "Dynamics of Wind Erosion II: Initiation of Soil Movement," Soil Science, Vol. 60, 1945, pp. 397-411.

18. Zingg, A. W., "Wind-Tunnel Studies of the Movement of Sedimentary Material," Proceedings of the Fifth Hydraulics Conference, Bulletin 34, State University of Iowa, Iowa City, 1952, pp. 111-135.

19. Haefeli, R., "The Stability of Slopes Acted upon by Parallel Seepage," Proceedings of the Second International Conference on Soil Mechanics and Foundation Engineering, Vol. I, Rotterdam, June 1948, pp. 57-62.

20. Bernatzik, W., Baugrund und Physik, Schweizer Druck-und Verlagshaus, Zürich, 1947, p. 133.

21. McNown, J. S., H. M. Lee, M. B. McPherson, and S. M. Engez, "Influence of Boundary Proximity on the Drag of Spheres," Proceedings of the VII International Congress for Applied Mechanics, London, 1948, pp. 17-29.

22. Keller, J. B., "Viscous Flow through a Grating or Lattice of Cylinders," Journal of Fluid Mechanics, Vol. 18, Part 1, 1964, pp. 94-96.

23. Bernatzik, W., "Grenzneigung von Sandböschungen bei gleichzeitiger Grundwasserströmung," Die Bautechnik, Vol. 55, 1940, pp. 634-642.

24. Havlicek, J., "Tekuty Pisek," Stavebnicky Casopis, Vol. 2, 1962, pp. 80-98.

25. Turcotte, D. L., "A Sublayer Theory for Fluid Injection into the Incompressible Turbulent Boundary Layer," Journal of the Aerospace Sciences, Vol. 27, No. 9, September 1960, pp. 675-678.

26. Todd, D. K., Ground Water Hydrology, John Wiley and Sons, New York, 1960, p. 49.

27. Eckert, E. R. G., A. J. Diaguila, and P. L. Donoughe, "Experiments on Turbulent Flow Through Channels Having Porous Rough Surfaces With or Without Air Injection," NACA TN 3339, Washington, D. C., February 1955, 45 pp.

28. Burnage, H., "Contribution a L'Etude de L'Ecolement Turbulent dans une Conduite Cylindrique a Paroi Poreuse," Notes Techniques No. 114, Publications Scientifiques et Techniques, Du Ministere de L'Air, Paris, 1962, 44 pp.

29. Dutton, R. A., "The Effects of Distributed Suction on the Development of Turbulent Boundary Layers," Aeronautical Research Council R. and M. No. 3155, London, 1960, 28 pp.

30. Lamb, H., Hydrodynamics, Dover Publications, 6th Edition, New York, p. 369.

31. Putnam, J. A., "Loss of Wave Energy due to Percolation in a Permeable Sea Bottom," Transactions of the American Geophysical Union, Vol. 30, No. 3, June 1949, pp. 349-356.

32. Wiegel, R. L., "A Presentation of Cnoidal Wave Theory for Practical Application," Journal of Fluid Mechanics, Vol. 7, Part 2, February 1960, pp. 273-286.

33. Jacobi, C. G. J., Gesammelte Werke, Vol. 1, Berlin, 1881, p. 175.

34. Copson, E. T., Theory of Functions of a Complex Variable, Oxford Press, 1935, p. 97.

35. Jolley, L. B. W., Summation of Series, Dover Publications, Second Edition, New York, 1961, p. 222.

36. Hunt, J. N., "On the Damping of Gravity Waves Propagated over a Permeable Surface," Journal of Geophysical Research, Vol. 64, No. 4, April 1959, pp. 437-442.

37. Keller, J. B., "The Solitary Wave and Periodic Waves in Shallow Water," Communications in Pure and Applied Mathematics, Vol. 1, 1948, pp. 323-339.

38. Laitone, E. V., "The Second Approximation to Cnoidal and Solitary Waves," Journal of Fluid Mechanics, Vol. 9, 1960, pp. 430-444.

39. Wedernikov, V. V., "Über die Sickerung und Grundwasserbewegung mit freier Oberfläche," Zeitschrift für Angewandte Mathematik und Mechanik, Vol. 17, 1937, pp. 155-168.

40. Keulegan, G. H., "Laws of Turbulent Flow in Open Channels," Research Paper RP 1151, Journal of Research, U. S. National Bureau of Standards, Vol. 21, 1938, pp. 707-741.

41. Rouse, H., Engineering Hydraulics, John Wiley and Sons, New York, 1950, p. 104.

VITA

Charles Samuel Martin was born in Augusta County near Middlebrook, Virginia, on May 22, 1936. He attended local schools and graduated from the Augusta Military Academy, Fort Defiance, Virginia, in June of 1953. He graduated from the Virginia Polytechnic Institute, Blacksburg, with a Bachelor of Science in Civil Engineering in June of 1958. He was employed by the Virginia Department of Highways during the summer of 1958. He attended the Graduate Division of the Georgia Institute of Technology from September 1958 to September 1959. From September 1959 to May 1960 he was employed by the Newport News Shipbuilding and Dry Dock Company, Newport News, Virginia, as a designer of hydraulic machinery. Excluding the summer of 1961, he attended the Graduate Division of the Georgia Institute of Technology from May 1960 to the present. During the summer of 1961 he worked for the United States Mine Defense Laboratory, Panama City, Florida, as a hydraulic engineer. He was awarded a Master of Science in Civil Engineering in June of 1961.

While at the Georgia Institute of Technology he was employed as a graduate teaching assistant and as a graduate research assistant. During the school year of 1961-1962 he was a recipient of a Ford Foundation Fellowship-Assistantship for prospective engineering teachers. As a research assistant he was employed by the Engineering Experiment Station on a sponsored federal government project. Part of the study associated with the project is the problem reported in this thesis.

He is currently an Assistant Professor in the School of Civil

Engineering of the Georgia Institute of Technology.

He is a member of the honorary societies Tau Beta Pi, Sigma Xi, and Chi Epsilon; a student member of the American Geophysical Union; and an associate member of the American Society of Civil Engineers.

He is single.